A STUDY OF COAL OXIDATION

Thesis by

William Samson Kalema

In Partial Fulfillment of the Requirements

for the Degree of

Doctor of Philosophy

California Institute of Technology

Pasadena, California

1985

(Submitted July 9, 1984)

To the memory of my father

William W. Kalema, 1926-1972

Acknowledgments

I am very grateful to my thesis advisor, Dr. George R. Gavalas, who provided many valuable insights and guided me towards productive work, while allowing me the freedom to be creative. I was also privileged to have worked with the late Dr. William H. Corcoran, whose example of personal integrity, self-discipline and compassion will always be an inspiration to me. He cared about me and encouraged me to grow, both personally and academically.

George Griffith gave unstinting help and advice in the construction of the experimental apparatus. Like others before me, I have benefited greatly from his humanity and his dedication to Caltech.

For the FTIR work, I was fortunate in having access to the excellent facilities and expert guidance of Dr. Peter R. Griffiths and his research group at the University of California, Riverside. Dr. Paul Painter of Penn State was also helpful and informative. Dr. James Yesinoski of the Southern California Regional NMR Facility kindly read over parts of the manuscript and suggested useful changes. Dr. Bruce Hawkins and Mark Davis of the Colorado State Regional NMR Facility at Fort Collins gave me the benefit of their expertise in the NMR spectroscopy of solid coal. The Penn State Coal Bank provided the coals used in this work. The service they provide is invaluable.

I wish to express my warm thanks to Kathy Lewis for helping with the typing, and to Valerie Purvis for making the illustrations.

I gratefully acknowledge the financial support of the California Institute of Technology. I thank Martin Aliker and Ned Munger, who first

encouraged me to apply to Caltech. Ned has been a good friend and counselor throughout my time in Pasadena.

I have enjoyed my time at Caltech and learned a lot, both formally and informally. I appreciated the good company of my colleagues in the Corcoran group and the Gavalas group, among them, Ajit Yoganathan, Dan Hanle, Teri Weston and Sergio Edelstein.

My wife, Felleng, has been patient and understanding and cared for me lovingly. She and I have enjoyed the fellowship of Knox Presbyterian Church and the company of many friends in this area.

This thesis is one step in a lifelong process of learning our personal growth, which started in the warmth and security of a loving home. I thank my mother for her encouragement and support over the years, and dedicate this thesis to the memory of her late husband.

Table of Contents

Page

Abstract

Three coals were oxidized in a fluidized bed, using air at temperatures from 175°C to 280°C and total pressures from 126 kPa. to 274 kPa., for periods of up to 24 hours. An infra-red analyzer was used to measure concentrations of carbon oxide gases in the fluidizing stream. Both CO and CO_2 rates declined with time and increased with total pressure. The CO_2/CO ratio increased with oxidation temperature.

Oxidation at 200°C for 12 hours caused about a 10% loss in coal heating value, with most of that loss occurring in the first two hours. The loss of heating value correlated well, according to Dulong's formula, with the decrease in carbon and hydrogen content. The total and carboxylic ion-exchange capacities of the coal increased significantly with oxidation. The enhanced cation exchange capacity could be used to introduce calcium or other cations, which could help reduce emissions of sulfur oxides during coal combustion by forming sulfates in the ash.

FTIR spectra of coal samples were obtained using diffuse reflectance spectroscopy and peak overlap was reduced significantly using the fourier self-deconvolution technique. The spectra of oxidized coal samples showed the progressive reduction in the intensities of aromatic, methyl, and methylene C-H peaks and the appearance or enhancement of a number of carbonyl peaks.

Carbon-13 NMR spectra of solid coal samples were obtained using the cross-polarization technique together with magic-angle spinning, and carbon aromaticities were estimated which, when combined with analyses for carbon and ash content, allowed the calculation of overall consumption of aromatic and aliphatic carbon. Both aromatic carbon and aliphatic

carbon were consumed, even at 175°C. This finding disproved a previous theory that aromatic rings were oxidized only above 225°C.

List of Tables

List of Figures

1. INTRODUCTION

Our interest in coal oxidation developed out of earlier work on the desulfurization of coal [1,2,3], notably the results of Kralik's investigations into oxidative desulfurization using nitrogen dioxide. He had noted that, when washed with sodium carbonate solution, the oxidized coal took on sodium ions by cation exchange. Upon subsequent combustion up to 95 % of the sulfur in the coal was trapped as sulfate in the ash, instead of appearing as gaseous sulfur oxides. Thus it appeared that, under the right conditions, oxidative pre-treatment offered a potential method for achieving coal desulfurization.

Historically, the oxidation of coal has been studied for a number of different reasons. One reason was to investigate the physical changes which occur when coal is exposed to air at ambient conditions. Typically, the heating value falls slightly and the coal loses its caking properties. If the coal is stored in a large stockpile, the heat released by oxidation may build up and raise the temperature within the stockpile, causing greater loss of heating value and even ignition. Oxidation has also been used to achieve coal desulfurization, as in the Ames process [4]. Others oxidized coal using air and other oxidizing agents, observed changes in the coal and characterized the extract from the oxidized coal, and were then able to draw conclusions about the chemical structure of the coal. Thus, although early interest in coal acids was stimulated by interest in their potential usefulness as raw materials for the chemical industry [5,6], some workers soon recognized that the study of those acids could also help elucidate coal structure.

Our purpose in this work was to gain an understanding of the chemistry of coal oxidation, and to obtain data that could be useful in evaluating the economic viability of coal-pretreatment processes based on cation exchange; in

particular, the process whereby oxidized coal takes on metal cations from solution by ion exchange following which, on combustion, a significant proportion of the sulfur in the coal is trapped in the ash as sulfate, rather than being emitted into the atmosphere. In our experiments we oxidized coal with air, using a fluidized-bed reactor. We measured reaction rates at different temperatures and pressures, and studied how operating conditions affected the rate and products of oxidation. The concentrations of various oxygen-containing groups in oxidized coal were estimated using wet chemical methods. We sought to understand how acidic functional groups were formed, and cation-exchange capacity increased, during oxidation. We measured the heating values of coals oxidized under different conditions. Nuclear magnetic resonance and infra-red spectroscopy were used to study chemical changes in oxidized coals. The kinetic, analytical, and spectroscopic data were used in developing a model of coal oxidation.

1.1 The Structure of Coal

Coal is a carbon-rich sedimentary rock derived from plant matter, originally laid down as peat. In the course of some 60-300 million years, the peat became progressively less oxygen-rich and at the same time incorporated inorganic matter, forming a heterogeneous " fruit cake " consisting of clusters of several organic macerals and various inorganic compounds, along with small amounts of volatile gases and water.

Coals are most commonly described in terms of their Rank, which is a measure of the degree of coalification . The lowest rank is lignite or "brown coal" and the highest rank is meta-anthracite. Intermediate ranks are represented by sub-bituminous, bituminous, and anthracite coals. Most commercially useful coals are bituminous. Oxygen content, moisture, and volatile-matter content

decrease steadily with coal rank while heating value, carbon content and carbon aromaticity increase [7].

Coal owes much of its scientific interest to the complexity of its structure, which is heterogeneous, non-uniform, and porous. No two coals are exactly alike. Differences exist between coals of different geographical origin and geological history. The challenge of current research is to be able to make valid general statements based upon the behavior of a wide range of coals.

The organic material in coal is composed of three major kinds of macerals; vitrinites, inertinites (fusinite and micrinite) and liptinites (exinite, resinite, and bitumen) [8]. Under the microscope, those maceral types can be physically distinguished by their reflectance of light. Vitrinites, which appear gray in color, typically represent 70 -85 % of the organic matter in bituminous coals. They are derived from the lignin and cellulose in the original plant matter. The light-colored inertinites, which usually account for about 10 -20 % of the organic matter, tend to occur as discrete particles embedded within the vitrinite. Liptinites are very dark in color and are derived from a variety of substances, such as the resin, cutin and cork cell walls of the original plant matter and oily material from algea.

The inorganic compounds present in a particular coal reflect the geological environment in which the coal was formed. They include the dissolved carbonate, sulfate, and chloride salts of sodium, calcium, magnesium, and other cations. Other minerals such as silicates, carbonates, and pyrites also occur in discrete grains within the coal. There is increasing evidence that the mineral matter may sometimes catalyze the chemical reactions of coal [9]. The mineral matter is also noticeable in the infra-red spectra of coals [10].

In the present work, we are particularly interested in the oxygen content of coal, especially the oxygen in the organic coal structure. The oxygen-containing compounds in mineral matter, such as silicates, carbonates, sulfates, and nitrates are not significantly affected by oxidation below 300 ^{0} C. In the process of coalification, plant matter was converted to humic acids and then to peat, then lignite, and finally to bituminous coal and anthracite. All the present-day analogs of the original precursors of coal contain oxygen. Cellulose and lignins have ether linkages and phenolic and alcoholic hydroxyl groups. Tannins contain ether, phenolic and carboxylic oxygen. Alkaloids have alcohol and methoxy groups. Plant protein contains carbonyl, carboxyl and phenolic groups. And so on. The oxygen-containing groups, though gradually depleted during coalification, are found in varying amounts in all coals. Methods for estimating total oxygen content and the distibution of oxygen among functional groups are described in Chapter 3.

In general, researchers are mainly interested in the reactions of the organic portion of coal. Several different approaches may be used. Some workers have looked at particular coal macerals, notably vitrains [11,31]. Others have used extracts of coal in various solvents. Tars and other products of coal pyrolysis have also been used to gain some insight into the nature of coal. The structure and reactions of coal liquefied using hydrogen or donor solvents have also been studied extensively [12] Typically, the heavy coal liquids are fractionated by distillation and solvent extraction and the different fractions then characterized in terms of average molecular weights and representative molecular structures, based on spectroscopic and other evidence [12,13]. Thus structural analysis has developed as a useful tool for characterizing coal. Another approach is to react the coal with other chemical substances, usually oxidizing agents, and then observe the resulting products.

1.2 Oxidation of Coal

In the past, research workers have oxidized coal using liquid or gaseous oxidizing agents, for a variety of reasons - the study of atmospheric oxidation and weathering [14,15], the production of humic and other acids [5,6], oxidative desulfurization [1,2,4], and the study of coal structure [16-33].

There is a fundamental difference in chemical mechanism between gas-phase and liquid-phase oxidation. Liquid-phase oxidation is initiated by electrophilic attack while gas-phase oxidation occurs by a free-radical mechanism. Therefore conclusions drawn from liquid-phase systems are not necessarily applicable to oxidation by gases.

In general, oxidation with air at moderate temperatures has less drastic effects on the chemical structure of coal than does oxidation with oxidizing liquids. Oxidation with air is also more selective and more easily controlled. In this section we review previous studies of coal oxidation by gases and liquids.

1.2.1 Oxidation by Liquids

Liquid-phase oxidation has generally been used to fragment the organic coal matrix into identifiable products of lower molecular size. The severity of the conditions used would depend on the purposes intended. Thus, to produce humic, polyaromatic, and polycarboxylic acids, coal was reacted with hot nitric acid, hydrogen peroxide, or alkaline potassium permanganate. Insight into the structure of the coal could then be gained by identifying the smaller molecules produced by rupture of the organic coal matrix.

Some oxidizing agents, such as nitric acid and potassium permanganate, attack mainly the benzylic or aliphatic part of the coal, producing humic and benzenecarboxylic acids of high molecular weight, whose structure bears a

resemblance to the aromatic fraction of the coal. Alternatively, an oxidizing medium can be used which selectively attacks the aromatic rings and preserves the aliphatic chain. The structure of the small aliphatic compounds thus produced provides clues to the chemical structure of the non-aromatic part of the coal. An example of such an oxidant is the mixture of hydrogen peroxide, sulfuric acid, and trifluouroperoxyacetic acid (TFPA) at 85 ^{0} C. Using that mixture, Deno *et al.* [16,17] found that C_3-C_8 aliphatic diacids and triacids, arising from polycyclic systems consisting of hydroaromatic and aromatic rings, accounted for 50-90 % of all the observed products from the digestion of coal. By identifying the acids, they were able to characterize the aliphatic structures of various coals, based on the results of model compound studies. Those studies had shown the direct correspondence between the aliphatic-chain length of the acid and that of the original hydrocarbon. For example, propyl benzene was converted to butyric acid, and ethyl benzene to propionic acid. Thus they reasoned that the presence of acetic acid in the liquid product of digested coal implied that the starting coal contained aryl-methyl groups, while the presence of succinic acid implied that Ar-CH_2-CH_2-C methylene groups were present.

Likewise, characterization of the humic acids produced by oxidation of the aliphatic fraction of the coal can be used to elucidate coal structure. The acids range from simple aliphatic acids such as oxalic acid to acids with molecular weights as high as 10,000. Generally the low-molecular-weight acids are water-soluble while the high-molecular-weight acids are alkali-soluble.

Kamiya [18] produced aromatic polycarboxylic acids by reacting a Japanese bituminous coal with oxygen in an alkaline solution at 27 ^{0} C. The extract consisted of oxalic acid, aromatic acids, and humic acids. The acids were separated into different fractions. Benzenepolycarboxylic acids accounted for

about 45 % of the carbon contained in the aromatic-acid fraction. Those acids included three dicarboxylic acids (phthalic, iso-phthalic, and terephthalic), two tricarboxylic acids (trimellitic and hemimellitic), as well as tetracarboxylic, pentacarboxylic, and haxecarboxylic acids. A naphthalene tricarboxylic acid was also identified. High-molecular-weight humic acids were identified as the pre-cursors of benzenecarboxylic acids.

Moschopedis [19] characterized humic acids using chemical and spectroscopic techniques. He identified quinones and other oxygen-containing groups in humic acids. For one humic acid extract he estimated the quinonic content as 0.8 mg.equiv per gram of dry, ash-free (d.a.f) coal and the contents of carboxylic, phenolic, and methoxy-group content as 4.4, 2.9, and 1.7, respectively. Another study [20] indicated that about 80 % of the carboxylic acid groups were present as adjacent pairs, capable of forming anhydrides in the same way as phthalic acid, for example, forms the anhydride.

During the late 1950s and the 1960s, Mazumdar and his colleagues at the Indian Central Fuel Research Institute conducted extensive systematic studies of coal oxidation [21-24,29,30]. An essential starting point of their studies was the characterization of oxygen-containing functional groups in various coals [21,22].

Mazumdar *et al.* [23] reacted six coals of different rank with a 1:1 mixture of concentrated nitric and sulfuric acids at - 14 to + 15 ^{0} C, for three hours. Chemical analysis for oxygen-containing functional groups showed a significant increase in –COOH groups and very small increases in the concentrations of –OH and –CO groups. When the reacted coal was heated to 350 ^{0} C, the amount of CO_2 released was consistent with that expected from decomposition of the carboxylic groups. The authors concluded that, in the presence of concentrated

nitric and sulfuric acids, the aromatic rings were nitrated while methyl groups alone were oxidized to carboxylic acids. The authors also noted in a subsequent paper [24] that nitrated coal yielded no methane when pyrolyzed, thus suggesting to them that nitric acid had converted all the methyl groups to carboxylic acids. However, carboxylic-acid groups could also have been produced by the oxidation of methylene and other aliphatic C-H groups.

Some highly significant findings emerged from a systematic series of oxidation experiments conducted by Yokokawa *et al.* [25], using some thirty pure model compounds as well as lignin, lignite humic acids, and the methylated derivatives of lignin and humic acids. The model compounds used were representative of the oxygen-containing species and other functional groups of coal. They performed two sets of oxidation experiments. In the first experiments all the compounds were boiled in 1 N nitric acid for about 5 hours. The other oxidizing agent they used was alkaline potassium permanganate. The pure compounds were oxidized at 20 deg C, and the humic acids were oxidized at 25-50 deg C . They reported the following findings. The aromatic rings of uninuclear phenols were easily oxidized to CO_2 and oxalic acid. Naphthols were also similarly oxidized, but much more slowly. With nitric acid, aromatic rings were simultaneously nitrated, giving products which were very resistant to further oxidation. Methyl ethers produced by the methylation of phenols were not oxidized. The hydroxyl group apparently activated aromatic rings towards oxidation. Hydroaromatic structures containing alcoholic hydroxyl groups were even more reactive. Alicyclic structures containing –OH groups, such as 4-methyl hexanol and 1,2,3,4- tetrahydro-2-naphthol, were oxidized with the greatest ease, producing large quantities of CO_2 but very little oxalic acid. Lignin and lignite humic acids, but not their methylated derivatives, were easily oxidized, to give CO_2 , oxalic acid, and water-soluble acids. Hydrocarbons

without substituted hydroxyl groups, such as tetralin, decalin, 5,6,7,8-tetrahydro-1-naphthoic acid and γ-cyclohexyl propionic acid, were not oxidized at all.

When Kralik [1] studied the oxidative desulfurization of a bituminous coal by nitrogen dioxide he performed experiments in which he used water and carbon tetrachloride as carrier liquids. The NO_2 combined with residual water in the coal to form nitric and nitrous acids and several reactive electrophilic species including the nitronium ion and the nitrosonium ion. The two latter species are known powerful nitrating species, while nitric and nitrous acids are oxidizing agents. Thus, as well as incorporating significant amounts of nitrogen, the coal acquired an enhanced capacity for cation exchange, consistent with the creation of phenolic and carboxylic acid groups.

1.2.2 Air Oxidation

Air oxidation is a common cause of loss of heating value in coal. When coal is stockpiled, the enthalpy of oxidation can cause a large rise in the temperature within the pile, to values above 100 ^{0} C, leading to more rapid oxidation of the coal and even to spontaneous combustion. If the temperature rise due to stockpiling is avoided, coal does not deteriorate significantly under atmospheric conditions. Measurements of the loss of heating value of coal stored in small piles where spontaneous heating was avoided showed that there was no noticeable deterioration after several years' exposure [26]. The more significant changes which occur are physical. Ambient air oxidation dramatically reduces caking, which otherwise would cause agglomeration, loss of permeability, and blockage of feed lines during coking or gasification of coal. At higher temperatures, the physical changes are enhanced and chemical changes become apparent. Kona *et al.*[27] oxidized coal with air at 200-300 ^{0} C and found that

caking properties virtually disappeared after a few hours. Grindability, as measured by the Hardgrove grindability index, also fell drastically. Plasticity was substantially reduced, and the free-swelling index dropped.

Liotta *et al.* [14] made claims for significant chemical reaction at ambient temperature, based on the reaction of an Illinois bituminous coal at 20-30 ^{0} C for 56 days, but the evidence offered was not convincing. They reported a dramatic 26 % increase in the amount of organically-bound oxygen in the coal coal but, curiously, no increase in the amounts of carboxylic and phenolic groups. They defined ether-group content as the difference between the total concentration of organic oxygen and the sum of phenolic and carboxylic groups. So they concluded that the additional oxygen had been chemically incorporated in the form of ether linkages. Actually the oxygen could also have been present as carbonyls, quinones, aliphatic hydroxyl groups or, most likely, hydroperoxides. Fourier-Transform Infra Red spectroscopy indicated no increase in the intensities of the carbonyl or quinonic peaks, but there was an increase in overall peak intensity in the region 900-1200 cm^{-1}, which the authors associated with ether groups. In fact tertiary alcohols, peroxides, and sulfates also absorb in the same region. Sulfates, for instance, could have been produced by the oxidation of pyrite, which is present in coals. The free-radical mechanism proposed to explain the formation of ether linkages included an implausible step and differed from the generally-accepted mechanism of autoxidation [28]. The authors also proposed that changes in physical properties were caused by the loss of cross-linked polymeric properties, which somehow resulted from the formation of the ether linkages. No scientific theory relating cross-linking to physical properties was proposed, however.

Mazumdar and his colleagues made important contributions to the study of

air oxidation [29,30]. In one investigation Mukherjee *et al.*[29] oxidized coal in an air oven at 200 ^{0} C for up to 1300 hours. They took periodic samples of oxidized coal, from which humic acids were extracted by refluxing in alkali solutions and then recovered by precipitation in the presence of a strong mineral acid, followed by extraction and drying. The cation-exchange capacities of the coals were determined using barium solutions. By varying the pH of the solutions the amounts of –COOH and –OH could be separately estimated. As expected,the cation-exchange capacity increased with oxidation time. The results also indicated the oxidation of low-rank coals, initially containing high concentrations of –COOH and –OH groups, tended to produce almost exclusively –COOH while high-rank coals, which had very low concentrations of –COOH and –OH, increased their concentrations of both. The –OH/–COOH ratio of the humic acids increased with oxidation time, suggesting that the –COOH groups were the more susceptible to thermal degradation. In reference [30], Mazumdar *et al* presented data to show that the ring indices of several coals increased with oxidation, and thereby concluded that air oxidation at 170 ^{0} C had no effect on condensed aromatic structures. The ring index was used as a measure of aromaticity, but there was some ambiguity about the way it was calculated. Even assuming the correctness of Mazumdar's ring-index calculation, the change in the index would not be sufficient proof of the non-oxidation of the aromatic structure. An increase in the value of the index would simply imply that the condensed rings were less severely oxidized than the aliphatic fraction. In further experiments reported in the same article [30] the authors slowly increased the temperature in the oven while monitoring the weight of the coal and the production of CO, CO_2, and water. At the beginning, the powdered coal was laid on a Petri dish in the oven at 170 ^{0} C, through which a stream of air was passed. When the evolution of carbon oxides ceased, the coal sample was

weighed, the oven temperature was raised by 10 ^{0} C, and oxidation was continued at the higher temperature. Thus the temperature was progressively increased, up to 240 ^{0} C. There was little change in the amount of carbon oxides evolved or the weight of coal until the temperature reached 230 ^{0} C. Then substantial loss of organic matter became evident. The weight of a sample of vitrain fell by 40 % between 220 ^{0} C and 230 ^{0} C. Mazumdar *et al.* attributed this loss to the incipient oxidation of the aromatic fraction of the coal. Actually, the evidence that no aromatic material was oxidized below 230 ^{0} C was only circumstantial. The functional groups first oxidized at 230 ^{0} C could have been other relatively unreactive groups, not neccesarily aromatic material. The phenomenon observed at that temperature could also have been the result of a sudden change in the pore structure of the coal, making the coal more accessible to oxidation and thus rendering the coal much more reactive.

Another interesting observation from ref. [30] was that the rate of oxidation of vitrains was at least 50 % slower than the rate of coals, and the maximum percentage weight loss was significantly lower for the vitrains; indeed, the high-rank vitrain actually showed a small net *gain* in weight. Further, the estimated concentration of unreactive oxygen was much higher for vitrains than for their corresponding coals. Those results imply that the chemistry of vitrains is somewhat different from that of coals. The authors suggested that the difference was due to catalytic action by mineral matter in coal.

1.2.2.1 Mechanism of Coal Oxidation

Following from the work of Jones and Townsend [31], Moschopedis *et al.*[19,20], and Jensen *et al.*[32], a general mechanism of coal oxidation began to emerge. Oxidation in air was believed to proceed in four main stages: first, the formation of coal-oxygen surface complexes, especially peroxides, second, oxidation of the

coal to produce alkali-soluble species collectively known as humic acids, third, progressive thermal degradation of the humic acids into smaller molecules soluble in acids and water and finally, the breakdown of those molecules into carbon monoxide, carbon dioxide, and water. The four stages were believed to overlap, with CO, CO_2, and water being by-products in the last two steps.

Jensen *et al.*[32] first proposed the existence of a separate "burn-off" reaction by which water and carbonic gases would be produced without decomposition of humic acids.

In 1979 Berkowitz [7] summed up the prevailing view of how air oxidation of coal occurs, as follows: Initially oxygen is chemisorbed at readily-accessible aromatic and aliphatic surface sites and reacts to form carboxylic, carbonyl, and phenolic groups and, in the presence of water, peroxide and hydroperoxide complexes. The peroxides are unstable above 70 ^{0} C. In time the coal substance is degraded to humic acids which are further broken down into progressively smaller molecules. Humic acids are only formed in significant amounts above 150 ^{0} C and decompose to give water and carbonic gases, especially above 250 ^{0} C. Water and carbonic gases are also formed, at all temperatures, by a direct "burn-off" reaction. The overall scheme is shown in Figure 1.1 At higher temperatures, the above processes are merely accelerated. The oxidation of aromatic structures follows Tronov's scheme, shown in Figure 1.2 , and similar reactions cause the oxidation of hydroaromatic structures. Tronov's scheme is similar to the mechanism of the gas-phase oxidation of naphthalene.

The existence of the "burn-off"reaction in the general mechanism described by Berkowitz is rather doubtful. A dual-path mechanism seems superfluous. We would expect the carbonic gases and water to arise from some oxidized intermediate species not necessarily humic acids, which are chemically stable.

Both Mazumdar *et al.*[30] and Kam *et al.*[33] reported that there was a change in mechanism at about 230 ^{0} C. Mazumdar *et al.*ascribed that change to the incipient oxidation of the aromatic fraction of coal while Kam *et al.*believed that it was due to the predominance of "site-oxygen" reactions over "site-site" reactions at higher temperatures.

In fact the evidence for a change in mechanism at 230 ^{0} C is by no means conclusive. The apparent change could have been an artifact of the particular experimental systems used.

1.3 Spectroscopic Analysis of Coal

The combined use of chemical and spectroscopic analysis can contribute greatly to a better understanding of the structure and chemical reactions of coal. Both infra-red (IR) and nuclear magnetic resonance (NMR) spectroscopy have been used to characterize coal and its products. Although spectra of coal-derived liquids can be analyzed in fine detail, the spectroscopic analysis of solids is still a developing science, especially with NMR. Further progress will depend on improvements in instrument design , continued breakthroughs in theoretical analysis, and advances in the techniques of nuclear decoupling and spectral resolution. In this section we discuss both IR and NMR.

1.3.1 Infra-Red Spectroscopy

Infra-Red spectroscopy was first used to characterize coal following the development of more sensitive diffraction-grating spectrometers in the 1950's. Much of the early work was concerned with developing reliable methods of sample preparation [34,35,36,37] and with the correct assignment of i.r absorption bands to given C-H and C-O bonds [34,37,38,39]. Currently,the most widely-used procedure for sample preparation is the potassium halide method,

in which coal is ground with potassium chloride or bromide under specified conditions, and pelletized into a disc whose i.r spectrum is then obtained.

For the study of coal oxidation, the most interesting regions of the spectrum are: the 2980-2860 cm^{-1} region, corresponding to the aliphatic C-H stretching modes, 3400 cm^{-1}, due to associated OH and NH, 3030 cm^{-1}, due to aromatic C-H stretching, 1800-1500 cm^{-1}, representing C-O stretching frequencies for a number of different functional groups, and various C-H and C-O bending frequencies in the 1500 to 900 cm^{-1} range.

Any mineral matter present obviously contributes to the i.r spectrum. In the past, interference due to mineral matter was often avoided by working with vitrains rather than whole coals [39,40]. Today some use spectral subtraction techniques, in conjunction with Fourier Transform Infra-Red (FTIR) spectroscopy.

The amount of information obtainable from a spectrum depends on the precision of the instrument. Fourier-Transform Infra-Red (FTIR) spectrometers give the best spectra. The advantage of FTIR spectrometers derives mainly from their unique optical system, which utilizes an interferometer to scan a wide range of frequencies at the same time, producing an interferogram. A fast-fourier-transform algorithm implemented by an on-line computer is used to convert the interferogram into a frequency spectrum. By this design, the FTIR spectrometer has much higher spectral resolution and much higher signal/noise ratios than the conventional spectrometer, producing a sensitivity which is particularly advantageous in analyzing an opaque material such as coal. Because the spectra are stored by the computer, they can be conveniently compared and analyzed. The subtraction of spectra from different samples, to highlight their differences, is just one simple example. The high resolution

makes possible the use of effective techniques for resolving broad bands of closely-spaced, overlapping peaks, which could not be separated otherwise. Two such techniques are least-squares curve fitting and fourier self deconvolution [41,42]. Using those procedures in conjunction with FTIR we are able to follow more closely the fate of given C-H and C-O bonds in the coal, and thereby realize great improvements on past studies of the infra-red spectra of coal.

1.3.2 Nuclear Magnetic Resonance Spectroscopy

Proton and carbon-13 NMR spectroscopy of coal-derived liquids gives fairly detailed, quantitative information of the functional distribution of protons and carbon atoms in the sample. The combination of data from FTIR and NMR spectroscopy can help characterize coal liquids unambiguously.

Carbon-13-NMR spectra of whole, solid coals can be obtained using the combined techniques of cross-polarization and magic-angle spinning. Such spectra do not, however, show the detailed disposition of functional groups in the sample. The major result from those spectra is an estimate of the carbon aromaticity of the coal. Thus we can investigate whether a given treatment - such as oxidation - causes changes in the aromaticity of the coal.

1.4 Objectives

Our purpose was to identify the products and understand the mechanism of coal oxidation in air, with particular interest in the formation of ion-exchange structures, in view of their potential usefulness. We investigated the origin of the carbon oxides produced during oxidation. We sought to observe and explain the effects of temperature and oxygen concentration on the rate of oxidation. We measured cation-exchange capacity for coals oxidized under different conditions. While the literature suggests that carboxylic groups are derived

from methyl groups in the coal, the chemical precursors of phenolic groups are not clearly identified. Using chemical analysis and FTIR spectroscopy we observed the functional groups affected by oxidation. A number of workers had reported an apparent change in the mechanism of oxidation around 225 ^{0} C. We wished to investigate whether that change was real and whether it was indeed caused by the incipient oxidation of the aromatic fraction of coal. NMR was used to measure possible changes in aromaticity.

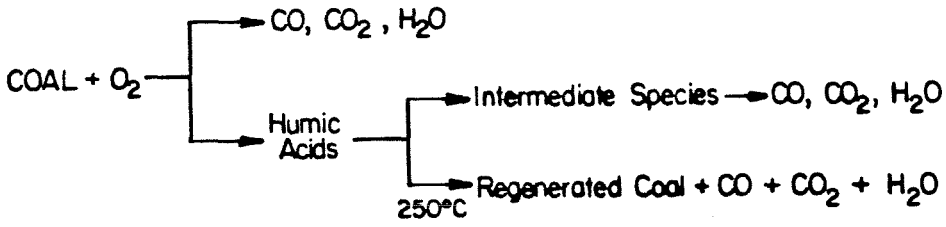

FIGURE 1.1: Mechanism of Coal Oxidation in Air, Proposed by Berkowitz (7)

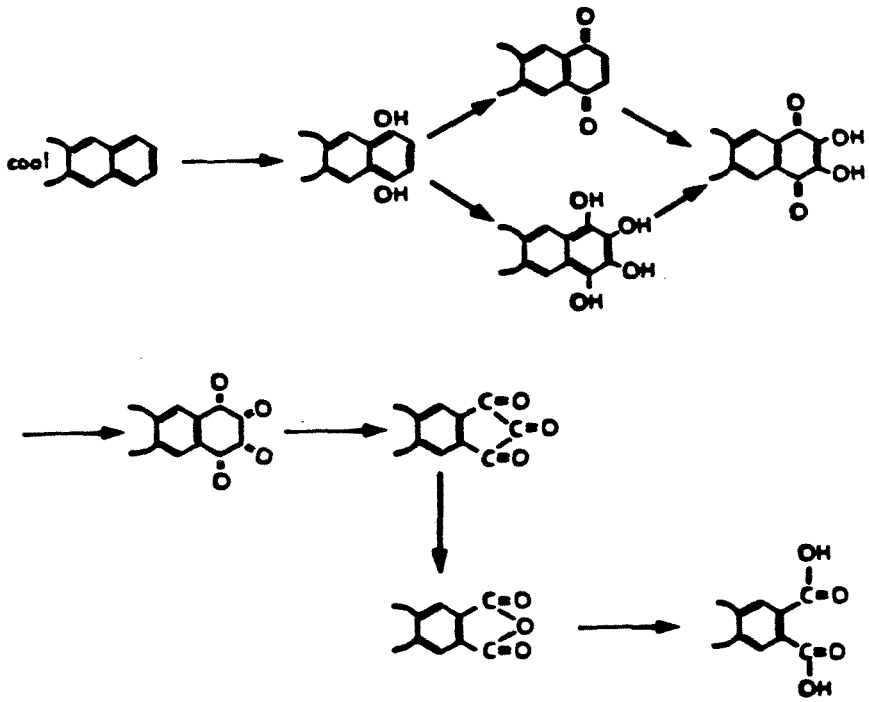

FIGURE 1.2: Tronovs' Scheme for the Oxidation of Coal in Air

References

[1] Kralik J.G, Ph.D Thesis, California Institute of Technology, Pasadena, 1981

[2] Vasilakos N, Ph.D Thesis, California Institute of Technology, Pasadena, 1981

[3] Attar A and Corcoran W.H Ind. Eng. Chem. Prod. Res. Dev., **17**, 102, 1978

[4] Friedman S, Lacount R.B, and Warzinski R.P, in Coal Desulfurization, ACS Symp. Ser. No.64, American Chemical Society, Washington D.C, 1977

[5] Frankie N.W, Kiebler M.W, Ruof C.H, Savich T.R, and Howard H.C, Ind. Eng. Chem, **44**, 2784, 1952

[6] Friedman L.D and Kinney C.R, Ind. Eng. Chem.,**42**,2525,1950

[7] Berkowitz N, An Introduction to Coal Technology, Academic Press, New York,1979

[8] Gorbarty M.L and Ouchi K (Eds), Coal Structure, Adv. in Chemistry Series No. 192, American Chemical Society, Washington D.C, 1981

[9] Z. Abdel-Baset, P.H. Given, and R.F. Yarzab, Fuel, **47**, 95, 1978

[10] Painter P.C, Snyder R.W, Starsinic M, Coleman M.M, Kuehn D.W, and Davis A, Appl. Spectrosc., **35**, 475, 1981

[11] Conrow R.B, Durie R.A, Shannon J.S, and Sternall S, Fuel, **42**, 275, 1963

[12] Petrakis L, Allen D.T, Gavalas G.R, and Gates B.C, Anal. Chem., **55** , 1559, 1983

[13] Allen D.T, Ph.D Thesis, California Institute of Technology, Pasadena, 1983

[14] Liotta R, Brons G, and Isaacs J, Fuel, **62**, 781, 1983

[15] Yohe G.R, Fuel, **44**, 135, 1965

[16] Deno N.C, Greigger B.A, and Stroud S.G, Fuel,**57**,455,1978

[17] Deno N.C, Jones A.D, Koch C.C, Minard R.D, Potter T, Sherrard R.S, Stroh J.G, and Yevak R.J , Fuel,**61**,49,1982

[18] Kamiya Y, Fuel, **40**, 457, 1961

[19] Moschopedis S.E, Fuel, **41**, 425, 1962

[20] Wood J.C, Moschopedis S.E, and Den Hertog W, Fuel, **40**, 491, 1961

[21] Mazumdar B.K, Bhangale P.H, and Lahiri A, J.Sci Ind Research, **15B**, 44, 1956

[22] Bhowmik J.N, Mukherjee A.K, Mukherjee P.N, and Lahiri A Fuel, **41**, 443, 1962

[23] Mazumdar B.K, Chatterjee A.K, and Lahiri A, Fuel, **46**, 379, 1967

[24] Chatterjee A.K and Mazumdar B.K, Fuel, **47**, 93, 1968

[25] Yokokawa C, Wanatabe Y, Kajiyama S and Takegami Y, Fuel, **41**, 209, 1962

[26] Schmidt L.D and Elder J.L, Ind.Eng. Chem., **32**, 249, 1940

[27] Kona N.R, Fairbanks H.V, and Leonard J.W, Fuel, **47**, 177, 1968

[28] Walters W.A, Mechanisms of Oxidation of Organic Compounds, John Wiley & Sons, New York, 1964

[29] Mukherjee P.N, Bhowmik J.N, and Lahiri A, Fuel, **36**, 417, 1957

[30] Mazumdar B.K, Chakrabarty S.K, Saha M, Anand K.S, and Lahiri A, Fuel, **39**, 469, 1959

[31] Jones R.E and Townsend D.T.A, J. Soc. Chem. Ind., **68**, 197, 1949

[32] Jensen E.J, Melnyk N, Wood J.C, and Berkowitz N, in Coal Science, Given P.H (Ed), Advances in Chemistry Series No. 55, American Chemical Society,

Washington D.C, 1966

[33] Kam A.Y, Hixson A.N, and Perlmutter D.D, Chem. Eng. Sci., **31**, 821 , 1976

[34] Brooks J.D, Durie R.A, and Sternhell S, Aust. J. Appl. Sci., **9**, 63, 1958

[35] Czuchajowski L, Fuel, **39**, 377, 1960

[36] Albers G, Lenart L, and Oelert H.H, Fuel, **53**, 47, 1974

[37] Painter P.C, Rimmer S.M, Snyder R.W, and Davis A, Appl. Spectrosc., **35**, 102, 1981

[38] Rao H.S, Gupta P.L, Kaiser F, and Lahiri A, Fuel, **42**, 417, 1963

[39] Adams W.N and Pitt G.J, Fuel, **34**, 383, 1955

[40] Osawa Y and Shih J.W, Fuel, **50**, 53, 1971

[41] Kuehn D.W, Snyder R.W, Davis A,and Painter P.C, Fuel, **61**, 692, 1982

[42] Griffiths P.R, Department of Energy Report No. DOE/PC/30210-T3, 1982

2. OXIDATION OF COAL IN AIR

The work described in this chapter was undertaken to obtain information that would be helpful in modeling the kinetic mechanism of coal oxidation, and to obtain samples of oxidized coal for subsequent chemical and spectroscopic analysis. The effects of external heat and mass transfer resistance had to be minimized, so that the rates measured could be interpreted chemically. Using a fluidized-bed reactor, we obtained data free of external transport effects. We investigated how rates of production of CO and CO_2 depended on coal type, temperature, oxygen concentration and time. We looked for a change in the CO/CO_2 ratio at some temperature, possibly indicating a change in the mechanism of oxidation.

Several authors had reported an apparent change in mechanism at 225°C. We sought to determine whether this apparent change was real and if so whether of chemical or physical origin. If the change was chemical, we wished to establish whether it resulted from the decomposition of carboxylic groups or, as some authors had supposed, from the incipient oxidation of aromatic rings.

2.1 Previous Work

Most of the early published data on coal oxidation indicated that the rate of oxidation in air tends to decay with time. Several workers measured the amount of oxygen consumed and fitted their data to equations such as (1), in which q is the cumulative amount consumed and C and n are empirical constants. The exponent n was reported as -0.5, by Frey [1] and -0.25 by Schmidt and Elder [2]. Other workers [3,4] expressed their data in terms of the Elovich equation, shown below as Eqs. (3) and (4), in which the quantities α, t_0 and B are empirical constants.

$$\frac{dq}{dt} = Ct^n \tag{1}$$

Elovich Equation :

- Differential Form

$$\frac{dq}{dt} = be^{-\alpha q} \tag{2}$$

- Integral Form

$$q = \left(\frac{2.3}{\alpha}\right) \log (t+t_0) - \left(\frac{2.3}{\alpha}\right) \log t_0 \tag{3}$$

The Elovich equation was in fact originally proposed in 1940 as an empirical relation. Later, several workers, notably Taylor and Thon [5] justified it by a theory of chemisorption involving the creation and subsequent deactivation of active sites on the surface. Thus, Wood argued that his data, taken at 30°C indicated that chemisorption was the key step in coal oxidation. The same results, however, could have been obtained from a measurement of gas diffusion. Harris and Evans [6] have shown that numerical values consistent with the Elovich equation, subject to a suitable choice of the constant t_0, can be generated from the standard mathematical solution to the problem of unsteady diffusion into a sphere, viz. Eq. (4):

$$\frac{q}{q_\infty} = 1 - \frac{6}{\pi^2} \sum_{n=0}^{n=\infty} \left[\frac{1}{n^2} e^{\left(-\frac{D_e n^2 \pi^2 t}{r^2}\right)}\right] \tag{4}$$

where r is the radius of the sphere, t is the time, D_e is the effective diffusivity, and q is the total amount of diffusing species taken up by the sphere at time t.

The empirical relations of Eqs. (1)-(3) should not be taken too literally because they were based on data that were generally not very accurate. The values of (dq/dt) used by the authors of Refs. [1-4] were obtained by estimating the slope of the q vs. t curve, using measurements of q which were not precise

because the experimental systems used were somewhat crude.

As an example, consider the experimental system used by Carpenter and Giddings [4]. They put coal in a packed bed within a closed system through which air was recirculated slowly by means of a pump. The water and CO_2 produced by reaction were removed by adsorbents contained in U tubes and the CO was oxidized over an electrically-heated platinum wire, to produce CO_2 which was then removed by adsorption. Every 15 minutes the recirculation pump was stopped and a known amount of oxygen was added to the closed system, sufficient to reestablish the total pressure of the system. That amount was defined as the amount of oxygen consumed by coal oxidation. Thus, they measured the rate of oxygen consumption. They assumed that the oxygen required to oxidize the CO was negligible, whereas in fact it represented up to 30% of all the oxygen consumed. Apart from errors in measuring oxygen consumption, the overall rate was also influenced by gas-to-particle mass transfer resistance because gas recirculation was slow.

In the work of Schmidt and Elder [2], about 180 lbs of - 1/4-inch coal were placed in a rotating drum and a mixture of nitrogen and oxygen was passed through it. The effluent gases were analyzed chemically for oxygen, CO and CO_2. The temperature of the drum was maintained using a gas burner. Because of low flow rates and large particles, the overall rate was again affected by external mass transfer.

The different authors reported different orders of reaction with respect to oxygen concentration. Carpenter and Giddings [5] oxidized six coals at 95°C and reported orders of 0.32 to 0.67 . Elder [2] quoted 0.61. Because of external mass-transfer resistance, no valid mechanistic interpretation can be placed upon those orders of reaction. Likewise, the value of 12 kcal/g mole for the

activation energy of the oxidation reaction, reported in Ref. [2], may be subject to error.

Perlmutter and co-workers [7-9] used a packed-bed reactor to study the oxidation of seven coals of different rank and geographical origin. The range of oxidation temperatures was 200-277°C and the partial pressure of oxygen was varied from about 0.1 atmospheres to about 0.4 atmospheres. Experiments were performed with three particle-size fractions: -6 to -14 mesh (1.41 to 3.36 mm), -14 to -18 mesh (1.0 to 1.41 mm), and -18 to -50 mesh (0.3 to 1.0 mm), which had external surface areas of 3.25, 5.25 and 15.25 m^2/kg, respectively. They monitored the concentrations of oxygen, CO and CO_2 in the effluent gas using a gas chromatograph and measured the amount of water produced by absorption in the drying agent anhydrone.

A dual-path model was proposed for the reaction between coal and oxygen, similar to that of Berkowitz which is shown in Figure 1.1. Reaction was assumed to occur only at the external surface, and intra-particle diffusion was neglected. The burn-off reaction, path I, was assumed not to be rate-limiting. Rapid chemisorption of oxygen would create "activated complex" reactive sites, which would then decay by further reaction with oxygen and by bimolecular site-site deactivation reaction, such as free-radical recombination.

At 200 and 225°C, the rates of evolution of CO and CO_2 were constant with time; and at 250 and 277°C the rates decayed exponentially with time. At a given temperature the ratio of CO_2 to CO produced remained constant with time. Their data, reproduced in Table 2.1, show that this ratio had its minimum value at 225°C. Actually, as we shall see later, their data may have been confused by the use of large overall oxygen conversions, causing concentrations and temperatures within the packed-bed reactor to be highly non-uniform and

significantly different from their nominal values.

The authors speculated that the apparent change in mechanism was caused by the predominance of the activated site-oxygen reaction over bimolecular site-site deactivation, at the higher temperatures.

The experimental system used by Kam et al. [8] [8] and Avison et [9] al. [9] represented a significant improvement over previous systems. The rates of consumption of oxygen and production of carbon oxide gases were more accurately measured than in previous investigations. Relatively high flow rates of air were used and thus the influence of gas-to-particle mass transfer resistance was minimized. Using typical values of operating parameters for an oxidation run, as given in Ref. [8], we estimated (see calculation in Appendix A) that gas-film mass-transfer resistance accounted for about only 0.24% of the total difference in oxygen concentration between the bulk gas and the reaction interface. In other words, the overall rate was controlled by the rate of chemical reaction and, perhaps, by intra-particle diffusion but not by external mass transfer. This statement contradicts one of the conclusions of Kam et al. [8].

In Ref. [8], it was stated that the overall rate was affected by external mass transfer. That conclusion was based on the observation that the reaction rate increased with decreasing particle size and with increasing air flow rate. To explain why the rate of reaction increased with increasing air flow rate, we note that, for the experiments described in Ref. [8], the overall conversion of oxygen typically ranged from about 70% at the beginning of an oxidation experiment to about 30% after six hours of reaction. Those figures are extracted from data reported in Ref. [8], and evaluated in Appendix A. At such high levels of conversion, increasing the air flow rate raises the mean oxygen concentration and thereby causes the overall rate of reaction to increase. Considering that

the oxidation of coal is an exothermic reaction, we would expect that the large concentration gradients within the bed also led to significant temperature gradients and possibly also to "hot spots"; because of the well-known difficulty of maintaining uniform temperatures in packed beds. The higher reaction rate observed with smaller particles could be due also to possible higher bed temperatures, caused by agglomeration and poor air circulation.

The very high conversion of oxygen used by Kam et al. invalidated the assumption made, in developing their mathematical model of reaction [7], that the packed bed could be regarded effectively as a differential reactor, allowing them to linearize the standard design equation for the plug flow reactor. Consequently, much of the quantitative interpretation of reaction rates presented in Ref.[8] was incorrect.

2.2 Oxidation of Coal in a Fluidized Bed Reactor

The benefits of fluidized-bed reactors have long been recognized [10,11]. A fluidized bed behaves as a turbulent system, characterized by large eddy diffusivities of heat, mass and momentum. In gas-solid systems, particulate (i.e. non-bubbling) fluidization minimizes gas by-passing, effectively giving complete mixing of the gas and solid phases.

The fluidized-bed reactor meets the important requirements of a good laboratory reactor for studying gas-solid reactions. Those criteria are given below.

1. Isothermal operation and ease of control of temperature.
2. Low conversion of key reactive component.
3. Minimal influence of external mass transfer on overall rate of reaction.

4. Facility for taking representative samples of reacted solids, where needed.

5. Low cost and ease of construction.

The measurement of reaction rates is simplified greatly if requirements (1) and (2) are satisfied. With an isothermal bed and low conversion of the reactive gas-stream component A, the bed can be treated as a differential reactor [12]. The instantaneous rate, r_A, is calculated readily from the molar flowrate F and the difference in molar concentrations (c_A) of A in the inlet and exit streams. Thus,

$$r_A = F\Delta c_A\,,\ \Delta c_A << c_A \qquad (5)$$

In our fluidized-bed oxidation experiments, the conversion of oxygen was typically 1.5% and, therefore, the conditions for the use of Eq. (5) were well satisfied.

A packed-bed reactor such as that used by Kam et al., by contrast, is an integral reactor. Such reactors are generally suitable for obtaining rate constants with systems for which rate expressions are available and where small concentration differences would be difficult to measure. The assumed rate expression is used to calculate the overall conversion by numerical solution of the coupled equations of heat and mass transfer and chemical reaction. The iterative calculation is repeated until the calculated conversion is arbitrarily close to the observed conversion. Clearly, good estimates of intrinsic reaction rates will not be obtainable unless the correct rate expression is used. The integral reactor is unsuitable for a system with multiple reactions or with unknown, or time-dependent, kinetics.

Appendix A shows the calculation in which we estimated the magnitude of external mass-transfer resistance under typical operating conditions of our reactor. Based on that calculation, we estimated that external mass transfer

accounts for only approximately 0.13% of the overall oxygen-concentration difference between the bulk gas and the particle. Thus we concluded that the overall rate of reaction was essentially independent of external mass transfer.

The possible influence of intra-particle mass transfer on the overall rate of reaction is discussed in Chapter 6 of this thesis.

The only other reported use of a fluidized-bed reactor to study coal oxidation was by Toynbee and Fleming [13], who oxidized a sub-bituminous coal with air at 200-325°C in a 2-inch diameter fluidized bed for up to seven hours. According to their account, the bed tended to heat up by about 75°C upon addition of coal, causing temperature control to be extermely difficult. The composition of the effluent gas at 325°C is shown in Table 2.2 . The table shows that the rates of production of carbon oxide gases declined markedly with time. The authors did not report any rates of reaction. In view of the high conversion of oxygen implied by the figures in Table 2.2, the true rate of reaction would have been difficult to evaluate.

2.3 Experimental Set Up

2.3.1 Apparatus

The experimental apparatus we used is shown schematically in Fig. 2.1. Air was taken from the 80 psig laboratory air supply. Any CO and CO_2 present in the air was removed by molecular sieve material contained in a cylindrical container. Fresh, regenerated molecular sieve was used in every experiment. For some special experiments, pre-purified nitrogen was used instead of air. The feed pressure of either gas could be adjusted to the desired value by adjusting the pressure regulators and the valves in the feed lines.

The 12-inch long reactor and the 4-inch long preheater were made from 3/4-inch o.d, 1/8-inch wall mild-steel tubing. Both sections were heated externally using copper heating blocks made by inserting electrical heating elements into specially-drilled holes in each of two identical copper blocks. The preheater was filled with 0.3-0.4 mm glass beads to increase its heat capacity and the area available for heat transfer. The reactor section and the preheater section were both well insulated with alumina blanket insulating material.

The power supplied to the heaters was controlled by two independent variacs. The preheater voltage was normally set at about twice the voltage of the reactor heater voltage. An on/off temperature controller was used to regulate the preheater. It was actuated by the voltage signal from a sheathed thermocouple inserted into the fluidized bed, about an inch above the distributor plate of the bed. The thermocouple readings were also recorded by a chart recorder. Bed temperature was controlled frequently to within $\pm$ 1°C.

Entrained particles in the exit stream were removed by a screen at the top of bed and by a solids trap consisting of a 3/4-inch tube filled with glass wool.

When required, samples of oxidized coal were withdrawn via a 1/8-inch diameter sample port, while keeping the bed fluidized. First the bed would be de-fluidized, then the plug on the sample port would be removed. Then the air supply valve would be opened momentarily, fluidizing the coal and causing it to issue out of the sample port. The duration of the pulse determined the quantity of sample taken.

The effluent gas from the reactor was cooled to room temperature in a coiled 1/4-inch diameter copper tube immersed in a water bath, and then passed through a millipore filter and thence to the Infra-Red Spectrometric Analyzer for CO and CO_2. The analyzer was a Series 702 Model, manufactured by Infrared

Industries Inc. of Santa Barbara, California. The range of the CO_2 scale was 0-1% and the range of the CO scale was 0-6%. The exit gas stream was not analyzed for oxygen because the total conversion of oxygen was very low, and a suitable accurate instrument to monitor oxygen concentration was not available.

2.3.2 Experimental Method

A 3/4-inch diameter fluidized bed made from lucite was used to establish minimum fluidizing velocities and optimum operating velocities for the different particle-size fractions used. The reactor was operated as a bubbling fluidized bed.

Before the start of each oxidation run, the infrared analyzer was checked fully using an oscilloscope, and then calibrated. Calibration consisted of a zero calibration and a span (proportionality) calibration. Pre-purified nitrogen was used for the zero check and a standard gas mixture containing known concentrations of CO and CO_2 was used for the span calibration. During a run, the zero calibration was repeated every hour and the span calibration was repeated every four hours. Typical CO concentrations represented less than 4% of the fullscale reading and were therefore rather inaccurate. CO_2 readings were about 10-50% of fullscale. Therefore, we based most of our quantitative analysis on CO_2 reaction rates.

At least four hours before the start of an oxidation run, the heaters were switched on and the temperature controller set to the temperature at which the oxidation run was to be performed. The air flow rate was also set to the value to be used in the experiment. The infrared analyzer was switched on, to allow sufficient warm-up time prior to calibration.

During warm-up, the temperature in the reactor was recorded by the

thermocouple recorder chart. Coal was added to the bed when the desired steady temperature had been attained. The flow of air was shut off and a known weight of coal, usually about 10 grams, was added to the bed through the coal feed line. The coal was allowed to heat up for about two minutes and then the flow of air was restored. The desired operating temperature was usually re-established in about 30 minutes.

Normally, several runs were made for each given set of operating conditions. Some runs were for measuring rate data, others were for obtaining samples of oxidized coal for subsequent chemical and spectroscopic analysis. When reaction rates were to be measured, no samples of oxidized coal were taken. The typical run lasted about 12 hours.

2.3.3 Experiments Performed

Three different coals were used: PSOC 704, a high-volatile bituminous "A" coal; PSOC 615, a low-volatile bituminous "B" coal; and PSOC 247, a lignite "A". All three coals were obtained from the Penn State Coal Bank in Pennsylvania. Table 2.3 shows analytical data on the coals, provided by the coal bank. PSOC 704 coal was used in most of our investigations.

2.3.3.1 Oxidation Experiments

We studied the air oxidation of coal at temperatures of 175-425°C and total pressures of 125 kPa. to 274 kPa. (3.5 to 25.0 psig) and used coal particles of four different size fractions. We measured rates of evolution of CO and CO_2. As mentioned earlier, oxygen consumption was not measured.

The following sets of oxidation experiments were performed:

1. Oxidation of PSOC 704, PSOC 615 and PSOC 247 coals at 200°C and 126 kPa. (3.5 psig), using 68-80 mesh (177-250 μm) particles, to compare rates of reaction for three different coal types.

2. Oxidation of PSOC 704 coal at 200°C and 126 kPa. (3.5 psig), using 42-48 mesh (297-354 μm), 60-80 mesh (177-250 μm) and 100-120 mesh (125-149 μm) particles, to investigate the effect, if any, of particle size or external mass transfer on the rate of oxidation of coal.

3. Oxidation of acetylated, 60-80 mesh PSOC 704 coal at 200°C and 126 kPa. (3.5 psig) to see what effect, if any, the blocking of free hydroxyl groups would have on the rate of oxidation of coal in air. The hydroxyl groups in the coal were blocked by forming their acetyl derivatives by refluxing the coal for 24 hours, using a 2:1 mixture of pyridine and acetic anhydride, as described in Chapter 3.

4. Oxidation of 60-80 mesh PSOC 704 coal, acid-washed using the procedure described in Chapter 3, at 200°C and 126 kPa. (3.5 psig) to investigate the possible catalytic effect of Fe^{+2} and other cations on the autoxidation of coal.

5. Oxidation of 60-80 mesh PSOC 704 coal at a series of temperatures in the range 280-325°C, noting how the CO_2/CO ratio varied with oxidation temperature.

6. Oxidation of 60-80 mesh PSOC 704 coal at 126 kPa. at temperatures of 175, 200, 230, 250, and 280 ^{0} C to study the effect of temperature on reaction rates.

7. Oxidation of PSOC 704 coal at 200°C, using 68-80 mesh (177-250 μm) particles and total pressures of 126, 181, 205 and 274 kPa. (3.5, 11.5, 15.0

and 25.0 psig), to study the dependence of reaction rate on oxygen partial pressure and measure the order of reaction with respect to oxygen.

2.3.3.2 Heating of Oxidized Coal in a Stream of Pure Nitrogen

We used 60-80 mesh PSOC 704 coal for these experiments. We observed the effect of heat on oxidized coal by measuring the concentration of CO_2 and CO in the effluent gas stream and by analyzing samples of the coal before and after prolonged heating. Two sets of heating experiments were performed:

In the first set of experiments, set A, a sample of oxidized coal was subjected to heating at four successively higher temperatures, from 200 to 250°C. The coal had been oxidized at 200°C for nine hours using air, and then the flow of air replaced by a stream of pre-purified nitrogen, while maintaining reactor temperature at 200°C. The concentration of CO_2 in the effluent stream was monitored. A few measurements of CO concentrations were also made but, because the CO scale was relatively insensitive, we did not use them to calculate CO evolution rates. After heating at 200°C for four hours, the bed temperature was raised to 210°C within 30 minutes and maintained at 210°C for 3.5 hours and then to 250°C for three hours. The results are shown in Fig. 2.11.

In the second set of experiments, set B, samples of coal were oxidized for six hours at 126 kPa. (3.5 psig) and at temperatures of 200°C and 250°C, respectively, and then heated at the given temperature for 6-12 hours in a stream of pure nitrogen. We had established that the hold-up time between the gas inlet valve and the CO/CO_2 analyzer was about four minutes. Allowing for that delay, we determined initial CO_2 rates for the heating experiment at each temperature, and compared that rate with the oxidation rate. The results are shown in Fig. 2.12 and Table xx.

2.4 Results and Discussion

Reaction rates for the oxidation experiments and heating experiments are summarized in this section. Some of the implications of those results are discussed briefly. In Chapter 6 of this thesis we will attempt a fuller explanation of the important aspects of coal oxidation, encompassing our findings from chemical analysis and spectroscopy of oxidized coal as well the results summarized here.

2.4.1 Oxidation Experiments

Figures 2.2 and 2.3 show CO_2 and CO rates at 200°C for the three coals used in this study. The lignite PSOC had the highest rate of reaction and the low-volatile bituminous PSOC 615 the lowest. Rates of evolution of CO and CO_2 declined with time, at different rates for each coal, with the steepest decline occuring in the early stages of oxidation. Presumably, the rate of oxidation fell as reactive species in the coal are depleted.

Below about 250°C, the ratio CO_2/CO decayed fairly slowly with time. With the higher rates of oxidation at higher temperatures the CO_2/CO ratio decreased with time, apparently indicating preferential consumption of CO_2-producing reactive functional groups. The value of this ratio at 200°C was 1.71 for PSOC 247, 0.99 for PSOC 704 and 1.26 for PSOC 615. Clearly, the ratio depends on the nature of the reacting coal. In Fig. 2.10 we see that the ratio was also a function of temperature. Figure 2.10 shows a fairly linear increase in CO_2/CO ratio for PSOC 704 coal, from 0.87 at 175°C to about 1.5 at 300°C. In contrast to the data of Kam et al. shown in Table 2.1, we found no minimum in the value of the CO_2/CO ratio at some temperature. Above 300°C the ratio did not increase further, but actually began to show a faster rate of decline with increasing time

of oxidation. Our data suggest no sharp change in oxidation mechanism between 175 and 300°C.

The effect of temperature on the rate of oxidation of PSOC 704 coal is shown in Figs. 2.4 and 2.5. The absolute rate and the slope of the rate vs. time curve increased sharply with temperature. From an Arrhenius plot of initial CO_2 rate against the reciprocal of the temperature, Fig. 2.6, we estimated the activation energy as 68.2 MJ/kg mol (16.3 kcal/g mole). A similar plot of the initial CO rate gave an activation energy of 49.0 MJ/kg mol (11.7 kcal/gmole).

Measured CO_2 rates at 200°C for PSOC 704 particles of different size showed that particle size has no effect on the overall rate of CO_2 evolution. Rates of CO evolution for different-sized particles were also similar.

Figure 2.7 shows that blocking free OH groups by acetylation does not cause a decrease in the rate of oxidation; indeed, the reaction rate is marginally increased, probably because the pyridine solvent used extracted some organic material and possibly opened up the micropore structure. In addition, the CH_3 of the acetyl group may also have contributed to the slightly higher initial oxidation rate of the acetylated coal.

The rates of production of CO and CO_2 were not affected by prior washing of the coal with dilute HCl. Therefore, we conclude that the air oxidation of coal at 200°C is not catalyzed by acid-soluble cations.

The influence of oxygen partial pressure on the CO_2 evolution rate is shown in Figs. 2.8 and 2.9 and in Table 2.4. The apparent order of reaction was 2.1 initially, 1.5 at six hours and 1.6 at 12 hours. The error in these values was about ± 10%, and so we may say that the initial rate is bimolecular in oxygen. The change in reaction order with time indicated that the reactions occurring were complex and, perhaps, sequential.

2.4.2 Heating of Oxidized Coal in a Stream of Pure Nitrogen

Figures 2.11 and 2.12 show rates of evolution of CO_2 as a function of time, for samples of PSOC 704 coal heated in a stream of pure nitrogen following oxidation in air.

Results of the set "A" experiments are shown in Fig. 2.11. We note that the thermal CO_2 rate decayed much faster than did the oxidation rate at the same temperature. Evidently, the thermal reaction involved the rapid decomposition of oxygenated species which, in the absence of oxygen, were not replenished. From the initial rates of the thermal reaction at 210, 230 and 250°C, we estimated that the activation energy of the thermal reaction was about 63 MJ/kg mol (15 kcal/g mol), roughly equal to the activation energy of the oxidation reaction. The CO scale of our infrared analyzer was unfortunately not sensitive enough to give us reliable readings of CO concentration in the nitrogen stream; nevertheless, the few readings we obtained suggested that the CO_2/CO ratio for the thermal reaction was approximately equal to that of the oxidation reaction at the same temperature.

Figure 2.12 shows the sudden decline in CO_2/CO rate when nitrogen was substituted for air, at 200°C and 250°. We estimated the initial rates of the thermal reaction by extrapolation. The rates are summarized in Table 2.5 .

Samples of oxidized coal and heated coal were analyzed for total acidity and carboxylic acidity. The results are shown in Table 2.6. Clearly, the thermal reaction was not fast enough to cause significant depletion of the carboxylic-acid groups in coal. That conclusion is consistent with the observed low rates of evolution of carbon oxide gases in the thermal experiments. At 200°C, the thermal CO_2 rate is about 4×10^{-9} kg mol/kg coal-sec so that, in eight hours, about 1.15×10^{-4} kg mol/kg coal of CO_2 is produced. Assuming that an equal

amount of CO is evolved, we see that if the carbon oxide gases were derived from carboxylic groups the carboxylic acidity would be reduced by 0.23 g mol/kg coal in eight hours. The fact that the carboxylic acidity of the coal is unchanged after heating suggests that the carbon oxides were derived from some oxygenated intermediates other than carboxylic acid groups. On the other hand, there is a notable decrease in the phenolic content of the coal, which strongly suggests that, on heating, the phenolic groups undergo condensation and form ether groups.

The observation that the concentration of carboxylic-acid groups is not affected greatly by heating, whereas the thermal CO_2 rate decays rapidly, implies that those acid groups are not the proximate source of the carbon oxide gases. Those gases must be produced from some other oxygenated intermediates whose concentration falls off rapidly when not replenished by the reaction of coal and oxygen.

Table 2.1

Relative Rates of Production of CO_2 and CO

in Packed-Bed Oxidation Experiments of Kam *et. al.* , Ref. [8]

Temperature (^{0}C)	CO/CO_2 ratio
200	1.57
225	1.06
250	1.38
277	1.51

Table 2.2

Composition of Reactor Exit Gas in

Fluidized-Bed Oxidation Experiments of Toynbee and Fleming, Ref. [13]

Gas	Percentage of Gas in Exit Stream	
	After 27 Minutes of Oxidation	After 6.5 Hours of Oxidation
CO_2	8.7	3.4
CO	2.5	1.8
O_2	7.6	17.6
CO_2/CO Ratio	3.5	1.9

Table 2.3

Data on Coals Used in Oxidation Experiments

	Penn State Coal Bank Number		
	PSOC 704	PSOC 615	PSOC 247
Origin	West Virginia	Pennsylvania	North Dakota
Coal Province	Eastern	Eastern	N. Great Plains
Coal Region	Appalachian	Applachian	Fort Union
Rank	High Volatile A Bituminous	Low Volatile Bituminous	Lignite A
Proximate Analysis (% , moisture-free)			
Ash	8.24	15.73	11.29
Volatile Matter	40.55	19.25	41.00
Fixed Carbon	51.21	65.02	47.73
Elemental Analysis (% , moisture-free)			
C	75.29	72.17	65.88
H	5.18	3.97	4.22
N	1.02	1.14	1.32
Organic S	1.71	0.78	0.44
O (diff.)	6.71	4.02	15.36
Min. Matter	10.09	17.92	12.77
Total S	3.37	1.08	0.47

Note: Data and Coals were provided by the Penn State Coal Bank.

Table 2.4

Effect of Oxygen Partial Pressure on Rate of CO_2 Evolution for 60-80 Mesh PSOC 704 Coal Oxidized at 200 ^{0} C

Total Pressure (kPa.)	Oxygen Partial Pressure (kPa.)	CO_2 Rate (kg mol/kg coal-s)× 10^7		
		Initial Rate	Rate at τ = 6.0 hr	Rate at τ = 12.0 hr
125.5	26.3	5.2	4.0	3.8
180.6	37.8	12.3	7.2	6.3
204.7	42.9	16.7	8.7	7.3
273.7	57.3	25.7	13.0	12.3
Apparent Order of Reaction (± 10 %)		2.1	1.5	1.6

Table 2.5

Rates of Evolution of CO_2 from PSOC 704 Coal

Temperature (^{0} C)	200	250
CO_2 Rates (kg mol/kg coal-s)		
- R_1, Oxidation Rate at τ= 6 hr	4.00×10^{-8}	1.06×10^{-7}
- R_2, Initial Heating Rate, at τ = 6 hr 4 min	1.58×10^{-8}	2.75×10^{-8}
- R_3, Heating Rate at τ = 6 hr 30 min	7.4×10^{-9}	1.23×10^{-8}
Ratio R_2 / R_1	0.396	0.260
Ratio R_3 / R_1	0.185	0.116

Table 2.6

Acidity of PSOC 704 Coal Samples Oxidized in Air and Heated in a Stream of Pure Nitrogen

Oxidation		Heating in N_2		Acidity (g eq./kg coal)		
Temp (^{0} C)	Time (hr)	Temp (^{0} C)	Time (hr)	Total	Carboxylic	Phenolic
200	12	-	-	5.27	2.12	3.15
	12	200	8	4.11	2.15	1.96
250	12	-	-	7.72	3.73	3.99
	12	250	6	5.69	4.05	1.65
	12	250	12	5.23	3.99	1.24

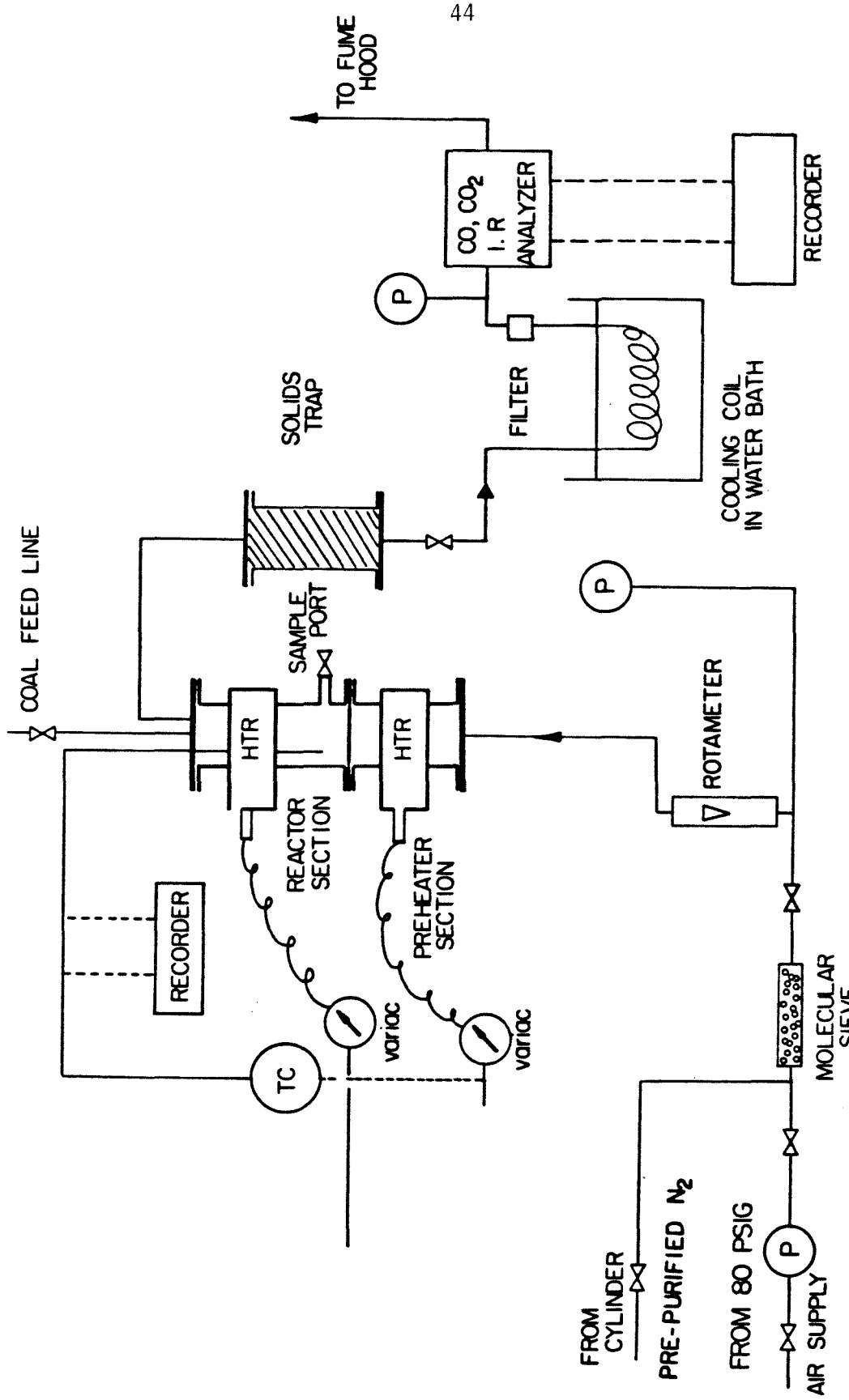

FIGURE 2.1: Fluidized-Bed Oxidation Apparatus

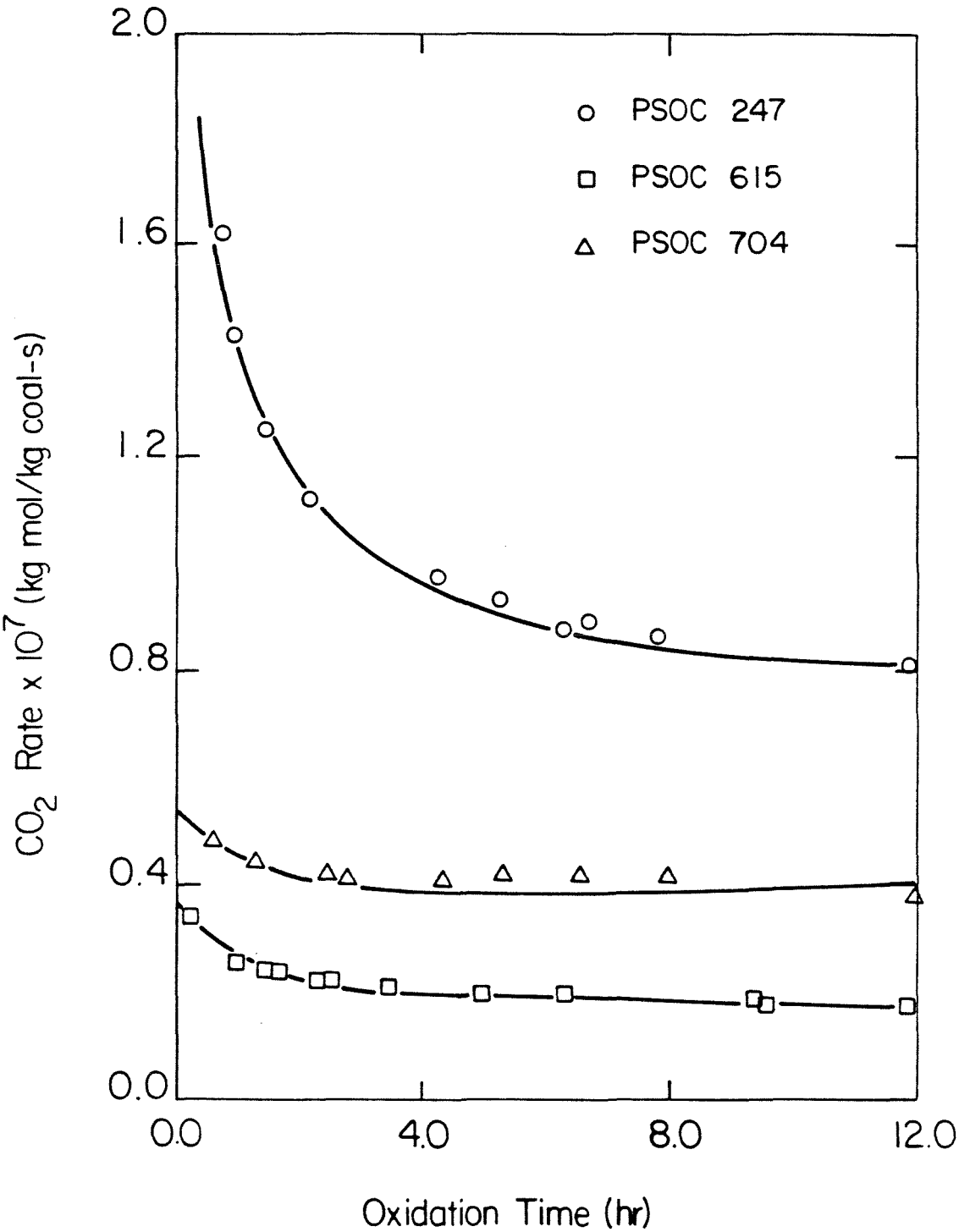

FIGURE 2.2: CO_2 Rate vs. Time for Different Coals Oxidized in Air at 200°C and 126 kPa Total Pressure

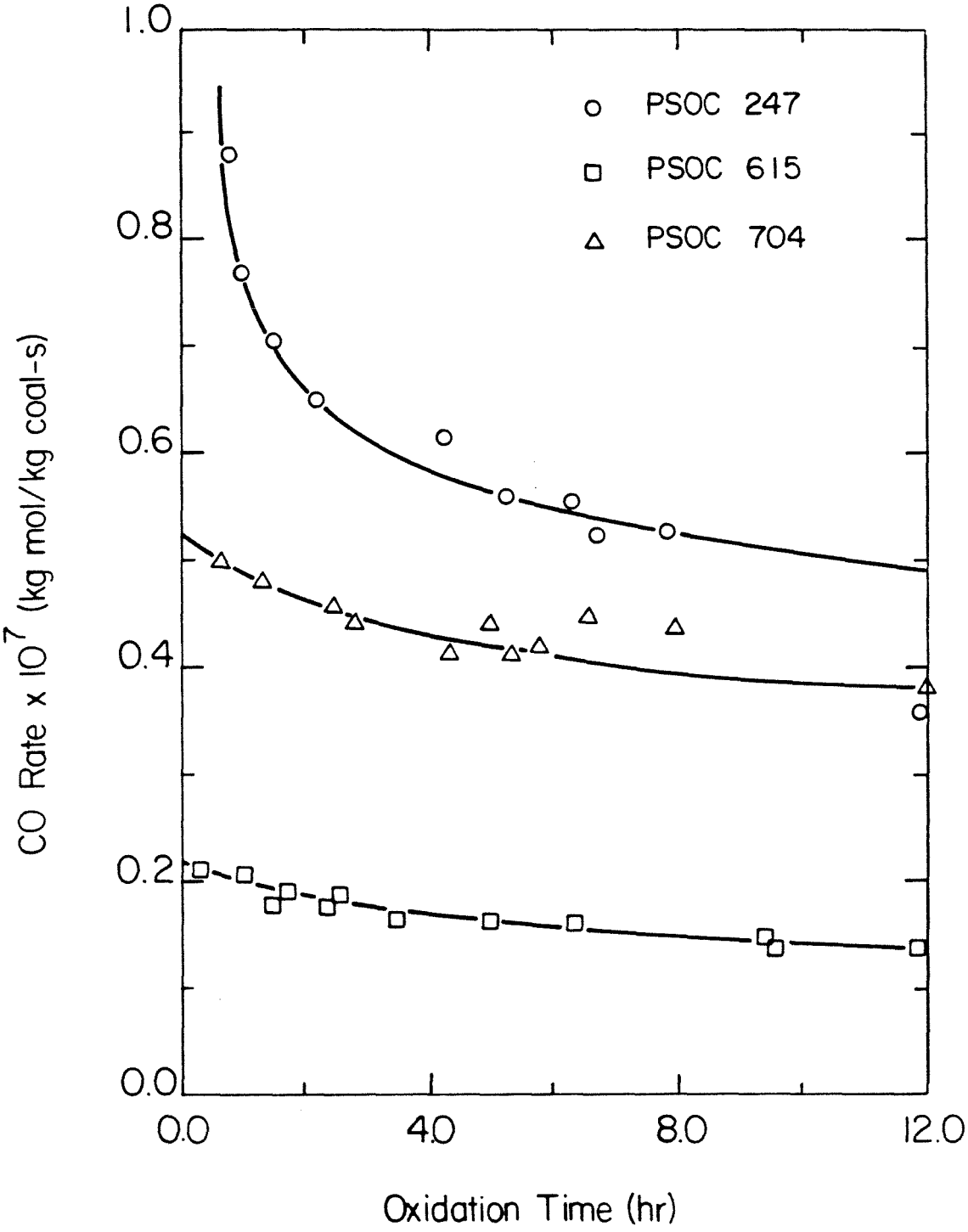

FIGURE 2.3: CO Rate vs. Time for Different Coals Oxidized in Air at 200°C and 126 kPa Total Pressure

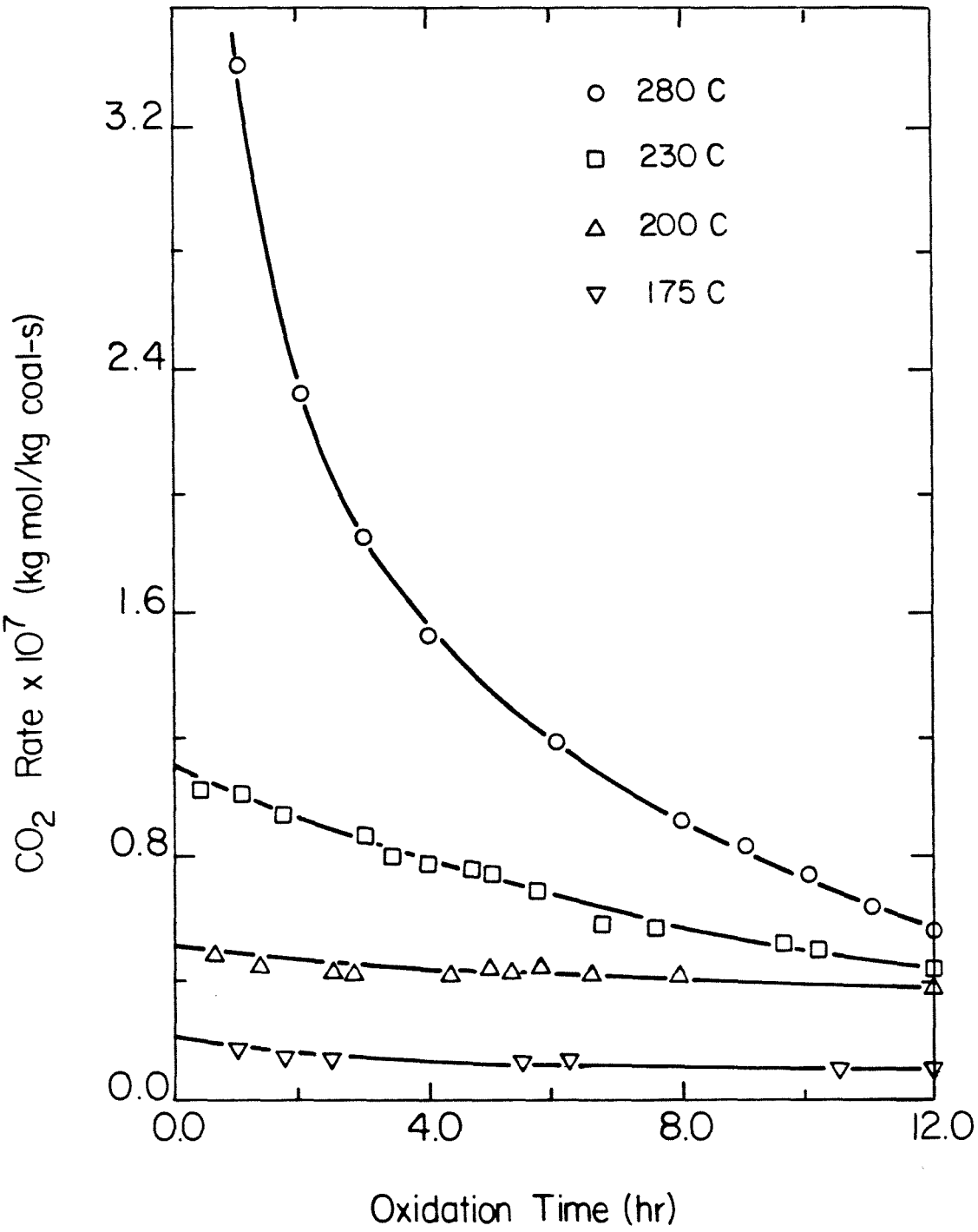

FIGURE 2.4: CO_2 Rate vs. Time for PSOC 704 Coal Oxidized in Air at Different Temperatures, at 126 kPa Total Pressure

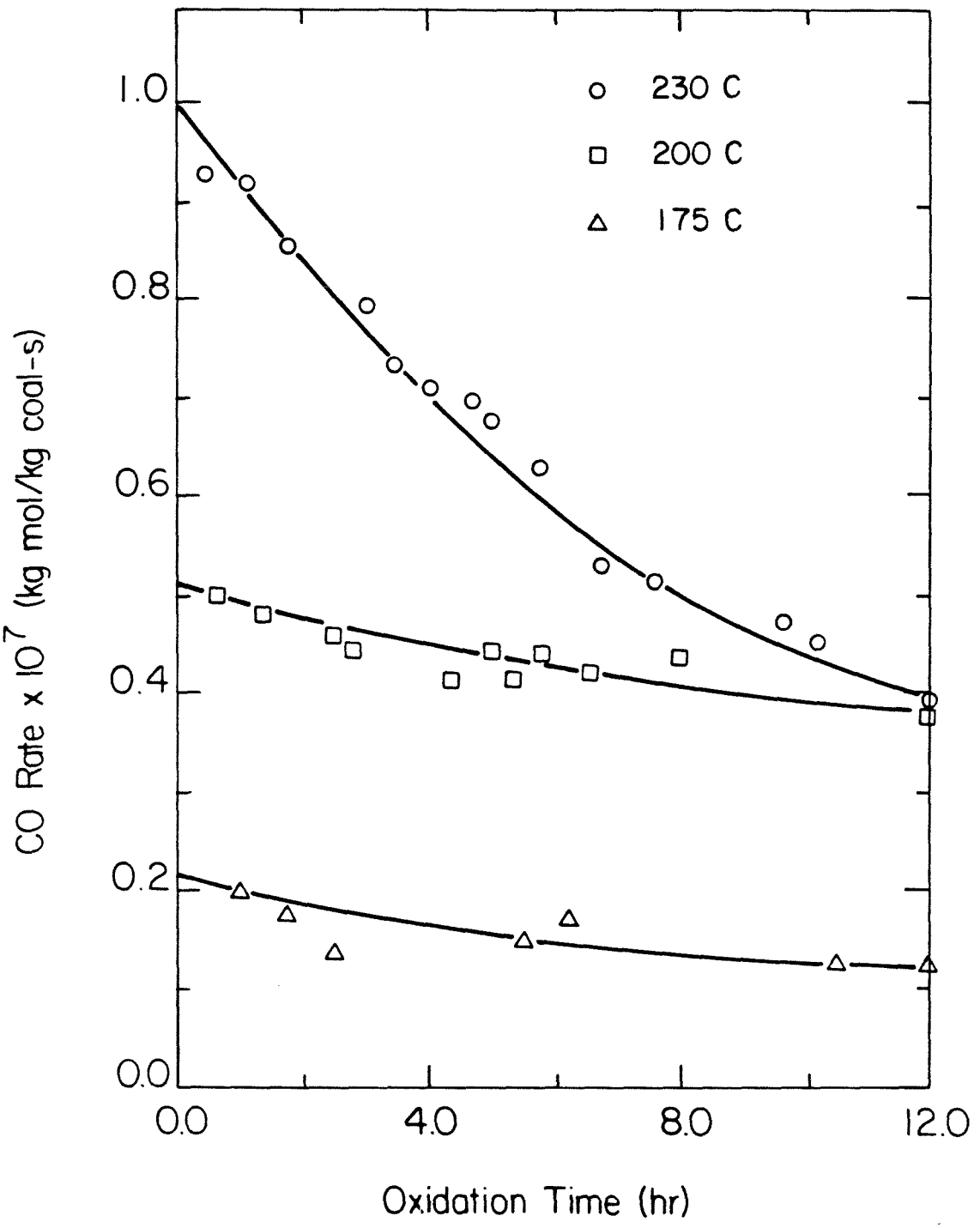

FIGURE 2.5: CO Rate vs. Time for PSOC 704 Coal Oxidized in Air at Different Temperatures, at 126 kPa Total Pressure

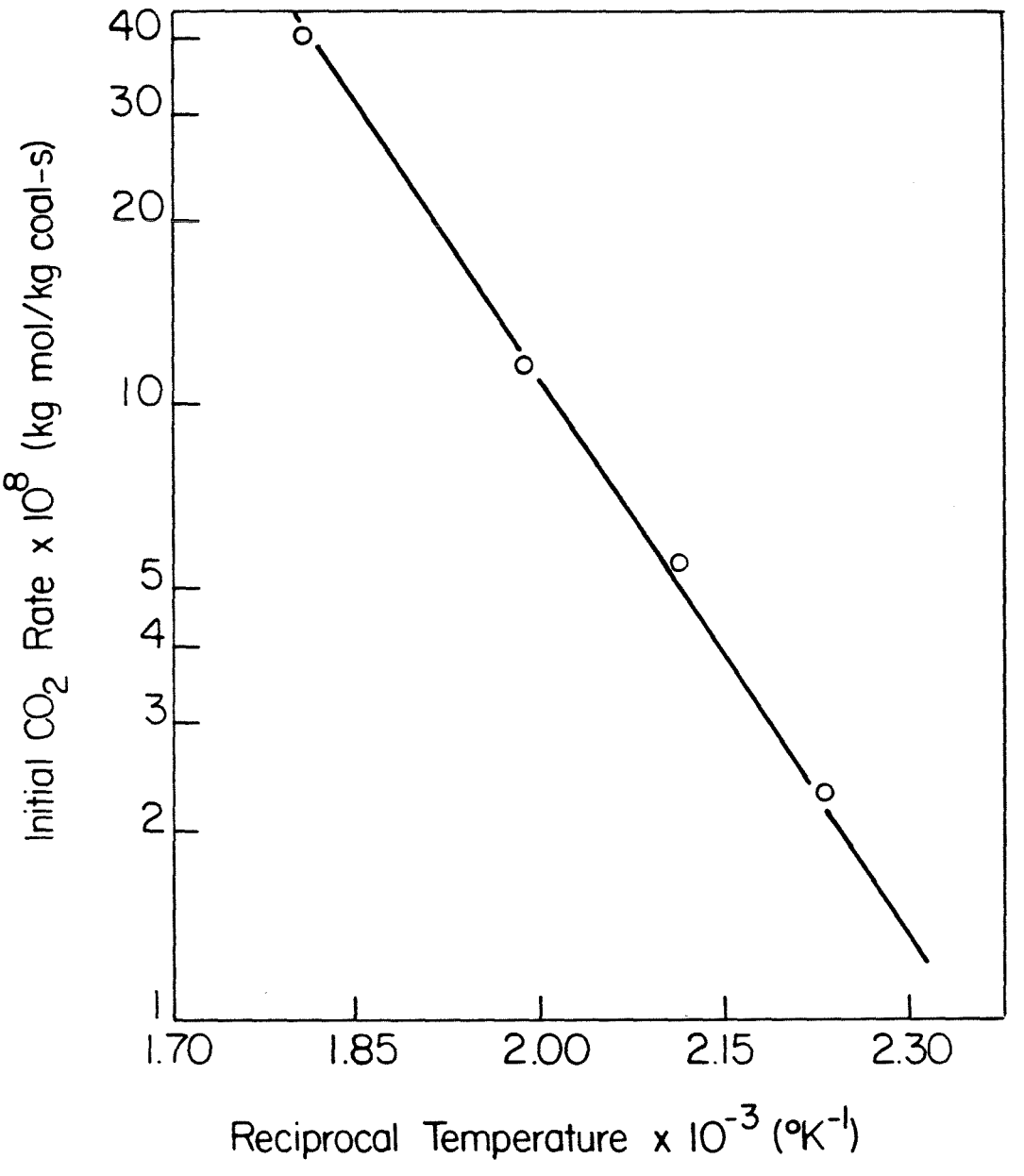

FIGURE 2.6: Arrhenius Plot for CO_2 Rate for PSOC 704 Coal Oxidized in Air at 126 kPa Total Pressure

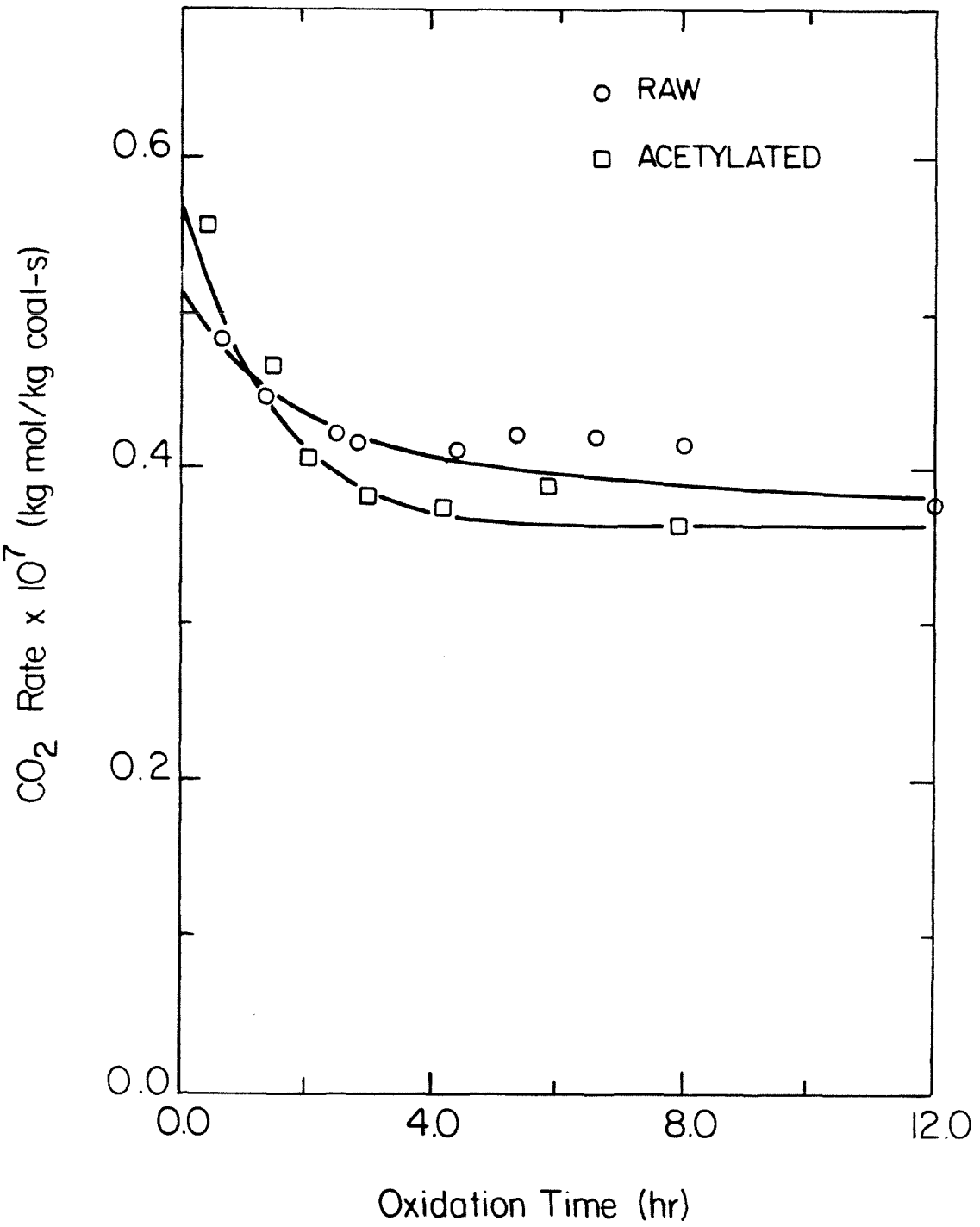

FIGURE 2.7: CO_2 Rate vs. Time for Raw and Acetylated PSOC 704 Coals Oxidized in Air at 200°C and 126 kPa Total Pressure

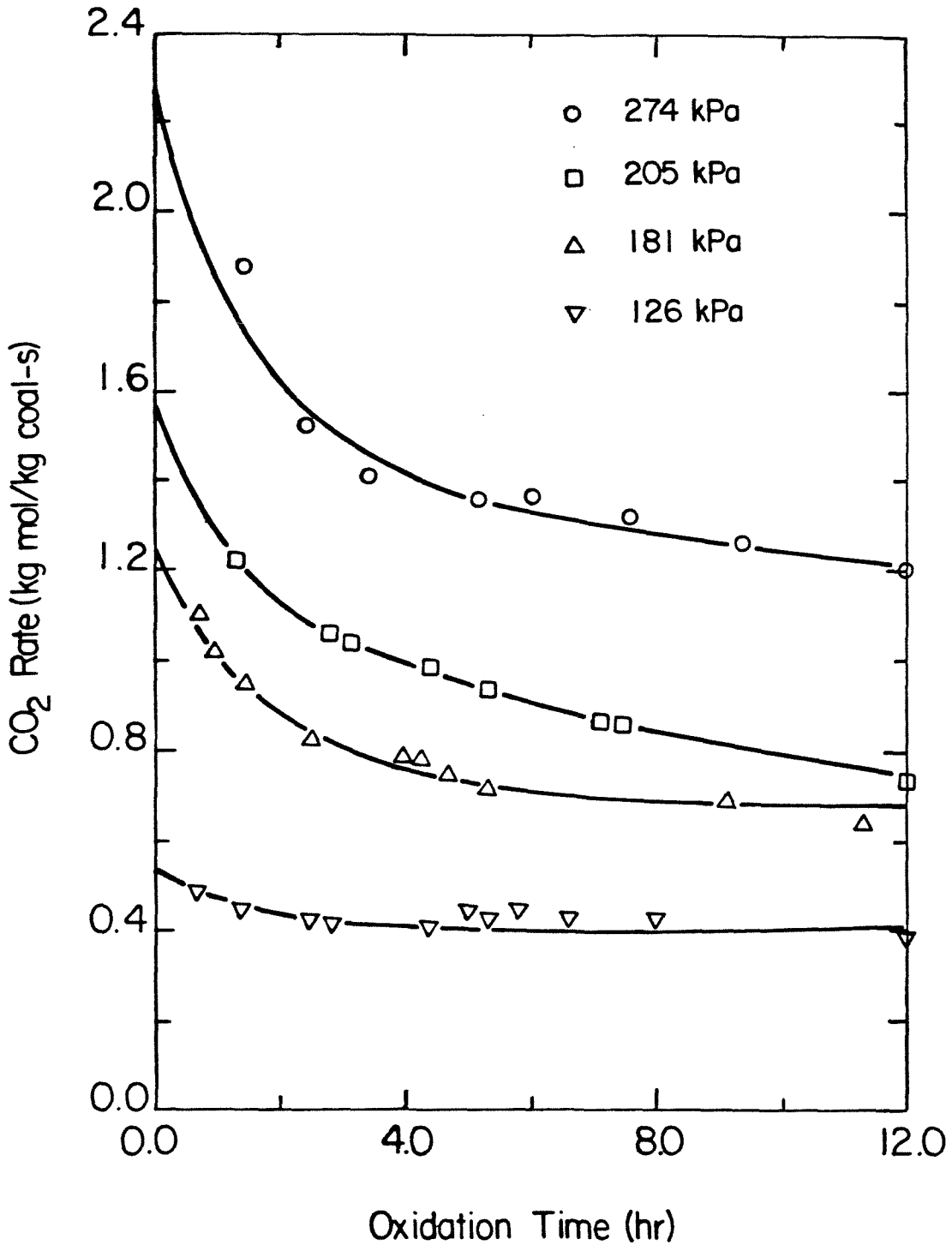

FIGURE 2.8: CO_2 Rate vs. Time for PSOC 704 Coal Oxidized in Air at 200°C at Different Total Pressures

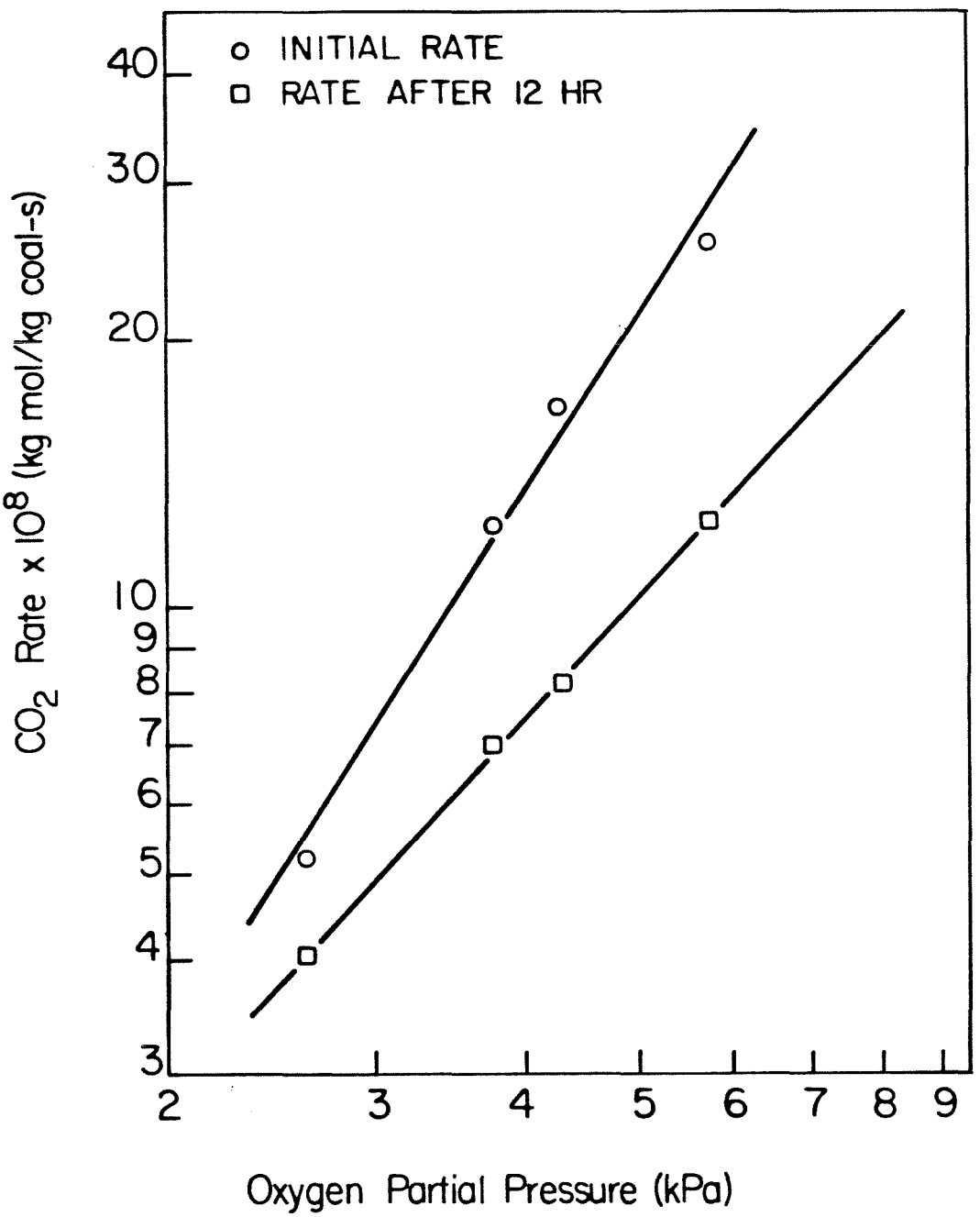

FIGURE 2.9: CO_2 Rate vs. Oxygen Partial Pressure for PSOC 704 Oxidized in Air at 200°C.

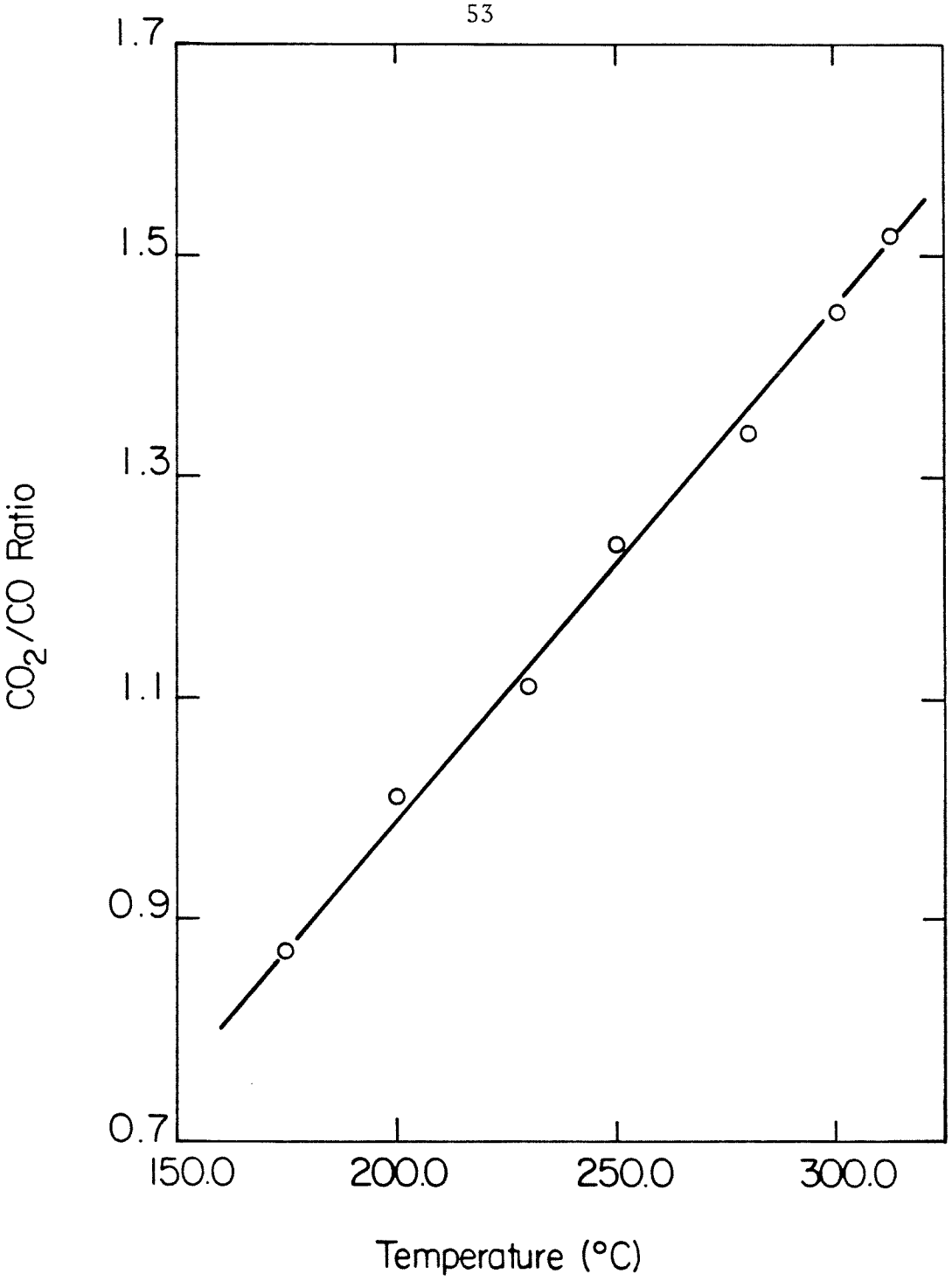

FIGURE 2.10: CO_2/CO Ratio vs. Temperature, for PSOC 704 Coal Oxidized in Air at 126 kPa Total Pressure

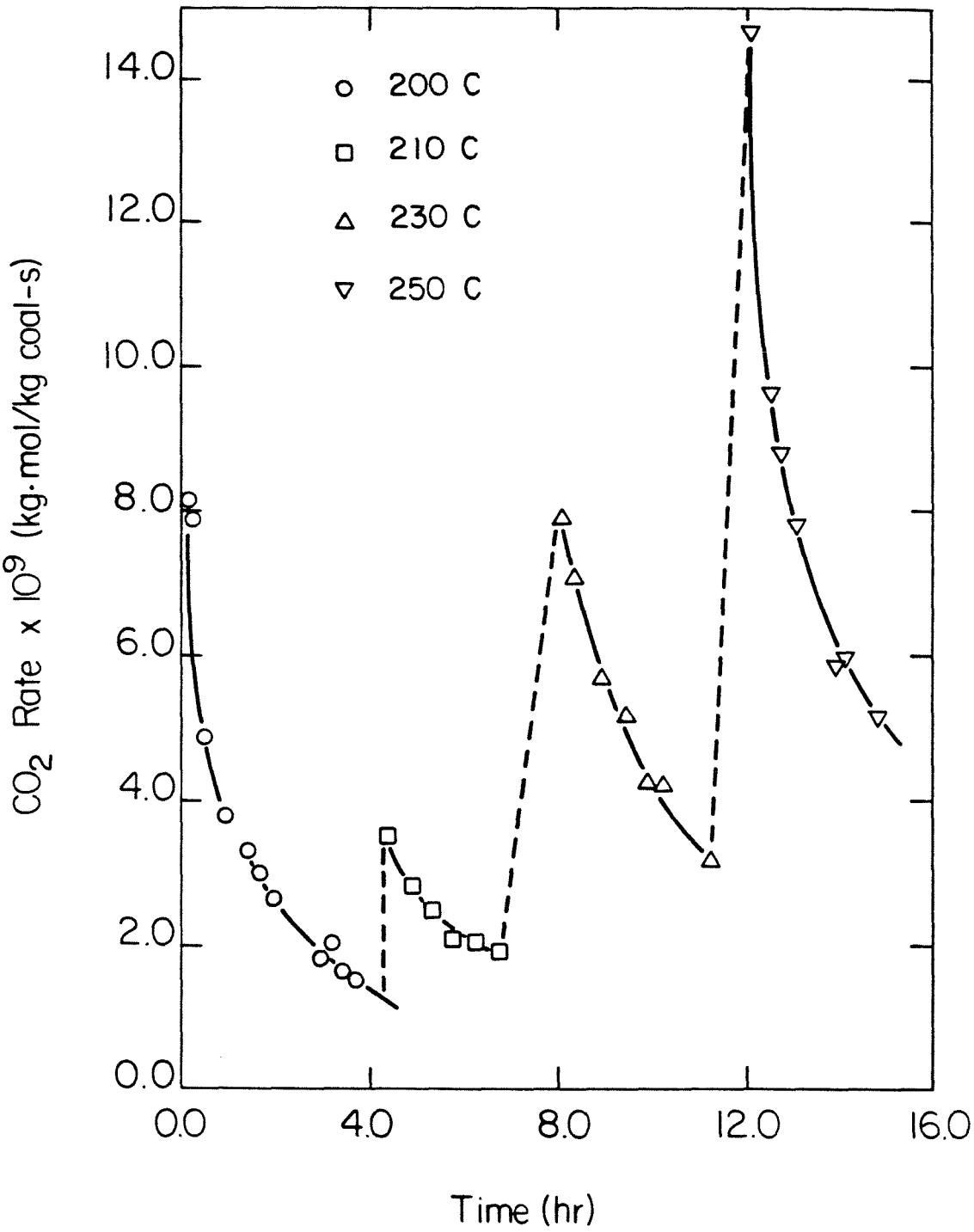

FIGURE 2.11: CO_2 Rate vs. Time for Oxidized PSOC 704 Coal Heated in Pure Nitrogen at Different Temperatures

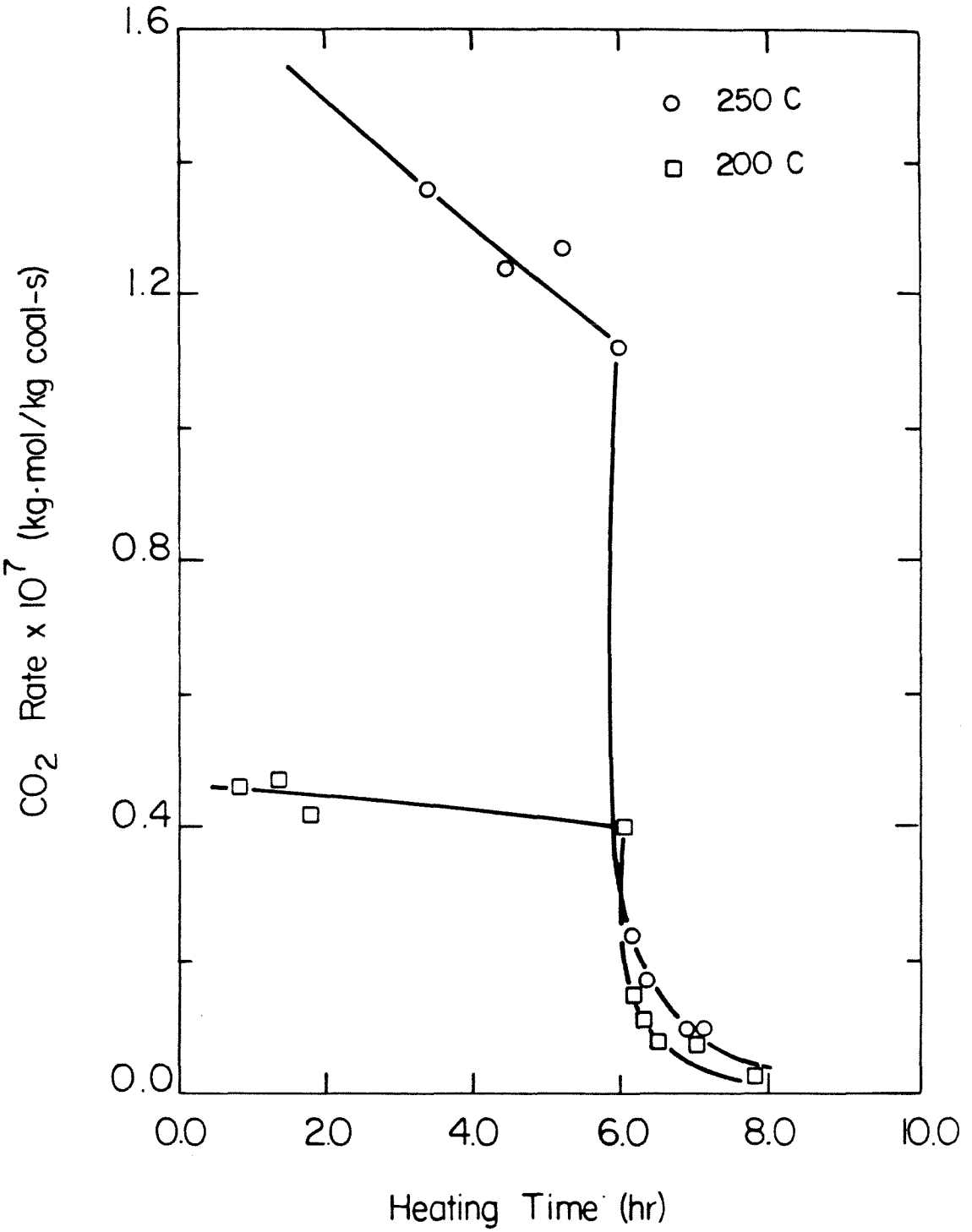

FIGURE 2.12: CO_2 Rate vs. Time for PSOC 704 Coal at 126 kPa Total Pressure. Fluidizing Gas Changed from Air to Nitrogen after 6 Hours

References

[1] Frey, Ol. u, Kohle **39**, 603, 1943.

[2] Schmidt, L. D. and Elder, J. L., Ind. Eng. Chem. **32**, 249, 1940.

[3] Wood, T. J., Appl. Chem. **8**, 565, 1958.

[4] Carpenter, D. L. and Giddings, D. G., Fuel **43**, 375, 1964.

[5] Taylor, H. A. and Thon, N., J. Am. Chem. Soc. **74**, 4169, 1952.

[6] Harris, J. A. and Evans, D. G., Fuel **54**, 277, 1975.

[7] Kam, A. Y., Hixson, A. N. and Perlmutter, D. D., Chem. Eng. Sci. **31**, 815, 1976.

[8] Kam, A. Y., Hixson, A. N. and Perlmutter, D. D., Chem. Eng. Sci. **31**, 821, 1976.

[9] Avison, N. L., Winters, R. M. and Perlmutter, D. D., AIChE J. **25**, 773, 1979.

[10] Davidson, J. F. and Harrison, D. (eds.), Fluidization, Academic Press, New York , 1971.

[11] Hanratty, T. J., Latinen, G. and Wilhelm, R. H., AIChE J. **2**, 372 , 1956.

[12] Pozzi, A. L. and Rase, H. F., Ind. Eng. Chem. **53**, 813, 1961.

[13] Toynbee, P. A. and Fleming, A. K., Fuel **42**, 379, 1963.

[14] Weekman, V. W., AIChE J. **20**, 833, 1974.

3. CHEMICAL AND PHYSICAL ANALYSIS OF COAL

The methods currently available for chemical characterization of coal are all subject to varying degrees of uncertainty, mainly because coal is an essentially non-homogeneous material. First, representative samples are sometimes difficult to obtain. Even when the ASTM procedure D 3172-73 is used, a representative sample may not be obtained if the coal particles are chemically non-uniform. An example of this problem is seen in the analysis of coal for iron content, where some particles may have chips of iron pyrite attached to them while others are essentially iron-free. A second common problem with coal analysis, especially where liquid reagents are used, as in functional-group analysis, is that often sites of reactive functional groups in the coal are physically inaccessible to the reagent molecules, due to mass-transfer limitation or steric hindrance. In some cases mass-transfer limitations can be reduced, and chemical reaction speeded up, by using small particles of coal and performing the reaction at elevated temperatures for long periods of time, on the order of days rather than hours. Solvents such as methanol and pyridine may also be used to swell the coal and open up the transitional pores in the the coal, allowing reagent to diffuse further into the coal. Most of the pore surface area in coal, however, is accounted for by the smallest pores, the micropores, which are impenetrable to all but the smallest molecules. Where analytical precision is essential, the experimentalist must resort to using coal-derived liquids, which can be reacted with chemical reagents without mass-transfer limitations. Unfortunately, the process of liquefaction alters some of the chemical characteristics of the coal. Heteroatoms such as oxygen and sulfur are lost while carbon and hydrogen escape as methane or ethane. Therefore results based on the analysis of coal-derived liquids are not always directly applicable to coal.

In this chapter we describe the analytical procedures which we used to characterize coal, and also give some estimate of the reproducibility of the data. Of course, reproducibility alone does not guarantee accuracy. In discussing the results we will also indicate, where applicable, the possible effects of diffusional and other limitations on the accuracy of the data. As long as we appreciate the limitations of the data, useful information about coal can be obtained from chemical analysis.

3.1 Analytical Procedures

3.1.1 Heating Values

Heating values were measured according to ASTM Method D 240-64, using the 1341 oxygen bomb calorimeter manufactured by the Parr Instrument Company. The method measures the higher heating value (HHV) . By taking all the neccesary precautions and carefully following the standard procedure we obtained results which were reproducible to within 233 kJ/kg (100 Btu/lb) , or about ± 1 % . The most critical experimental detail was ensuring that no coal was blown out of the combustion crucible while filling the bomb with pure oxygen under pressure, prior to combustion.

3.1.2 Ash Content

Ash content was determined according to ASTM method D 3174-73. A 1 g sample of coal of known moisture content was weighed into a crucible and placed in a cold muffle furnace. The furnace was slowly heated to 750 ^{0} C over a period of 2 hours and maintained at that temperature for four hours. The furnace was

switched off and allowed to cool down to room temperature, and the remaining ash was weighed. The sample was again heated, cooled and re-weighed until the final weight was constant.

3.1.3 Volatile Matter Content

Volatile matter content was determined in accordance with ASTM method D 3175-77. About 1 g of the sample was weighed into a nickel crucible of known weight. The crucible was covered with a lid and placed into a muffle furnace at 950 ^{0} C. After heating for exactly 7 minutes the crucible was removed from the furnace and allowed to cool, then weighed. The crucible was then weighed empty to find the net weight of the final coal residue. The volatile matter content of the coal was given by the percentage loss in weight minus the moisture content of the original coal sample.

3.1.4 Elemental Analysis

3.1.4.1 Carbon, Hydrogen, and Nitrogen

Analyses were performed at the Caltech Microanalytical Laboratory and also at Galbraith Laboratories Inc. in Tennessee. Analyses of PSOC 704 coal samples by the two laboratories gave slightly different results. The relative percentage differences between the two sets of values was about ± 0.5 % for carbon, about ± 7 % for hydrogen, and about ± 10 % for nitrogen. Those figures give a true indication of the degree of error associated with each elemental analysis.

The following procedure was used for C, H, and N at the Caltech Microanalytical Laboratories. 1-2 milligram samples of coal were combusted in a stream of pure oxygen and the products analyzed for percent carbon,

hydrogen, and nitrogen using a Perkin-Elmer model 240 A analyzer. A combustion aid, consisting of a mixture of vanadium pentoxide and tungsten trioxide, was used to ensure complete combustion of samples. Carbon and hydrogen contents were determined from the amount of carbon dioxide and water absorbed from the combustion gases. Nitrogen content was measured by a modified Dumas method, by which oxides of nitrogen were converted to nitrogen gas, whose concentration in the product stream was then measured by a thermal conductivity detector.

Because of the small size of the samples used in microanalysis, several determinations were usually required in order to obtain reproducible results.

3.1.4.2 Sulfur and Forms of Sulfur

The total sulfur content of coal was measured using a Leco furnace, in accordance with the high-temperature combustion method described in ASTM Method D 3177-75. A 0.5 g sample was placed into a boat made of refractory material and burned in a tube furnace at 1350 ^{0} C, in a stream of oxygen. The sulfur oxides produced by combustion were absorbed into a solution of hydrogen peroxide, producing sulfuric acid. After 15 minutes of combustion the flow of oxygen was stopped, and the furnace was purged for about 10 minutes using a stream of helium. The amount of acid produced was then determined by titration against a sodium hydroxide solution.

With coals that contain measurable amounts of chlorine, HCl is produced upon combustion and contributes to the acidity of the effluent gases. The ASTM procedure describes how to make the proper correction for chlorine. The coal we used, however, contained less than 0.01 % Cl and therefore no correction was neccesary.

There are three main forms of sulfur in coal - sulfates, pyritic sulfur, and organic sulfur. The ASTM Method D 2492-68, which we used, defines organic sulfur as the difference between total sulfur and the sum of sulfate and pyritic sulfur. Organic sulfur content is subject to the accumulated errors in the determination of the other forms of sulfur and therefore can be relatively inaccurate. The ASTM procedure, however was accurate enough for our purposes.

3.1.5 Total Acidity

The total acidity of a given coal is the total concentration of phenolic and carboxylic acid groups.

Total acidity was measured using a procedure based on barium cation exchange at 12.5, by a slight modification of the baryta method, first described by Syskov and Kukharenko [1], and later elaborated by Schafer [2,3]. This procedure requires that the coal sample first be washed in dilute acid, to remove any cations which may be associated with the acid groups in the coal and replace them with protons. The measured values of total and carboxylic acidity for acid-washed coal samples are usually higher than the values obtained without acid washing. The difference is greatest for lignites and oxidized bituminous coals. For example, Ruberto and Cronauer [4] reported that the measured carboxylic acidity of a particular lignite increased from 0.9 to 3.1 m.eq/g coal after acid washing.

Our procedure for acid washing was based on a slight modification of a procedure suggested by Blom *et al.* [5]. About 1 g of -60 mesh coal was added to 50 ml of 1N HCl in a beaker and then boiled for 3 hours on a heating plate. Then the coal was filtered and washed repeatedly with distilled water until the pH of

the effluent, as measured by a standard pH meter, was neutral. The coal was then dried in a vacuum oven at 105 ^{0} C. The dry, acid-washed sample was used in the cation-exchange procedures for the determination of total acidity and carboxylic acidity.

Total acidity was determined as follows: About 0.3-0.4 g of the coal sample was accurately measured and placed into a 200 ml flask containing 25.0 ml of a 0.1 N solution of barium hydroxide. About 50 ml. of distilled water was added, and the flask was purged of air, using nitrogen gas, and then sealed so as to prevent the absorption of CO_2 from the atmosphere while the contents of the flask were magnetically stirred for 24 hours. The protons released by cation exchange reacted with the hydroxyl ions in solution, thus reducing the alkalinity of the solution. The pH of the solution, initially about 12.5, fell to a steady final value of 12.2 within one day. The coal sample was filtered and washed, and the filtrate and washings were collected and used to determine the amount of alkali remaining after barium exchange, by titration against hydrochloric acid. The acid released by the coal sample was equated to the alkali consumed. Barium hydroxide tends to react readily with the CO_2 in air; therefore we performed a blank run from which we were able to establish that, using our procedure, the amount of alkali lost because of reaction with atmospheric CO_2 was negligible. The results we obtained were reproducible to within ± 3 % for the bituminous coals and ± 10 % for the lignite.

3.1.6 Carboxylic Acid Groups

The concentration of carboxylic acid groups was estimated by cation exchange, using barium acetate at pH 8.3. Variations on this method have been used by a number of workers in the past. Our procedure was based on the guidelines laid

down by Schafer [2,3].

Depending on the pH of the solution, cation exchange can affect phenolic groups as well as carboxylic acid groups. The acid released by cation exchange lowers the alkalinity of the solution, and the change in alkalinity then gives a direct measure of the acidity of the coal sample. In determining carboxylic groups we used a 1N solution of barium acetate, which has a pH of 8.3. Schafer had concluded from his investigations that complete exchange of carboxylic acid groups at room temperature would be achieved at pH 8.2-8.4, without exchange of the phenolic groups.

The procedure we used was as follows: About 0.3-0.9 g of coal was weighed and added to a 200 ml flask containing 75.0 ml of 1N barium acetate solution. The flask was flushed with nitrogen gas for about five minutes, a magnetic-stirring bar was placed in the flask, and then the flask was sealed with self-adhesive film, to exclude any CO_2 from the atmosphere, and placed on a magnetic stirrer. After 24 hours, the pH of the solution was measured using glass and calomel electrodes and sufficient 0.02N $Ba(OH)_2$ solution was added by burette to restore the pH to 8.3. The flask was again flushed with N_2 gas, re-sealed, and replaced upon the magnetic stirrer. It was essential that the titration be performed in the presence of the coal so that we could ensure that complete ion exchange took place at the stated pH of 8.3. The rate of ion exchange was quite slow under those conditions. Therefore the routine was repeated every 6-8 hours, with addition of a 0.02 N $Ba(OH)_2$ solution in the presence of coal, until a steady pH of 8.3 was attained. Usually about eight such titrations were neccesary. The acid released by cation exchange was equivalent to the total amount of $Ba(OH)_2$ solution required to restore the pH to a steady value of 8.3. To account for losses caused by reaction with atmospheric CO_2 and for any other errors, a

blank determination was made.

The coal samples were washed in dil HCl prior to cation exchange. Our results were reproducible to within ± 3 %.

3.1.7 Phenolic Groups

3.1.7.1 Difference Method

The phenolic-group content of the bituminous coals was defined as the differen ce between the total acidity, measured at pH 12.5, and the carboxylic acidity, measured at pH 8.3.

As can be seen from Table 3.4, some of the values of phenolic content determined by this method, especially for the lignite PSOC 247, appeared to be too high by comparison with corresponding values of total hydroxyl content, as determined by acetylation.

3.1.7.2 Direct Method

We investigated a method based on the direct reaction of coal with 2,4 dinitro flouro benzene (DNFB), according to the equation:

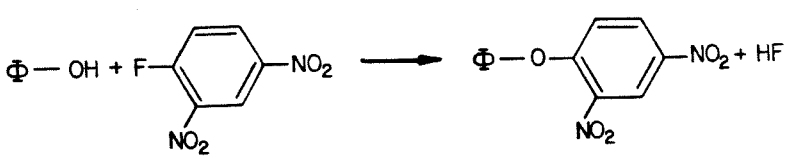

Zahn and Wurtz [6] had described the use of this reagent with model phenolic compounds in dimethyl formamide at room temperature, and the subsequent quantitative precipitation of the corresponding ethers. They had selected dimethyl formamide as the solvent because of its chemical inertness to DNFB. They had noted that thiols and amines would also react under similar conditions, and that even alcohols could react, however slowly. Fortunately for our work, thiols and amines are found in relatively low concentrations in coals. In our work with coal, we also required that the solvent be effective in penetrating coal. Two solvents we investigated were pyridine and methanol. When DNFB was dissolved into pyridine we found, as we had suspected, that chemical reaction occurred forming a clear reddish-brown solution which gradually darkened and became viscous until, after three days, it formed a sticky mess. Methanol, on the other hand, formed a clear, light yellow solution which showed no signs of any chemical reaction even when left standing for several months.

The following experimental procedure was used :

Into a 200-ml flask we added 2 g of DNFB and one gram of the coal sample together with 20 ml of methanol and 5 ml of 0.3 N sodium bicarbonate solution. We attached a reflux condenser to the flask and placed it on a hot plate at 80 ^{0} C for 24 hours. Then the flask was cooled, 100ml of water was added, and the coal was filtered and washed repeatedly with water, then soaked in methanol and again filtered and washed repeatedly in water, with boiling, in order to remove any residual unreacted DNFB. The washing was stopped when the color of the wash water changed from a clear yellow, formed by the DNFB in water, to colorless. The coal sample was then dried in a vacuum oven. Both the initial coal and the reacted coal were analyzed for nitrogen content. Two gram-atoms of nitrogen were incorporated for every gram-equivalent of phenol which

reacted. Therefore the indicated phenolic content was given by :

$$\text{Phenolic Content} = \frac{(N_f - N_i)}{14} \times \frac{1}{2} \text{ m.eq /gcoal}$$

where N_f and N_i are initial and final nitrogen content, respectively, expressed as kilograms of nitrogen per kilogram of coal.

3.1.7.3 Other Methods

The established methods for the quantitative determination of carboxylic and phenolic groups, which we did not use, were methylation and non-aqueous titration against sodium aminoethoxide.

Methylation may be achieved using dimethyl sulfate [7], diazomethane [5], or tetrabutyl ammonium hydroxide followed by methyl iodide [8,9]. and has been used in determining total acidities for some bituminous and sub-bituminous coals [9,10]. No results, however, have been reported for lignites. Methylation involves conversion of the acidic groups to methyl esters and ethers, respectively, followed by quantitative determination of the methanol released by alkali hydrolysis of the dried, methylated coal. According to the authors of ref [1], results obtained by the baryta method were similar to those found by methylation with dimethyl sulfate.

The determination of total acidity by non-aqueous potentiometric titration was described by Brooks and Maher [11]. In that method the coal sample is magnetically stirred in anhydrous ethylenediamine, until the potential difference between two antimony electrodes immersed in the reaction mixture reaches a steady value, and then potentiometrically titrated against a a 0.2 N solution of sodium aminoethoxide. The total and carboxylic acidities are calculated from the added volumes corresponding to the two points of inflection

in the curve. When Maher and Schafer [12] compared results of total and carboxylic acidities for 5 lignites, as measured by barium exchange and by non-aqueous titration [2,11], they found that the barium exchange method gave higher total acidities for two of the coals.

Both of the above methods are tedious to perform; and given that they had been tried before and not been shown to give more correct results than those given by cation exchange, we decided to investigate the use of a direct method for estimating phenolic groups, using DNFB, as described above.

3.1.8 Hydroxyl Groups

The hydroxyl-group content of coal samples was determined using the acetylation method, in which acetic anhydride is used to form acetyl esters of the aliphatic and phenolic OH groups. Later, the reacted coal is washed and filtered and then hydrolyzed with alkali, and the acetic acid released determined by steam distillation and titration. Acetic anhydride also reacts with primary and secondary amines and with thiols. The amino-group content of coal is generally very low, however, and the acetyl derivatives of amino groups are fairly stable to alkali hydrolysis. A number of authors had indicated a high degree of confidence in the acetylation method for OH groups. Blom *et al.* [5] considered it to be the definitive method. Painter and his co-workers [13] confirmed the completeness of the acetylation reaction by FTIR spectroscopy. Our results were obtained using the procedure recommended by Blom *et al.* [5], which we now describe.

About 500-800 mg of coal was carefully weighed into a 200 ml conical flask containing about 10 ml of a 2:1 mixture of pyridine and acetic acid. The pyridine was selected as a good solvent for coal. A condenser was attached, and

the contents of the flask were heated for 24 hours on a hot plate at 90 ^{0} C. Subsequently, the flask was cooled and about 100 ml of water was added to it. The hydroxyl groups were acetylated as shown in reaction (1) below :

$$2\ R{-}OH + (CH_3CO)_2O \quad = \quad 2\ R{-}O{-}CO_2CH_3 + H_2O \qquad (1)$$

The acetylated coal was filtered and washed thoroughly with distilled water, until the washings were completely free of acid, and then dried in a vacuum oven at 105 ^{0} C . Then the coal was transferred to a 250 ml flask containing 2 g of barium hydroxide dissolved in 100 ml of water. After boiling for about 5 hours, the flask and contents were left overnight on the steam plate, at low heat. The effect of the barium hydroxide was to hydrolyze the coal, releasing acetate ions as in equation (2) below :

$$2\ \Phi{-}O{-}CO_2CH_3 + Ba(OH)_2 \quad = \quad 2\ \Phi{-}OH + Ba(CH_3CO)_2 \qquad (2)$$

Next we added 3 ml of phosphoric acid, filtered the coal, and collected the filtrate and washings, now containing acetic acid (See eqn (3) below). The amount of acetic acid was determined by distillation.

$$3\ Ba(CH_3CO)_2 + 2\ H_3PO_4 \quad = \quad 6\ CH_3CO_2H + Ba_3(PO_4)_2 \qquad (3)$$

We then transferred the liquid into a 250 ml round-bottomed flask and distilled off 100 ml fractions, repeatedly adding water to the flask, and titrating the distillate fractions against sodium hydroxide. Distillation was ended when the titre fell to a constant value, t_0. The total amount of acetic acid, A was given by

$$A = \sum_{j=1}^{N} (t_j - t_0)\ \frac{N}{m}\ \text{g.eq/g.coal}$$

where N is normality of the alkali solution and m is mass of coal used, on moisture-free basis

As equations (1), (2), and (3) imply, the amount of hydroxyl group in the original coal is also given by A. Our results were reproducible to within ± 6 % .

A comparison between our reported values for the total OH contents of raw and oxidized coal samples and the corresponding values of phenolic hydroxyl content suggested that the reported values of the total OH content might be too low . We therefore decided to investigate the possibility that a significant portion of the coal might have been extracted by the pyridine used as solvent in the acetylation reaction, and subsequently lost during filtration and washing. We investigated the extraction of coal by pyridine under the conditions used in the Blom method. We weighed samples of the dry coal before and after the acetylation reaction. Our data showed that there was no significant extraction of coal.

3.1.9 Ether Groups

Ether groups are believed to account for up to one third of all the organic oxygen present in unoxidized bituminous coals. Unfortunately no accurate chemical or spectroscopic methods have yet been established for the direct, quantitative determination of the total ether-group content of coals. Infra-red spectroscopy cannot provide useful quantitative information because ethers absorb in a region of the spectrum where there is considerable overlap with absorptions due to a number of other functional groups as well as mineral matter. Chemical methods are limited because some ether groups are very unreactive. Although alkyl-aryl ethers and alkyl-alkyl ethers are cleaved by hydriodic acid, aryl-aryl ethers are relatively inert [14]. Aryl-aryl ethers have been identified in liquid extracts from bituminous vitrinite, in the form of chemical species such as benzofuran, benzonaphthofuran, xanthone, and

dibenzo-p-dioxin [15]. The oxygen contained in aryl-aryl ethers is sometimes called "unreactive oxygen", and is defined as the difference between organic oxygen and the sum of phenolic, carboxylic, carbonyl, and alkoxyl oxygen. Percent "Organic oxygen" is itself obtained by difference; it is defined as 100 minus the sum of the total contents of carbon, hydrogen, nitrogen, sulfur, and chlorine, as determined using mineral-matter-free coal [16]. Clearly, the reported values of unreactive oxygen are subject to the accumulated errors associated with the determination of all the above oxygen-containing functional groups and of organic oxygen. As such, reported data of unreactive oxygen may often have little meaning. Fortunately, our work required no estimate of unreactive oxygen groups which, by implication, would be unaffected by air oxidation.

We determined the total content of the alkoxy groups contained in alkyl-alkyl and aryl-alkyl, or "reactive" ether groups, using HI cleavage. The procedure, first described by Bhaumik *et al.* [17], is described below:

About 1 g of coal was refluxed with 8 ml of hydriodic acid at 130 ^{0} C for 24 hours and thereafter washed free of acid and dried in a vacuuum oven. A weighed amount of the dried sample was then used in the determination of total hydroxyl-group content, by the method described earlier. The increase in the OH content of the HI-reacted coal over that of the raw coal was a direct measure of the reactive ether groups in the coal. HI cleavage produces one hydroxyl group for each reactive ether group, thus:

$$\Phi\text{–O–}R_1 + HI \quad = \quad \Phi\text{–O–H} + R_1I$$

$$R_2{-}O{-}R_3 + HI \quad = \quad R_2{-}O{-}H + R_3I$$

where R_1, R_2, and R_3 are alkyl groups.

Our results were reproducible to within ± 6 %.

3.1.10 Carbonyl Groups

The method used for the chemical determination of carbonyl groups in coal was based on the procedure described by Brooks *et al.* [18].

The method depends on the reaction of the carbonyl group with phenylhydrazine to form the corresponding oxime.

$$>C{=}O + H_2N{-}R \quad = >C{=}N{-}R + H_2O$$

0.4 g of the coal sample was added to a flask containing about 20 ml of 0.2 N sodium acetate solution and 20 ml of a 0.1 M solution of phenylhydrazine, which was freshly made up using 1N HCl solution and standardized against potassium iodate before each experiment. The acid rendered the phenylhydrazine less sensitive to air oxidation. A reflux condenser was attached to the flask which was then heated on a hot plate at 100 ^{0} C for 6 hours. Afterwards, the contents of the flask were cooled and about 50 ml of water was added. The coal was filtered and thoroughly washed. The filtrate and washings were collected and the residual amount of phenylhydrazine was determined by titration against iodate. A blank determination was also neccesary because of the extreme sensitivity of phenylhydrazine to oxidation by air.

The titration followed the procedures recommended by Miller and Furman [19]. To the titration mixture were added 20 ml. of saturated mercuric chloride and sufficient concentrated HCl to give a 3 N solution. The mercuric ions

consumed the iodide ions released by the redox reaction and precipitated mercuric iodide, thus shifting the equilibrium to the right. At that level of acidity, and in the presence of mercuric ions, the redox reaction was:

$$3\ PhNNH_2 + 2\ KIO_3 + 3\ HCl \quad = \quad 3\ PhNNCl + 2\ KI + 6\ H_2O$$

The titration was performed using a potentiometer with a platinum electrode and a calomel reference electrode. At the point of equivalence the indicated emf rose sharply and the solution changed from colorless to yellow.

3.2 Results and Discussion

The analytical data are shown in Tables 3.1 through 3.5 and in Figures 3.1 through 3.11.

3.2.1 Ash Content

As can be seen in Table 3.1, the ash content of PSOC 704 coal increased with oxidation, reflecting the loss of organic material due to oxidation, in the form of carbon oxides and water. As expected, raising the oxidation temperature led to increased loss of organic matter.

3.2.2 Volatile Matter Content

Table 3.1 shows how the volatile-matter content of PSOC 704 coal varied with oxidation. At 200 ^{0} C, despite overall loss of organic material, the volatile-matter content remained virtually unchanged even after 24 hours of oxidation. Evidently, the loss of carbon and hydrogen in the form of water and carbon oxides was matched by the weight gain due to the incorporation of oxygen. At

230 ^{0} C, however, there was a net loss of volatile material, because of the increased rate of production of carbon oxides and water.

3.2.3 Heating Value

If those losses in heating value are are expressed on the basis of the original mass of the coal, allowing for a weight loss of about 4.5 % for the PSOC 704 coal and about 2 % for the PSOC 247 coal, the loss of heating value is fractionally higher. As shown by Figures 3.1 and 3.2 the heating value initially fell sharply during the first few hours of oxidation and then declined more gradually with further oxidation. Heating values for PSOC 704 and PSOC 247 were lower by 11.3 % and 8.4 % , respectively, after two hours' oxidation. Such large losses in heating value are clearly undesirable, as they would adversely affect the economic viability of coal-cleaning processes involving mild oxidation.

What caused the sudden loss of heating value ? . We have confidence in the reliability of the heating-value data, which were accurate within 1 % . The loss of heating value was real, and correlated well with the loss of carbon and hydrogen. Dulong's formula [20] gives the empirical relationship betwen coal heating value and C, H, O, and S content, expressed as decimal fractions, as follows:

$$HV\,(\,Btu/lb\,) \;=\; 14544\,C \;+\; 62028\,(\,H - O/8\,) \;+\; 4050\,S$$

Evidently the large, initial loss of heating value was caused by loss of carbon and hydrogen from the coal. As explained below, such loss of matter was probably due to rapid devolatilization.

3.2.4 Elemental Analysis

See Tables 3.2 and 3.3 and Figures 3.3 and 3.4.

The carbon and hydrogen data for PSOC 247 coal and PSOC 704 coal show similar trends, even though the initial fractional conversion of hydrogen is about four times higher than that of carbon. There is a significant drop in both carbon content and hydrogen content in the first two hours of oxidation, after which the C content declines more gradually with time while the H content continues to fall steeply.

The decrease in the carbon content of the PSOC 704 coal during the first two hours was about five times higher than the corresponding loss of CO and CO_2 during the same period, showing that some of the carbon was not lost in the form of carbon oxides but, possibly, as devolatilized hydrocarbons. With PSOC 247 coal, the decrease in carbon content was fully accounted for by the production of carbon oxides. In Table 3.3, the carbon content of PSOC 247 coal falls in the first two hours and then declines very slowly. The high rates of evolution of carbon oxides cause significant loss of organic material so that, while carbon is consumed, the carbon content on a percentage basis falls only gradually.

Thus a possible explanation for the large losses of C and H and the corresponding drop in coal heating value is that volatile hydrocarbon species are probably lost by desorption from the coal matrix.

Some desorption was observed by Vahrman and Watts [21] who heated a bituminous coal in a stream of pure nitrogen at temperatures of 50-500 ^{0} C, in 50 ^{0} C increments. The time required for complete evolution of volatile hydrocarbons at a given temperature ranged from 50 to 270 hours. Such a slow rate of desorption was taken to imply that the hydrocarbons were held in micropores, out of which they diffused by an activated process. The aliphatic compounds evolved between 150 ^{0} C and 250 ^{0} C amounted to 0.024 % by weight

of the dry mineral-matter-free (dmmf) coal while the corresponding aromatic products were 0.028 % of dmmf coal. Such small amounts, however, would not explain the precipitous drop in coal heating value during the first two hours of oxidation.

To investigate the possibility of devolatilization due to heating, we performed an experiment in which we added PSOC 704 coal into the fluidized bed reactor at 200 ^{0} C and maintained the temperature at 200 ^{0} C while fluidizing the bed with pre-purified nitrogen, for up to 12 hours. Samples of the heated coal were taken after 1, 2, 6, and 12 hours. The carbon and hydrogen contents of all those samples were virtually the same. Therefore, merely heating the coal did not cause loss of carbon and hydrogen.

The rapid loss of C and H during the first two hours of oxidation must have been due to some acceleration of the process of desorption and devolatilization, caused by a rapid increase in the temperature of the coal surface or by enlargement of the micropores, as reported by Oda *et al.* [22], leading to significant loss of volatile matter.

We had hoped to use the nitrogen analyses to obtain estimates of the possible consumption of nitrogen, but clearly the percentage error in the nitrogen values was so large that no meaningful conclusions could be drawn from them.

Table 3.4 shows the total content and distribution of sulfur in PSOC 704 coal before and after oxidation at 200 for 12 hours. The data show that there is no noticeable loss of sulfur from coal during air oxidation at 200 ^{0} C. We would have expected some pyrite to have been oxidized to sulfate, but the data do not indicate so in conclusive terms. The reproducibility of the sulfur analyses was not good. Possibly the individual coal particles all had different amounts of pyrite attached to them.

3.2.5 Total Acidity and Carboxylic Acidity

Oxidation creates phenolic as well as carboxylic groups, and both TA and CA increase as a function of time. Figures 3.5 through 3.11 show total acidity and carboxylic acidity for the three coals PSOC 247, PSOC 615, and PSOC 704 oxidized at 200 ^{0} C and 230 ^{0} C. In all cases the coals were oxidized at a fluidized-bed total pressure of 126 kPA (3.5 psig).

As shown in Figure 3.5, both TA and CA for PSOC 704 coal increased steadily with oxidation time at 200 ^{0} C, with TA increasing about twice as fast as CA. Figures 3.6 and 3.7 show how TA and CA increased with oxidation time at 200 ^{0} C and 230 ^{0} C. Figure 3.8 shows the effect of oxidation temperature on the TA and CA of 704 coal oxidized for 12 hours. Both TA and CA increase steadily as the oxidation temperature is increased.

Figures 3.9 and 3.10 show different relationships between total acidity and oxidation time for the three coals. PSOC 247, the lignite, had the highest acidity and was also the most reactive. When PSOC 247 was oxidized at 200 ^{0} C the total acidity (TA) rose to a plateau after four hours and did not increase further. At 230 ^{0} C, however, the TA rose steadily with increasing oxidation. We infer that some acid-producing functional groups were not oxidized appreciably at 200 ^{0} C. The results of PSOC 615 coal also pointed to a similar conclusion. There was practically no change in TA at 200 ^{0} C but we saw a slow increase in TA with oxidation time at 230 ^{0} C. Also, we noticed a small, apparent step change in the TA of PSOC 615 after oxidation for 8 hours at 230 ^{0} C.

The CA of PSOC 704 coal increased steadily with oxidation time. The CA of PSOC 247 passed through a maximum at about 4 hours and then apparently declined.

Values of total and carboxylic acidity were reproducible to within ± 0.1 g eq./ kg coal for the bituminous coals and about ± 0.3 g eq./ kg coal for the lignite. As can be seen in Figure 3.11, carboxylic acidity data for the lignite showed a high degree of scatter. Schafer [3] had also noted that the method of cation exchange could give anomalous results with lignites.

As described in Chapter 2, we measured rates of production of carbon oxide gases as a function of time. We now compare those rates with the rate of creation of carboxylic groups so as gauge the relative importance of the two processes.

Using data for PSOC 704 coal oxidized at 200 ^{0} C and 3.5 psig, we have

$$CO_2 \text{ rate} \approx CO \text{ rate} \approx 3.6 - 5.0 \times 10^{-8} \text{ kg mol/kg coal s}$$

and, from the rates of increase of TA and CA

$$[CO_2H] \text{ rate} \approx 4.5 \times 10^{-8} \text{ kg mol/kg coal s}$$

$$[\Phi\text{–OH}] \text{ rate} \approx 6.0 \times 10^{-8} \text{ kg mol/kg coal s}$$

Thus we infer that the production of carbon oxide gases and the creation of acidic groups at 200 ^{0} C were comparable in magnitude. At 230 ^{0} C, the correponding figures were :

$$CO_2 \text{ rate} \approx 0.75 - 1.10 \times 10^{-7} \text{ kg mol/kg coal s}$$

$$CO \text{ rate} \approx 0.70 - 0.95 \times 10^{-7} \text{ kg mol/kg coal s}$$

and,

$$[CO_2H] \text{ rate} \approx 1.0 \times 10^{-7} \text{ kg mol/kg coal s}$$

$$[\Phi\text{–OH}] \text{ rate} \approx 1.4 \times 10^{-7} \text{ kg mol/kg coal s}$$

Thus, at 230 ^{0} C, the rates of formation of carbon monoxide, carbon dioxide, and carboxylic acids are roughly equal, and all about 40 % lower than the rate of phenolic-group formation.

As noted earlier, the difference between total acidity (TA) and carboxylic acidity (CA) was defined as the phenolic content. In Table 3.4 some of the values of phenolic OH content given by the difference method appear to be too high, when compared with corresponding values of the total OH content, as determined by acetylation. The discrepancy in the phenolic and total OH values is most apparent for the lignite and the oxidized bituminous coal. If we define alcoholic OH content as the difference between total OH and phenolic OH then we find that, for some samples, the apparent values of alcoholic OH content are negative. Then we find that the alcoholic OH content, as defined, apparently decreases markedly as, presumably, alcohols are oxidized to aldehydes. There are two possible explanations for the observed discrepancy; either the phenolic OH values are too high or the total OH values are too low.

Firstly, the cation-exchange methods used to measure TA and CA could possibly be in error. The phenolic-group content would be overstated if TA was overestimated or CA underestimated. Clearly the apparent value of phenolic OH content depends on the assumed cut-off pH value for carboxylic acid groups. We adopted Schafer's [2,3] definition of carboxylic acidity as being equal to the cation-exchange capacity at pH 8.3 and total acidity as being the cation exchange capacity at pH 12.5. Schafer's choice of pH 8.3 could possibly be incorrect, at least for some coals, leading to wrong values of phenolic and

aliphatic OH contents.

Secondly the acetylation method, though generally accepted as reliable [5,13], may in fact underestimate total OH content. Either the acetylation reaction or the final hydrolysis step may not go to completion, due to intra-particle mass-transfer limitations. Also, some of the phenolic groups created during oxidation could conceivably be unavailable for acetylation either because of diffusional limitation or because of steric hindrance.

Table 3.5 shows values of phenolic content obtained using the direct method described earlier together with corresponding results obtained by the difference method. As can be seen in the table the direct method gave much lower values than those obtained by the difference method; and showed the oxidized coal as having a slightly lower phenolic content than the unoxidized coal. Clearly, the data given by the direct method appear to be less reliable than those given by the difference method.

3.2.6 Hydroxyl Groups and Ether Groups

Table 3.4 shows values of oxygen-containing functional groups for the three coals used in this work, before and after oxidation.

Data for the low-volatile bituminous coal, PSOC 615, show total OH increasing with oxidation. The total OH of the hvA coal PSOC 704 goes up from 1.86 to 2.93 g mol/ kg coal in four hours of oxidation and then seems to remain essentially constant , up to 24 hours of oxidation. Total OH for the lignite, PSOC 247, apparently decreases with oxidation. In view of the observed steady increase in phenolic-group content of coals with oxidation time, this result is somewhat surprising.

The ether content of PSOC 247 coal increases steadily with oxidation while that of PSOC 704 first declines and then begins to increase. Evidently, ether groups are formed by the condensation reactions of aliphatic and phenolic OH groups. As discussed earlier, the acetylation method could possibly underestimate the total OH content of a coal sample. If so, then our values for ether content could also be low.

3.2.7 Carbonyl Groups

Values of carbonyl-group content for three PSOC 704 coal samples are shown in Figure 3.6. They show the expected increase in carbonyl content with oxidation. The values may possibly be too low, in view of the difficulty, mentioned above, of ensuring completeness of reaction when using liquid-phase reactants with coal. For the moment, however, they are the best values available to us.

Table 3.1

Ash Content and Volatile-Matter Content for

PSOC 704 (HVA) Coal, on Moisture-Free Basis

Oxidation Temp (^{0}C)	Hours Oxidized	Ash Content Per Cent	Volatile-Matter Content, Per Cent
-	-	8.24	40.1
200	12	8.80	40.6
	24	9.24	40.5
230	12	9.60	38.3
	24	10.2	36.9

Table 3.2

Elemental Analysis and Heating Values of Oxidized

PSOC 704 (HVA) Coal, on Moisture-Free Basis

Oxidation Temp (^{0}C)	Hours Oxidized	Elemental Composition (%)			Heating Value	
		C	H	N	kJ/ kg	Btu/lb
-	0	77.08	5.49	1.34	32350	13920
200	2	72.97	4.74	1.25	28720	12350
	4	-	-	-	28170	12120
	6	72.11	4.38	1.19	28030	12050
	8	71.09	4.42	1.21	28140	12100
	16	70.16	4.04	1.19	26670	11470

Table 3.3

Elemental Analysis and Heating Values of

Oxidized PSOC 247 (Lignite "A") Coal, on Moisture-Free Basis

Oxidation Temp (^{0}C)	Hours Oxidized	Elemental Composition (%)			Heating Value	
		C	H	N	kJ/ kg	Btu/ lb
-	0	63.85	4.52	1.16	24210	10410
200	2	62.57	3.94	1.16	22180	9540
	4	61.93	4.05	1.15	22030	9470
	6	62.28	3.66	1.14	21730	9350
	8	61.24	3.71	1.12	21350	9180
	12	61.65	3.90	1.18	21560	9270

Table 3.4

Sulfur Contents of PSOC 704 (HVA) Coal Samples

Sulfur Analysis (%)	Unoxidized Coal	Oxidized Coal 200 ^{0} C, 12 hr
Pyritic Sulfur	2.91	3.10
Sulfate	0.28	0.32
Organic Sulfur	1.03	0.98
Total Sulfur	4.22	4.40

Table 3.5

Oxygen-Containing Functional Groups in Coal

Coal PSOC Number	Temp (^{0}C)	Hours Oxidized	Total Acidity	Carboxylic Acidity	Phenolic OH	Tot OH	Ether plus OH	Ether
704	-	0	0.73	0.18	0.55	1.86	2.84	0.98
	200	4	3.39	0.98	2.41	2.93	3.90	0.97
		12	5.27	2.12	3.15	3.07	3.28	0.21
		24	6.95	2.88	4.07	2.98	3.67	0.69
	250	12	7.72	3.73	3.99	3.39	-	-
247	-	-	5.82	3.13	2.69	3.37	5.34	1.97
	200	4	8.83	5.93	2.90	2.62	4.89	2.27
		6	8.50	4.06	4.44	2.38	-	-
		12	8.89	4.74	4.15	1.68	4.55	2.87
615	-	-	0.42	0.20	0.22	0.30	-	-
	200	12	0.83	0.45	0.38	1.01	-	-
		24	0.97	0.54	0.43	-	-	-
	230	24	4.20	2.58	1.62	-	-	-

All quantities are expressed as gram equivalents per kilogram, on a moisture-free basis.

Phenolic OH content was defined as Total Acidity minus Carboxylic Acidity.

Table 3.6

Phenolic and Carbonyl Content of PSOC 704 (HVA) Coal,

on Moisture-Free Basis

	Unreacted Coal	Oxidized 200 ^{0}C, 12 hr	Oxidized 200 ^{0}C, 24 hr
Carbonyl Content (g.eq/ kg coal)	0.06	0.15	0.24
Phenolic Content (g.eq/ kg coal)			
- Direct Method	0.56	0.52	0.64
- Diff. Method	0.44	3.15	4.07

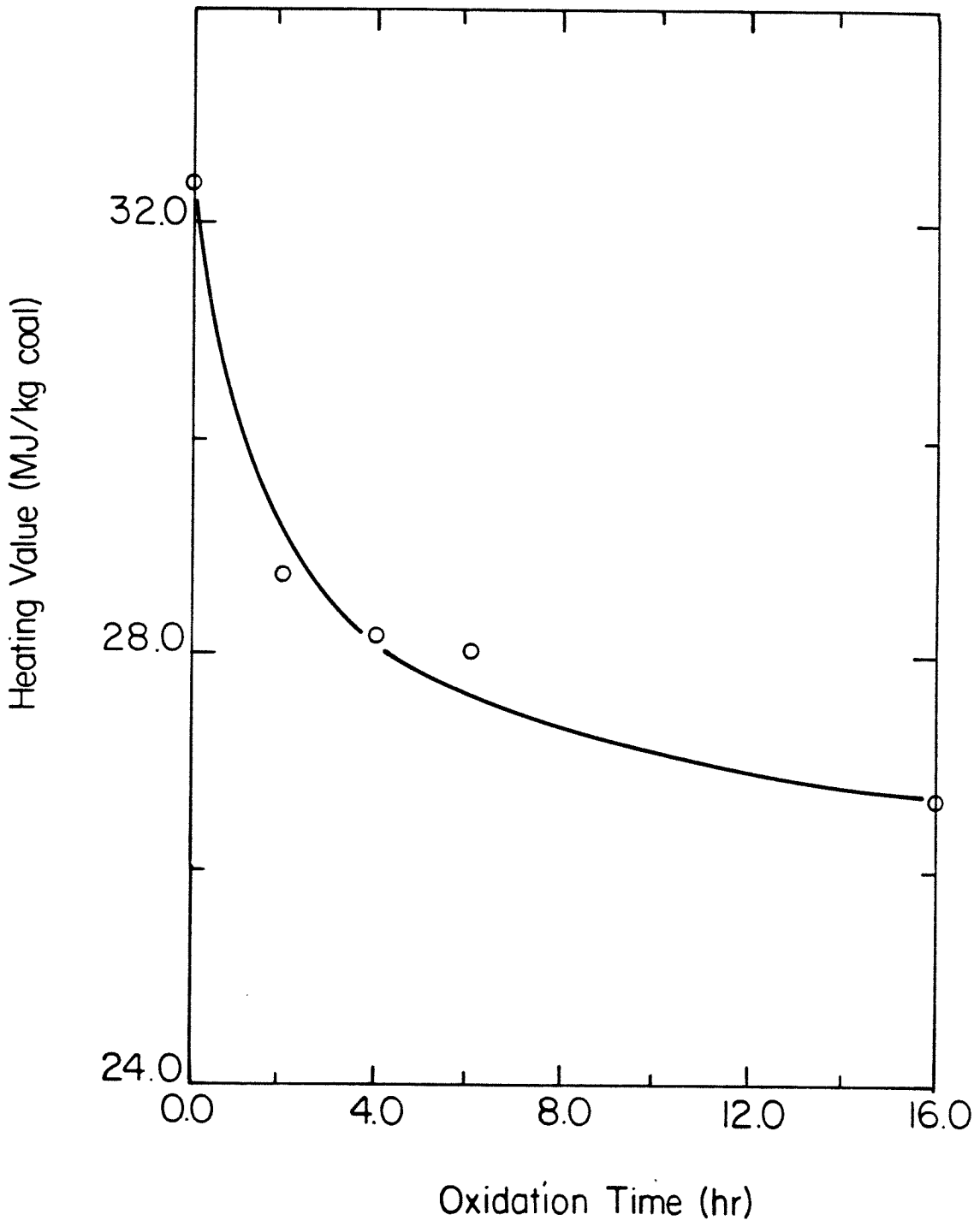

FIGURE 3.1: Heating Value of PSOC 704 Coal vs. Oxidation Time at 200°C and 126 kPa Total Pressure

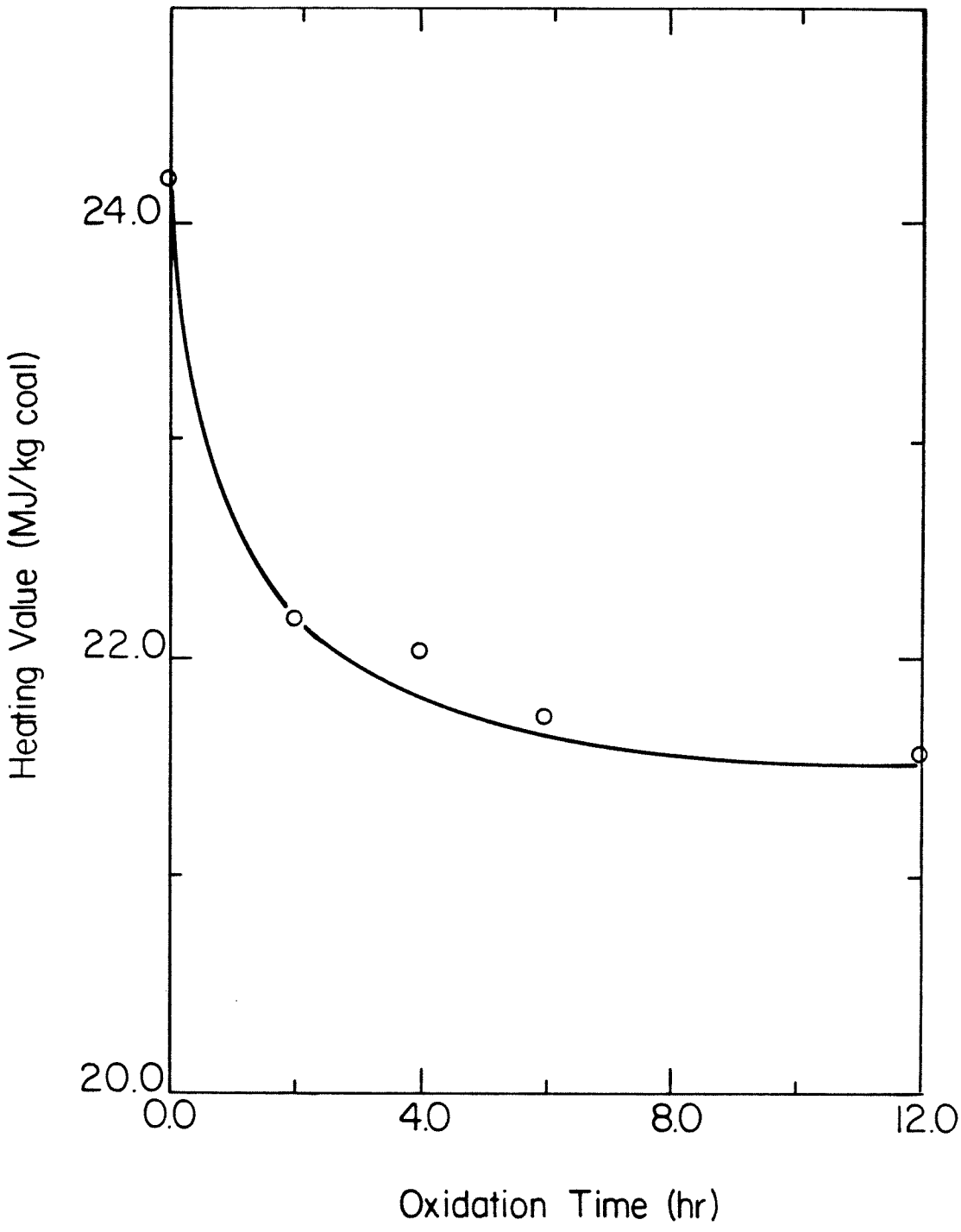

FIGURE 3.2: Heating Value of PSOC 247 Coal vs. Oxidation Time at 200°C and 126 kPa Total Pressure

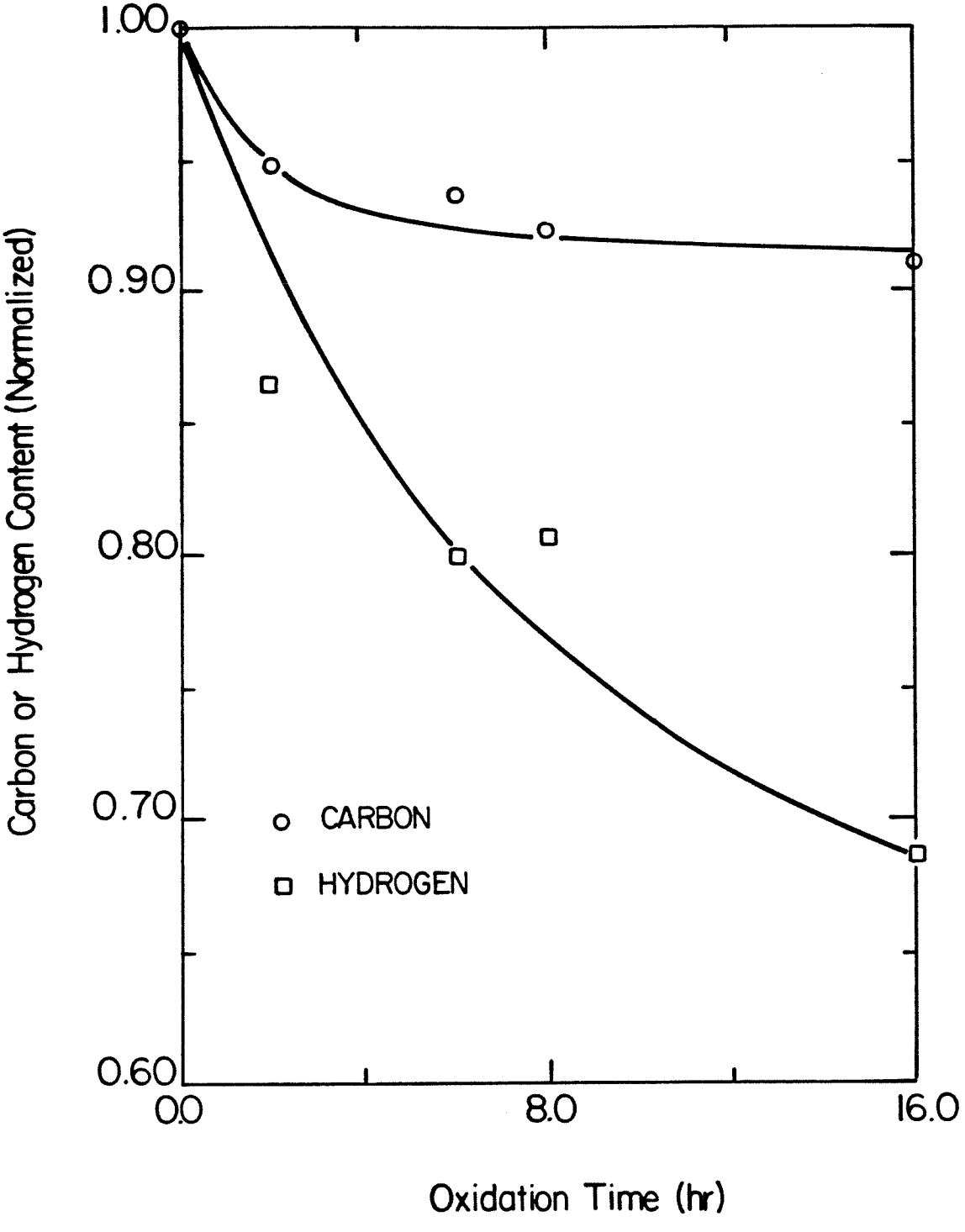

FIGURE 3.3: Ratios of Actual to Initial Percent Carbon and Hydrogen Content vs. Time for PSOC 704 Coal Oxidized at 200°C and 126 kPa Total Pressure

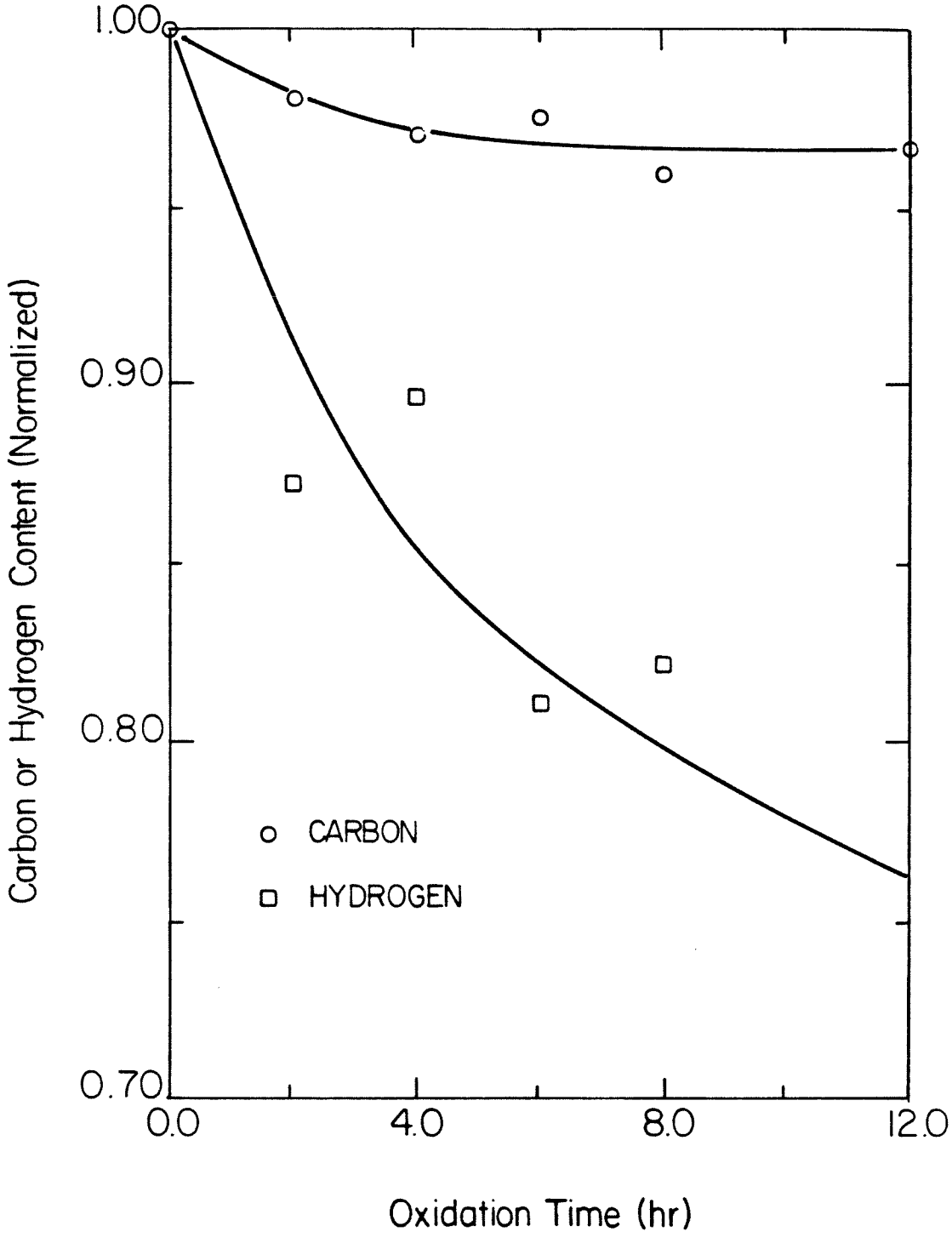

FIGURE 3.4: Ratios of Actual to Initial Percent Carbon and Hydrogen Content vs. Time for PSOC 247 Coal Oxidized at 200°C and 126 kPa Total Pressure

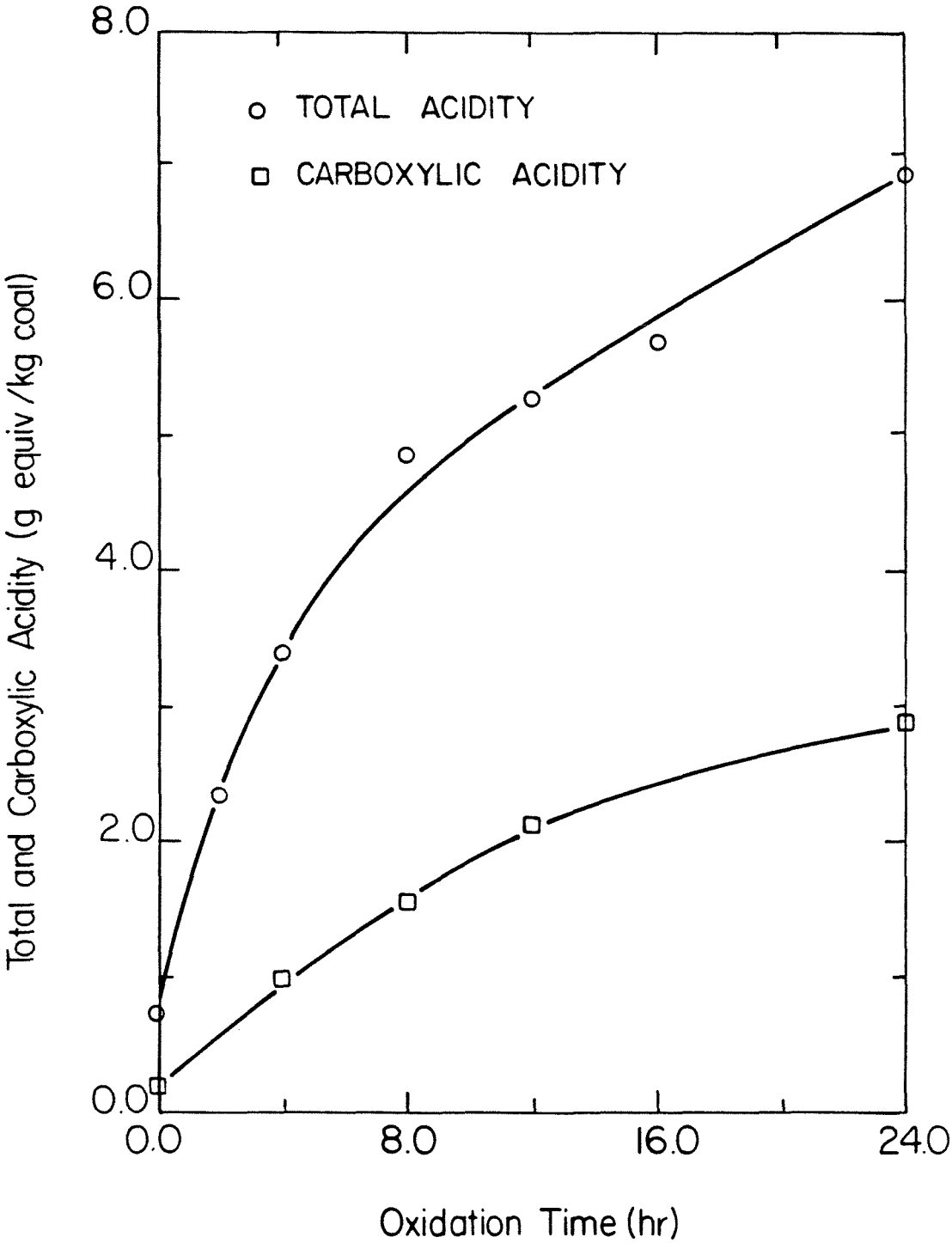

FIGURE 3.5: Total and Carboxylic Acidity vs. Oxidation Time for PSOC 704 Coal Oxidized in Air at 200°C and 126 kPa Total Pressure

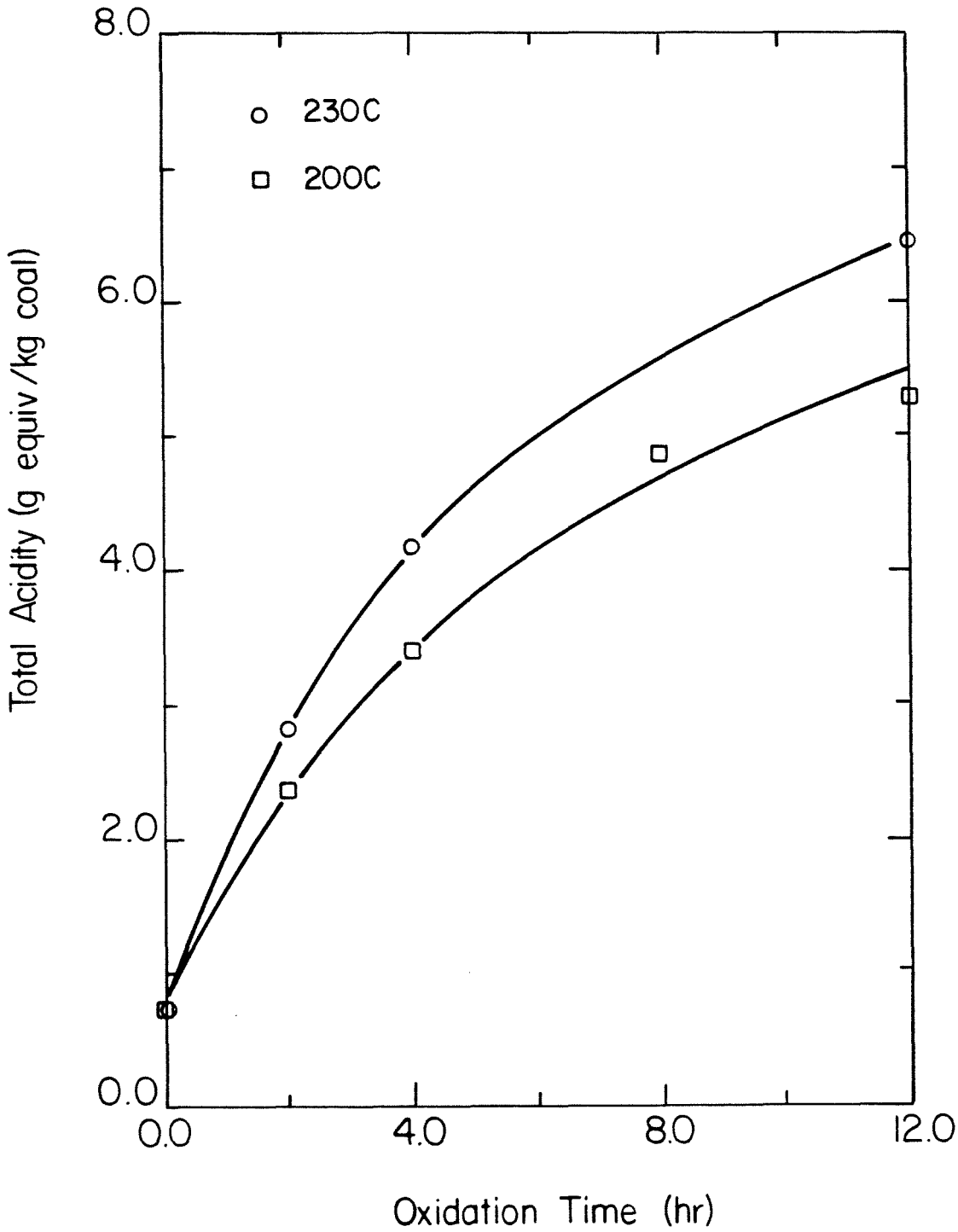

FIGURE 3.6: Total Acidity vs. Oxidation Time for PSOC 704 Coal Oxidized in Air at 126 kPa Total Pressure

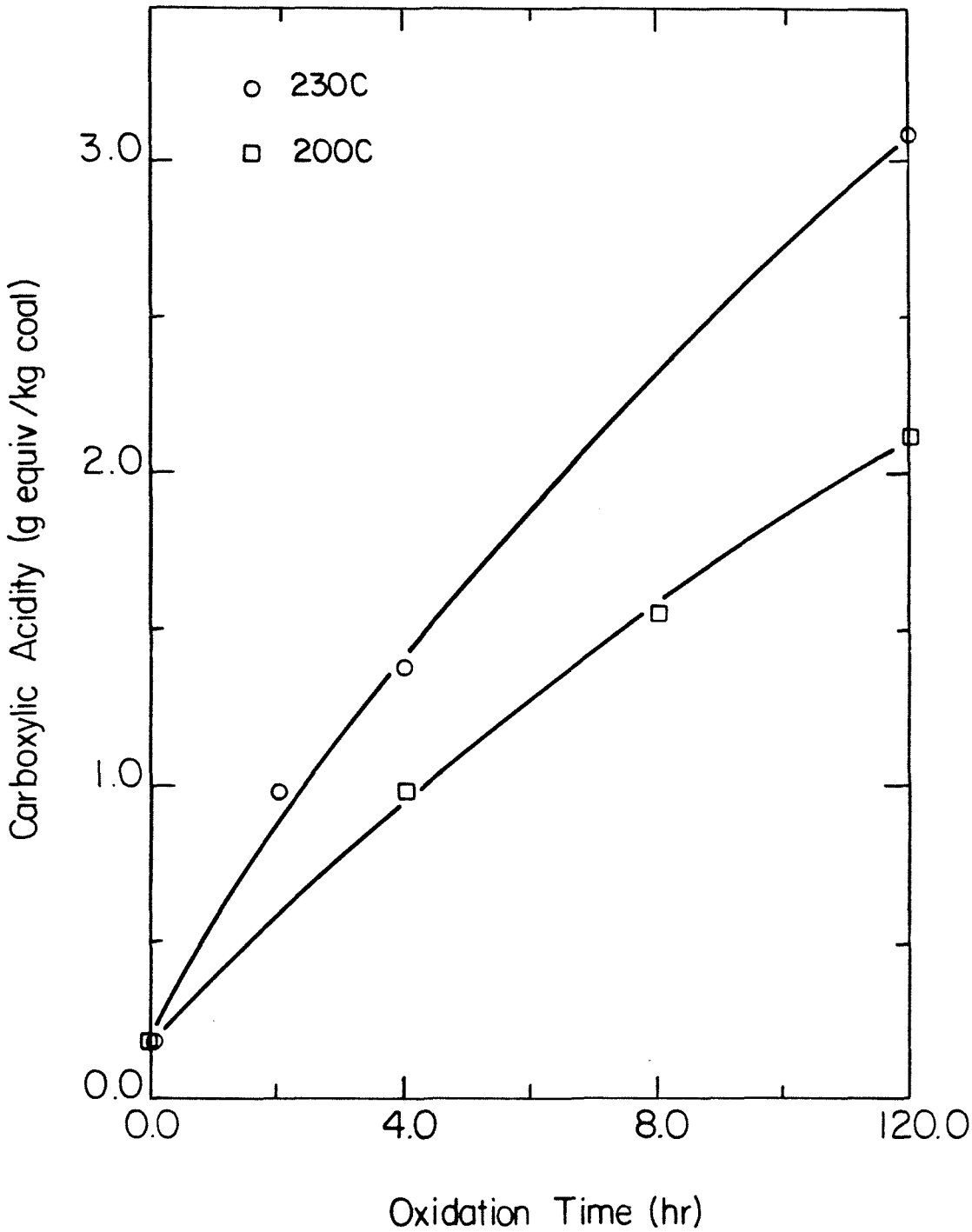

FIGURE 3.7: Carboxylic Acidity vs. Oxidation Time for PSOC 704 Coal Oxidized in Air at 126 kPa Total Pressure

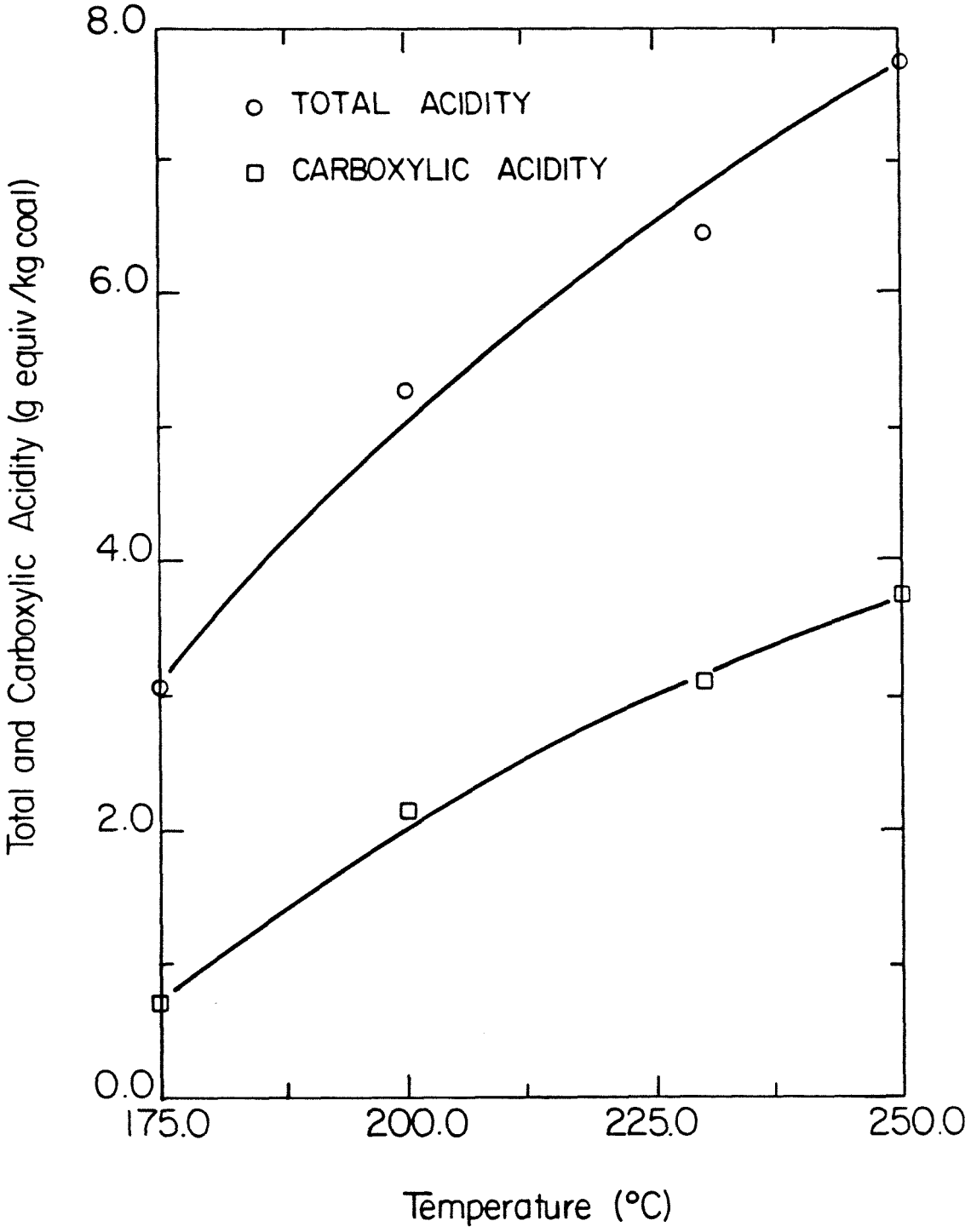

FIGURE 3.8: Total and Carboxylic Acidity vs. Oxidation Temperature for PSOC 704 Coal Oxidized for 12 Hours in Air at 126 kPa Total Pressure

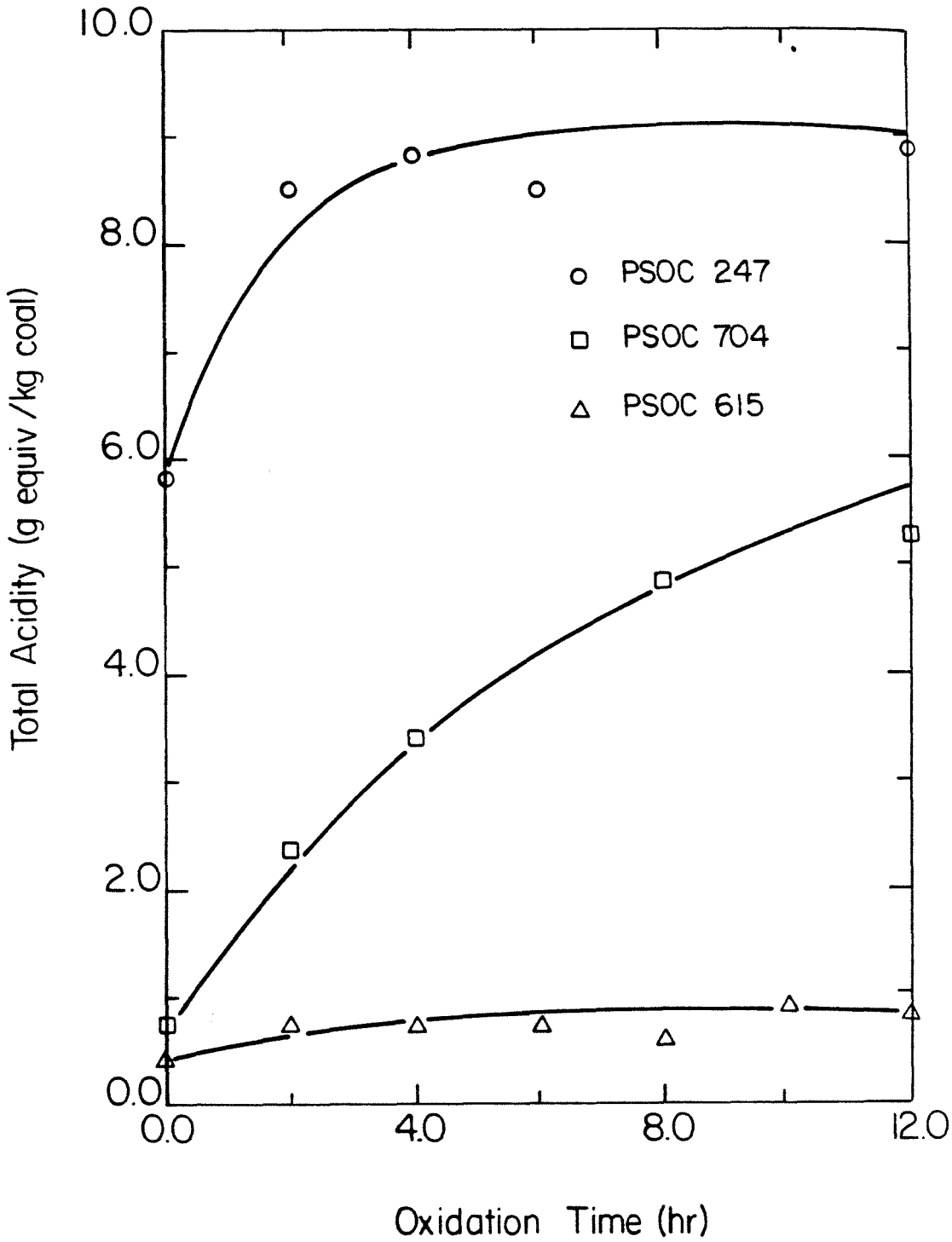

FIGURE 3.9: Total Acidity vs. Oxidation Time for Different Coals Oxidized in Air at 200°C and 126 kPa Total Pressure

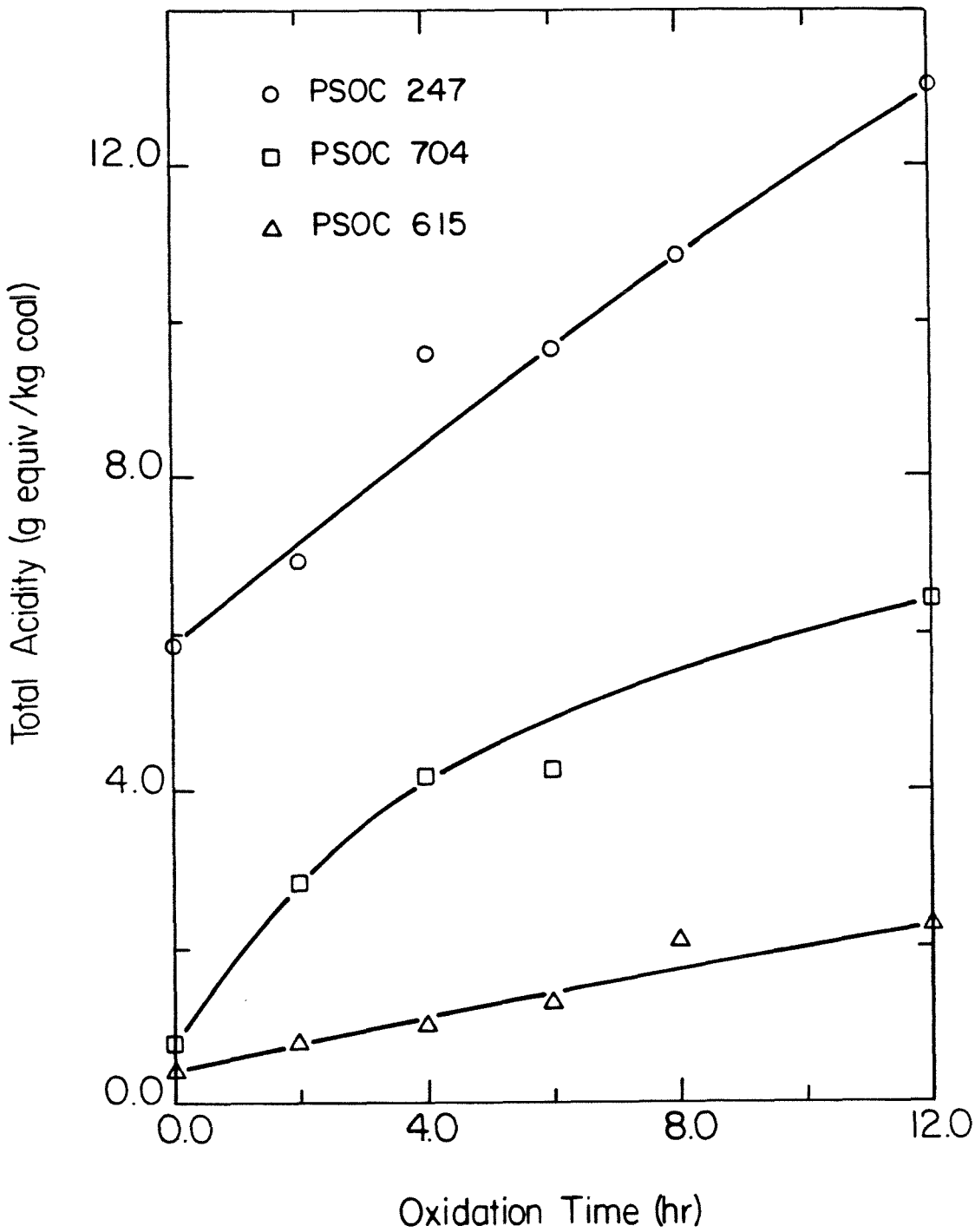

FIGURE 3.10: Total Acidity vs. Oxidation Time for Different Coals Oxidized in Air at 230°C and 126 kPa Total Pressure

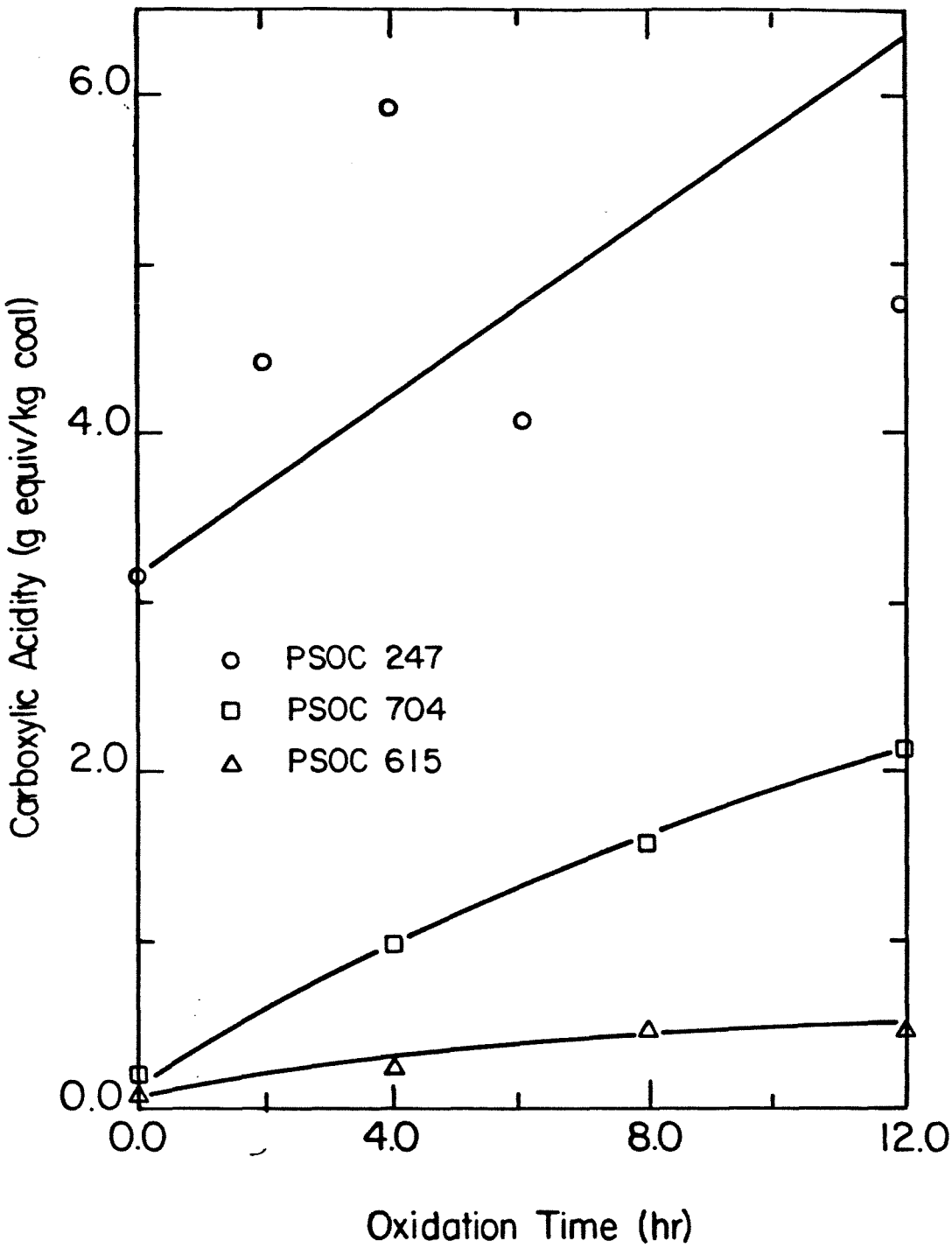

FIGURE 3.11: Carboxylic Acidity vs. Oxidation Time for Different Coals Oxidized in Air at 200°C and 126 kPa Total Pressure

References

[1] Syskov K.I and Kukharenko T.A, Zavodskaya Lab, **13**,25, 1947 and Chem. Abstracts, 5702, 1951

[2] Schafer H.N.S, Fuel, **49**, 197, 1970

[3] Schafer H.N.S, Fuel, **49**, 271, 1970

[4] Ruberto R.G and Cronauer D.C in Organic Chemistry of Coal, ACS Symposium Series No. 71, R.F Gould (Ed.), American Chemical Society, Washington D.C, 1978

[5] Blom L, Edelhausen L, and Van Krevelen D.W, Fuel, **36**, 135, 1957

[6] Zahn H and Wurtz A, A.Z. Anal. Chem., **134**, 183, 1951-52

[7] Yohe G.R and Blodgett E.O, J. Am. Chem. Soc, **69**, 2644, 1947

[8] Liotta R and Brons G, J. Am. Chem. Soc., **103**, 135, 1981

[9] Liotta R, Fuel, **58**, 724, 1979

[10] Liotta R, Rose K, and Hippo E, J. Org. Chem, **46**, 277, 1981

[11] Brooks J.D and Maher T.P, Fuel, **36**, 51, 1957

[12] Maher T.P and Schafer H.N.S, Fuel, **55**, 138, 1976

[13] Painter P.C, Rimmer S.M, Snyder R.W, and Davis A, Appl. Spectrosc., **35**, 102, 1981

[14] Hendrickson J.B, Cram D.J, and Hammond G.S, Oganic Chemisty, Third Edition, McGraw-Hill, New York, 1970

[15] Hayatsu R, Nature, **257**, 378, 1975

[16] Karr C (Ed), Analytical Methods for Coal and Coal Products, Vol.II, Academic Press, New York, 1978

[17] Bhaumik J.N, Mukherjee A.K, Mukherjee P.N, and Lahiri A, Fuel, **41**, 443, 1962

[18] Brooks J.D, Durie R.A, and Sternhell S, Aust. J. Appl. Sci.,**9**, 303, 19589

[19] Miller C.O and Furman N.H, J. Am. Chem. Scoc., **59**, 161, 1937

[20] Elliott M.A (Ed), Chemistry of Coal Utilization, Second Supplementary Volume, John Wiley and Sons, New York, 1981

[21] Vahrman M and Watts R.H , Fuel,**51**, 235, 1972

[22] Oda H, Takeuchi M and Yokokawa C, Fuel, **60**, 390, 1981

4. FOURIER TRANSFORM INFRA RED SPECTROSCOPY

4.1 Background and Review

The Fourier-Transform Infra-Red (FTIR) spectrometer has a higher signal-to-noise ratio (S/N) and a higher optical throughput than a comparable conventional instrument because of its optical system, which uses a Michelson interferometer instead of a diffraction grating. The laser reference beam used in the FTIR instrument also allows for excellent reproducibility of the frequencies. The frequency scale of the widely-used Digilab FTS 15B spectrometer, for example, is reproducible to within 0.2 cm^{-1}.

There are several other useful features of FTIR which arise from the necessary presence of a dedicated computer. For instance, we can use computer memory to co-add spectra from a large number of scans,or interferograms, and thereby average out random disturbances in the signal. We can also add or subtract spectra from other samples or from library routines. Routines have also been developed for separating overlapping peaks. In principle, the advantages of a computer can also be realized with a suitably-equipped conventional spectrometer. Extensive accounts of the general design and operating principle of an FTIR spectrometer are available in a number of textbooks, such as Ref 1.

The FTIR spectrometer samples a whole range of frequencies at the same time. If the spectral width of the range of interest is ν_1, then we have the equivalent of M channels, where

$$M = \frac{\nu_1}{\Delta\nu}$$

and $\Delta\nu$ is the resolution of the spectrum. Therefore, for measurements at the same resolution, optical throughput, and efficiency, using similar infra-red detectors, the FTIR data can be taken M times faster than with a conventional spectrometer. Clearly, this " multiplex ", or " Fellgett's " advantage is most significant at high resolution. On most FTIR machines, the resolution can be varied between 0.5 and 4 cm^{-1}. An alternative formulation of Fellgett's advantage says that, for equal measurement times, the (S/N) ratio of the FTIR spectrum is higher than that of a comparable conventional spectrum by a factor of $M^{0.5}$.

The second fundamental advantage of the Michelson interferometer is higher optical throughput, known as the Jacquinot advantage. It can be shown [1] that the ratio of the optical throughputs, Θ , of the interferometer (I) and the conventional spectrometer (G) is given by

$$\Theta^I / \Theta^G = \frac{2\pi A^I f a \nu^2}{h A^G \nu_1}$$

Thus the Jacquinot advantage is greatest at high frequencies.

One disadvantage of FTIR is that the infra-red detector required for rapid-scanning FTIR work, made of triglycine sulfate (TGS), produces a lot more measurement noise than that produced by the thermocouple detectors used with conventional spectrometers. Even so, FTIR spectrometers are several hundred times faster than conventional spectrometers operating with the same S/N ratio and spectral resolution.

4.1.1 Measurement of Spectra

When a beam of light strikes a solid sample, some of the light is scattered, some is transmitted, and the rest is absorbed. Spectroscopic information may be obtained by measuring changes in the transmitted beam or in the scattered beam or by studying changes in the absorbing sample, using photoacoustic methods.

In general, we are interested in characterizing the organic part of the coal. Interference due to mineral matter can be eliminated by careful use of spectral subtraction techniques [2,3]. Painter and his colleagues, for example, used a procedure whereby the FTIR spectrum of the low-temperature ash (LTA) of the coal was subtracted from that of the whole coal, in such a way as to eliminate the peaks known to belong to mineral matter. Acceptable results were also obtained in the study of oxidation by simply subtracting the spectrum of the raw coal from the spectrum of the oxidized coal. When that was done, any changes due to the oxidation of mineral matter neccesarily appeared in the difference spectrum as well.

Samples for FTIR analysis are usually prepared by grinding a small amount of coal with potassium chloride or bromide, under closely-controlled conditions. For transmittance spectroscopy the mixed powder is pressed to form a pellet which is then placed in the path of the infra-red beam. Most reported FTIR measurements on coal were made by this method. In diffuse reflectance spectroscopy the powder is loosely packed into a small sample cup and exposed directly to the infra-red beam, without pelletization. Griffiths and his co-workers [4,5], and other workers [6], have used this method for *in situ* observation of spectral changes accompanying the reactions of coal.

4.1.1.1 Transmittance Spectroscopy

The oldest and still most common method for preparing coal samples for transmittance infra-red spectroscopy is the potassium halide method. In this method, a small sample of coal is finely ground together with a potassium halide and formed into a pellet. At low concentrations, the classical Beer-Lambert law holds:

$$\text{Log}\left(\frac{I_0}{I}\right) = \varepsilon\, l\, c$$

where ε is the extinction coefficient

I_0 and I are intensities of incident and transmitted light

l is the path length

c is the concentration of the absorbing species

In practice, the Beer-Lambert law is not readily applied to coal because the various functional groups have different, and generally unknown, values of the extinction coefficient. In some cases, those values can be estimated by calibrating measured intensities against chemically-determined functional-group concentrations [7].

One major difficulty in using the pellet method is that any moisture present in the coal or the halide dominates the absorption in the 3000-3500 cm^{-1} region of the spectrum. The optimal grinding time and ratio of coal to halide for the sample must be established from trial experiments with a particular coal and grinding machine [8]. Painter and his co-workers [2,8] used a Perkin-Elmer Wig-L-Bug to grind a mixture of 1.3 mg of coal with 300 mg of KBr, for 30 seconds. Trials had shown that the area under the 700-900 cm^{-1} peak increased with grinding time but levelled off at 25 seconds. Despite strenuous efforts to dry the samples by heating in a vacuum at 120 deg C for two days the workers reported

residual absorption due to hydrogen-bonded OH . Therefore they recommended that the OH content should be measured from the infra-red spectra of acetylated coals. Nonetheless, Solomon *et al.* [9] reported that, with careful drying at 105 ^{0} C for 2 days, the OH content of samples could be estimated directly from the intensities of the OH peaks, to within 10 %.

A further problem with transmission spectra of coal is that the baseline of the spectrum is non-zero, and changes with frequency. Unless spectra are adjusted for baseline shift, measurements of peak intensities will be seriously in error and any quantitative estimates of functional-group concentrations will be quite wrong. Generally the baseline is a line of constant slope, extending over a given range of frequencies. Baseline-correction procedures are available for use with computerized FTIR instruments, but they must be applied carefully. In general, each region of the spectrum will have a different baseline.

Apart from complications caused by baseline scatter and by the presence of water, pelletization may also possibly cause minor changes in the vibrational spectrum of the coal. Fuller and Griffiths [5] noted that the spectrum of a pelletized sample of cholic acid in KCl was noticeably different from the spectrum of the pure acid, whereas the diffuse reflectance spectrum of the powdered sample was quite similar to that of the pure compound.

4.1.1.2 Diffuse Reflectance Spectroscopy

Diffuse Reflectance Infrared Fourier Transform (DRIFT) spectroscopy was used to obtain the spectra reported in this work.

In the DRIFT procedure the powdered sample, with particles of diameter less than 10 microns, is irradiated with a collimated infra-red beam from a Michelson interferometer. The diffused reflected light from the sample is

collected by an ellipsoidal mirror and then directed to a detector made of cadmium telluride. Thus the reflectance spectrum, $R_\infty(\nu)$, is measured. Experimentally, there is a linear relationship between the Kubelka-Munk function, $f(R_\infty)$, and the concentration of a dilute sample.

The relation is analogous to the Beer-Lambert law.

$$f(R_\infty) = \frac{(1-R_\infty)^2}{2\,R_\infty} = \frac{k}{s} = \frac{2.303\,\alpha\,c}{s}$$

c is molar concentration

α , the molar absorptivity, is a function of ν

k is the molar absorption coefficient

s is the scattering coefficient, which depends on the nature and size of the particles.

DRIFT requires less time in sample preparation, and is more sensitive with very dilute samples, than transmittance spectroscopy. With DRIFT, absorption is proportional to molar concentration, whereas the absorption of transmittance spectra is proportional to the square of the concentration [10]. Lastly, DRIFT requires no pelletization, and thereby avoids possible alteration of the coal spectrum.

4.1.2 Resolution of Overlapping Peaks

4.1.2.1 Least-Squares Curve Fitting

An excellent review of this technique is given by Maddams [11]. The method has been successfully applied to coal spectra by Painter and his co-workers at Penn State University [12]. The broad peak is considered to be a linear combination

of a number of smaller peaks, whose shape function is approximated by a combined Gaussian-Lorenzian function. First, the cordinates of the composite peak are digitized and fitted to a seventh-order Newton-Gregory polynomial. The position and approximate widths of the constituent peaks are determined from the minima and zeros of the second derivative of the polynomial. A least-squares iterative procedure, such as the one described by Fraser and Suzuki [13], is then used to establish the optimal widths, shapes and relative intensities of the constituent peaks. There are fundamental limitations to this technique, however. Two bands cannot be resolved if their peaks are separated by less than about 40 % of their half-widths [14]. Somewhat better resolvability is possible where the data are accurate enough to allow the use of third and fourth-order derivatives [15].

4.1.2.2 Fourier Self-Deconvolution

The spectra reported in this work were subjected to this method of spectral enhancement. Fourier deconvolution is a powerful technique for narrowing the band width of a given peak in the spectrum, and thereby reducing overlap. In fourier *self*-deconvolution the spectrum is deconvoluted with a function similar to its intrinsic line shape. It can be shown [16] that self-deconvolution produces the greatest narrowing of the band width. To avoid artifacts, the original spectrum should have a high signal-to noise (S/N) ratio, usually about 1000 or higher. The theory behind fourier-deconvolution is summarized below:

The frequency spectrum, $E(\bar{\nu})$ is the fourier transform of the interferogram, I(x).

$$E(\bar{\nu}) = F\{I(x)\}$$

$$I(x) = F^{-1}\{E(\bar{\nu})\}$$

The spectrum $E(\bar{\nu})$ can be expressed as the convolution of a lineshape function $G(\bar{\nu})$ and a modified spectrum $E'(\bar{\nu})$. Thus,

$$E(\bar{\nu}) = G(\bar{\nu})\ E'(\bar{\nu})$$

$$E(\bar{\nu}) = \int_{-\infty}^{\infty} G(\bar{\nu}')\ E'(\bar{\nu}-\bar{\nu}')d\bar{\nu}'$$

Taking inverse transforms we get, by the convolution theorem,

$$I(x) = F^{-1}\{G(\bar{\nu})\}\ I'(x)$$

Therefore,

$$I'(x) = \frac{1}{F^{-1}\{G(\bar{\nu})\}} I(x)$$

The fourier-deconvoluted spectrum, $E'(\bar{\nu})$, is then recovered by taking the fourier transform of $I'(x)$. The best peak resolution is obtained when the relevant peak is deconvoluted with its intrinsic line-shape function, i.e enhancement is maximized when $G(\bar{\nu}) = E_0(\bar{\nu})$

Consider a band described by a Lorenzian shape function:

$$E_0(\bar{\nu}) = \frac{\sigma/\pi}{(\sigma^2+\bar{\nu}^2)}$$

where 2σ is the peak width at half the height.

Now

$$F^{-1}(E_0(\bar{\nu})) = \exp(-2\pi\sigma x)$$

And thus

$$I'(x) = \exp(2\pi\sigma x)\, I(x)$$

The fourier transform of $I'(x)$ gives the fourier-deconvoluted spectrum $E'(\bar{\nu})$.

In the procedure used by Griffiths [4], the intrinsic line shape is assumed to be Lorenzian, and so the fourier transform of the spectrum is multiplied by an exponentially increasing function whose exponent, as seen above, is related to the peak width. The inverse fourier transform of the resulting function is then computed. The resulting spectrum has narrower bands than the original spectrum. The best value of the exponent is chosen by an optimization procedure designed to give maximum spectral enhancement without exhibiting undesirable features such as side lobes.

4.1.3 Use of FTIR to Study Coal Oxidation

Fourier Transform Infra-red spectroscopy is particularly well-suited to the study of qualitative and quantitative changes in the functional groups of coal. Spectral subtraction brings out important differences between raw coal and oxidized coal, and the difference spectra can be further analyzed using curve-resolution techniques.

4.1.3.1 Assignment of Absorption Peaks

The correct assignment of peaks has obvious implications for the validity of any conclusions based on analysis of spectra. Some of the major absorption bands of the infra-red spectrum of coal were assigned to principal functional groups during the early days of infra-red coal work, in the 1950's and 1960's. Usually

the peaks were generally identifiable from the spectroscopy of pure organic compounds. Coals were subjected to specific chemical treatments and the resulting changes in spectra then provided a basis for choosing between different possible assignments.

A few specific peaks were at first incorrectly assigned, however. Spectra obtained with older instruments were sometimes inaccurate or poorly resolved. Correct sample-preparation techniques had not yet been widely adopted. The effects of mineral matter on spectra were not always taken into account. Often, specific assignments were deduced from chemical experiments that were subject to several different interpretations. For example, the 1600 cm^{-1} band had been erroneously assigned to the carbonyl group, based upon some reactions which were later shown to be due to the presence of the carboxylate ion, whose frequency is 1575 cm^{-1}. Later, Painter [12] convincingly argued that the 1600 cm^{-1} peak was in fact due to the stretching vibration of the highly-conjugated, fused aromatic structure of coal.

In recent years, overlapping peaks have been resolved using the techniques of fourier self-deconvolution and least-squares curve fitting. The fourier self-deconvolution technique, in particular, revealed a number of peaks which previously were not distinguishable. Thus, for instance, the peak at 3050 cm^{-1} was resolved into an aromatic C-H stretch at 3070 cm^{-1} and an olefinic C-H stretch at 3040 cm^{-1}, and the CH_2 and CH_3 stretching frequencies at 2960-2850 cm^{-1} were resolved individually.

4.1.3.2 Previous Work

Some of the most significant investigations into coal oxidation were conducted by Painter and his colleagues at Penn State University [2,3,8,12]. Typically, a 5

gram sample of coal was placed in a ceramic boat and oxidized in a stagnant atmosphere of air, in a horizontal tube furnace. The FTIR difference spectra of samples oxidized at 100 ^{0} C were analyzed.

In the first stage of oxidation the spectrum was characterized by a reduction in the 2800-3000 cm^{-1} absorption, assigned to aliphatic C-H stretching, and the 1450 cm^{-1} absorption, due to CH_2 bending, but no change in the aromatic C-H stretching absorption at 3050 cm^{-1} or in the bending absorptions in the 700-900 cm^{-1} range. Two C-O peaks appeared in the difference spectrum; a carbonyl absorption at 1695 cm^{-1} and a carboxylate-ion frequency at 1575 cm^{-1}. The OH and ether-group absorptions were unchanged during the early phase of coal oxidation.

With increasing oxidation, the difference spectrum showed additional peaks at 3450 cm^{-1} , 1765 cm^{-1}, and 1260 cm^{-1} while the intensities of the 1695 cm^{-1} and 1575 cm^{-1} peaks increased. The new peaks were assigned to phenols, esters, and ethers, respectively. The phenolic OH absorption was, unfortunately, masked by the presence of water. The authors tried different techniques of sample preparation, but the problem was not fully solved. Heating the pellet would not remove all the water, and could have altered the coal sample through unintended further oxidation.

Later, the same authors [2] effectively avoided the water problem by acetylating the coal and then analyzing the acetylated coal. Using a mineral-free vitrinite, they were able to separate the FTIR peaks belonging to the acetyl derivatives of phenolic and aliphatic OH groups. They developed a least-squares, curve-fitting procedure to resolve the overlapping peaks. The 1620-1800 cm^{-1} band was resolved into five peaks; of which the 1635 and 1710 cm^{-1} were assigned to residual acetic acid and water, and the 1675, 1745, and 1770 cm^{-1}

peaks were believed to be associated with the acetyl derivatives of N-H, alkyl OH, and phenolic OH groups, respectively. At first, the relative intensities of the resolved peaks did not correspond to the known relative concentrations of aliphatic and phenolic OH groups [3]. The curve-fitting procedure was subsequently improved [17], and the relative peak intensities were found to be in fair agreement with estimates based on chemical analysis. Clearly, different functional groups have different extinction coefficients. The results thus indicated that acceptable results could be obtained by using an average extinction coefficient, applied to a narrow range of frequencies.

Fairly good quantitative results were obtained by Kuehn *et al.*[17], using a series of 21 vitrinite concentrates obtained from similar coals. Average extinction coefficients were derived, based on integrated peak intensities and on peak heights, for three regions of the spectrum: 2990-3100 cm^{-1}, for aromatic C-H stretching, 2700-2990, for aliphatic stretching, and the combined 1770 cm^{-1} and 1740 cm^{-1} peaks of acetylated OH groups. The vitrinites used were derived from bituminous coals which contain negligible amounts of carboxylic groups. Ignoring the hydrogen contained in small amounts of carboxylic groups in the bituminous vitrinites, they argued that the total hydrogen content (H_t) was related to the average extinction coefficients (ε) and integrated peak areas (A) for hydroxyl, aromatic and aliphatic hydrogen groups by the relation

$$H_t - \varepsilon_{OH}A_{OH} = \varepsilon_{Ar}A_{Ar} + \varepsilon_{Al}A_{Al}$$

H_t and $\varepsilon_{OH}A_{OH}$ were determined by well-established chemical methods. Best estimates ε_{Ar} and ε_{Al} were obtained by linear regression analysis of results from a large number of similar coals. Thus the distribution of hydrogen among OH, aromatic C-H, and aliphatic C-H was estimated for each of 21 vitrinites.

Results for different vitrinites were fairly consistent and realistic. And when the hydrogen distribution was calculated using ε values based on peak heights, the results were in reasonable agreement with those derived from ε values based on integrated peak areas.

The H_{Ar}/H_{Al} ratio ranged from 0.175 for vitrinites of 82-83 % carbon content to 0.4 for a vitrinite of 90 % carbon content. As would be expected, the aromatic hydrogen content of higher-rank vitrinites was higher most previously-reported data, because those data had generally been obtained with relatively hydrogen-rich solvent extracts of coals.

Griffiths [4] studied the oxidation of coal by heating a series of ten coals ranging in rank from semi-anthracite to lignite, in an air oven at 150 ^{0} C , for up to two weeks. Samples of the oxidized coals were analyzed by diffuse-reflectance FTIR at daily intervals. The spectra were enhanced using fourier self-deconvolution, which allowed a higher degree of peak resolution than had been achieved before, and provided significant new information about functional groups consumed and created during oxidation. Whole coals were used, rather than the mineral-free vitrinites which had been used by Kuehn *et al.*[17] and by several other previous investigators.

There were notable differences in the spectra of unoxidized coals of different rank. The absolute intensities of the aliphatic C-H peaks were seen to decrease with rank. The asymmetrical stretching modes of CH_2 and CH_3 were assigned to peaks at 2960 and 2948 cm^{-1} respectively. The ratio of the intensities of the symmetric CH_3 stretching peak (2872 cm^{-1}) and the symmetric CH_2 peak (2853 cm^{-1}) increased with coal rank, implying that the length of the aliphatic side chains and cross links decreases with coal rank.

The spectra of the oxidized coals showed a number of similarities as well as differences between coals of different rank. For all the coals the intensities of the carbonyl peaks at 1845, 1775, 1748, 1735, 1720, 1700, 1685, 1675, and 1655 cm^{-1} increased with oxidation time. The increase in the intensities of the carbonyl absorption frequencies was most evident for the low-rank coals. The 1845 and 1775 cm^{-1} peaks were tentatively assigned to acid anhydrides, the 1748 and 1735 cm^{-1} to aliphatic esters, 1720 cm^{-1} to aliphatic carboxylic acids, 1685 cm^{-1} to aromatic carboxylic acids, and the 1675 cm^{-1} to aromatic ketones. The 1655 cm^{-1} peak was not assigned. Anhydrides and esters were apparently formed by condensation between neighboring acid and hydroxyl groups. At least some of those groups were produced during oxidation.

For the high-volatile bituminous (HVB) coals, the formation of carboxylic acids and phenols was indicated by an increase in the intensity of the 3400 cm^{-1} band. The intensity of absorption in the 1350-1150 cm^{-1} range increased with oxidation as ethers, esters, and possibly alcohols, were formed. Sulfates, which are readily formed by the air oxidation of the pyrite present in coal, also vibrate in that frequency range.

Even though different peaks have different extinction coefficients, peak intensities can provide a useful basis for estimating changes in the relative amounts of different functional groups. The relative intensities of various C-H peaks showed some clear trends. An increase in the intensity of the 3070 cm^{-1} aromatic C-H stretching peak relative to the 3040 cm^{-1} olefinic C-H peak indicated that the aromatic C-H bonds were more stable than the olefinic. The MVB coals showed similar trends, although the apparent aromaticity increased much faster with oxidation than did that of the LVB coal. For all the coals, the intensity of the symmetric stretching peaks for the CH_3 group relative to the

CH_2 group increased with oxidation. For a sub-bituminous coal the ratio of those two intensities increased from 0.58 to 0.78 in eight days.

Wang and Griffiths (18) analyzed the C-H stretching and bending modes of fourier self-deconvolved FTIR spectra of a number of coals. They resolved the broad bands at 3040, 2940, and 2870 cm^{-1} into several constituent peaks. The aromatic C-H stretching band at 3000-3100 cm^{-1} was further resolved into four peaks located at 3050, 3030, 3020, and 3010 cm^{-1}. The asymmetrical methyl C-H peak was also further resolved into three peaks at 2975,2960, and 2948 cm^{-1} representing methyl groups in different environments. The C-H bending mode near 1450 cm^{-1}, due to a combination of asymmetrical C-H bending of CH_3 and CH_2 groups and in-plane aromatic C-H deformation, was resolved into a doublet with peaks at 1454 and 1440 cm^{-1}. The former peak decreased in intensity with increasing rank while the latter increased, and so they were assigned to aliphatic and aromatic bending respectively. Bands near 870, 820, and 755 cm^{-1} were assigned to out-of-plane C-H aromatic bending. Wang and Griffiths tentatively assigned those peaks, respectively, to isolated aromatic C-H, two-neighboring aromatic C-H, and four-neighboring aromatic C-H. Such detailed resolution was not possible before the fourier self deconvolution technique was developed.

4.2 FTIR Analysis of Coal Samples

4.2.1 Experimental

All the spectra were measured in Professor Peter Griffiths's laboratory at the University of California, Riverside. The FTIR equipment at Riverside was used to obtain diffuse-reflectance FTIR spectra of PSOC 247, PSOC 615, and PSOC 704 coal samples and fourier self-deconvolution routines were applied to resolve

overlapping peaks. The correct deconvolution parameters had previously been established from studies of coal spectra using a number of different coals [4].

Samples for FTIR analysis were prepared by grinding for 2 minutes using a Wig-L-Bug grinder and then drying for 5 days in a vacuum oven at 105 ^{0} C. This procedure was necessary because previously, when samples were dried before grinding, some water remained in the sample and subsequently evaporated slowly when the sample was placed in the focused i.r beam, causing interference with the coal FTIR spectrum, especially in the carbonyl region. The interference had rendered deconvolution impossible. The ground, dried sample was packed into a special receptacle which was then placed in the spectrometer and irradiated with an infra-red beam. The spectrometer was specially constructed using a Digilab Model 296 spectrometer as a second optical head of a Digilab FTS-20 spectrometer, as previously described by Fuller and Griffiths [19]. The spectral resolution used was 4 cm^{-1} and spectra were obtained by co-adding one thousand interferograms.

4.2.2 Results and Discussion

Figure 4.1 shows the general appearance of the FTIR spectrum of a bituminous coal.

Fourier self deconvolution reveals many features that otherwise would not be apparent. The sharp difference between ordinary spectra and deconvolved spectra is clear in Figure 4.2. In the C-H stretching region we see the aromatic peak at 3050 cm^{-1} deconvolved into two peaks centered at 3050 and 3020 cm^{-1} and the peaks at 2920 and 2860 are each split into a doublet. The assignment of these peaks by Griffiths [4] was discussed earlier in this chapter. Upon deconvolution, the broad peaks in the 1100-1900 cm^{-1} range are resolved into

many smaller peaks, many of which have been assigned. A number of the small peaks seen in the 700-1100 cm^{-1}region of the deconvolved spectrum are not yet assigned.

The difference between the spectrum of the acetylated coal and that of the raw coal can be seen in Figure 4.3. The intensity of the broad phenolic band in the 2600-3600 cm^{-1} region falls dramatically. In the spectrum of the acetylated coal, the sharp peak at 1770 cm^{-1} is due to the carbonyl stretch of acetyl esters and the spike at 1360 cm^{-1} is due to the C-H bending frequency of acetyl groups The very strong, sharp peak at 1200 cm^{-1} is assigned to ester C-O-C bonds. Peaks at 1600 cm^{-1} (aromatic ring stretch) and 1445 cm^{-1} ($-CH_2-$ and $-CH_3-$ groups) are unaffected by acetylation.

Spectra of the three different coals used in this study are shown in Figure 4.4. The spectrum of PSOC 247, a lignite, shows a prominent hump in the 2600-3600 cm^{-1} region, due to hydrogen-bonded phenolic and carboxylic groups. On the other hand the spectrum of PSOC 615 coal shows a much lower OH intensity. Also, the lignite spectrum appears to have mainly broad bands and not many prominent small peaks. The LVB, by contrast, gives a spectrum containing many small, distinct peaks and a strong absorbance centered at about 1030 cm^{-1}, which is due to mineral matter.

We were mainly concerned with the effects of coal oxidation. Some of those effects can be seen from a comparison of spectra for unoxidized coal and coal oxidized at 200 ^{0} C for 12 hours, shown in Figures 4.5, 4.6, and 4.7. With oxidation,the intensity of the H-bonded hydroxyl band increases. The C-H stretching peaks at 2800-3100 cm^{-1}, especially the aliphatic, decrease in intensity, as does the CH_2 , CH_3 bending peak around 1450 cm^{-1}. A broad carbonyl peak at around 1700 cm^{-1} intensifies. On deconvolution (see Figure

4.6) it is resolved into separate peaks at 1840, 1775, 1740, 1725, 1710, and 1690 cm^{-1} which have been assigned by Griffiths [4] to aliphatic acid anhydrides, aromatic acid anhydrides, esters, aliphatic carboxylic acids, aliphatic aldehydes and ketones, and aromatic carboxylic acids. The broad band appearing at 1150-1350 cm^{-1} in the spectrum of the oxidized coal in Figure 4.5 is probably due to the formation of ethers or possibly even iron sulfate, which results from the oxidation of the iron pyrite present in coal. The 700-1150 cm^{-1} region, shown in Figure 4.7, is complicated by the presence of several peaks assignable to mineral matter. Based on FTIR spectra of the low-temperature ash (LTA) from similar coals [18] the peaks at 1115, 939, 913, 891, 800, and 780 have been assigned to mineral matter. We note that oxidation also causes a reduction in the intensities of the three peaks at 755, 813 and 874 cm^{-1} . The possible assignment of those three peaks was mentioned earlier. The doublet at 1013 and 1034 cm^{-1} is due to mineral matter in the coal.

Figures 4.8 through 4.12 show FTIR spectra of PSOC 704 coal oxidized at temperatures of 175-280 ^{0} C for periods of up to 24 hours. In Figure 4.8 we see the steady consumption of C-H groups, aromatic and aliphatic, reflected by the steady fall in the intensity of the stretching frequencies at 2800-3100 cm^{-1} and decline in the intensity of the 1450 cm^{-1} peak due to CH_2 and CH_3 bending modes. Likewise the overall intensity of the bands at 750-1000 cm^{-1} decreases. The same trends are seen in Figure 4.9 where spectra of coals oxidized for 12 hours at 175 ^{0} C and 250 ^{0} C are compared with the spectrum of the unoxidized coal. For the 2800-3200 cm^{-1} range in Figure 4.10 we see the greater consumption of C-H groups and increase in hydrogen-bonded, phenolic and carboxylic, content for the coal oxidized at 250 ^{0} C. A visual comparison of peak heights also shows that the aliphatic groups are consumed faster than the aromatic groups. The deconvolved spectra of the 100-1900 cm^{-1} region

unfortunately do not contain much significant information.

The major observations from Figures 4.11 and 4.12, showing the spectra of unoxidized coal and of coals oxidized at temperatures of 200 ^{0} C and 280 ^{0} C for 24 hours, is also the decline in intensity of the C-H stretching peaks, reflecting the consumption of those groups during oxidation. Again the 1000-1900 cm^{-1} region of the deconvolved spectrum shows little additional detail.

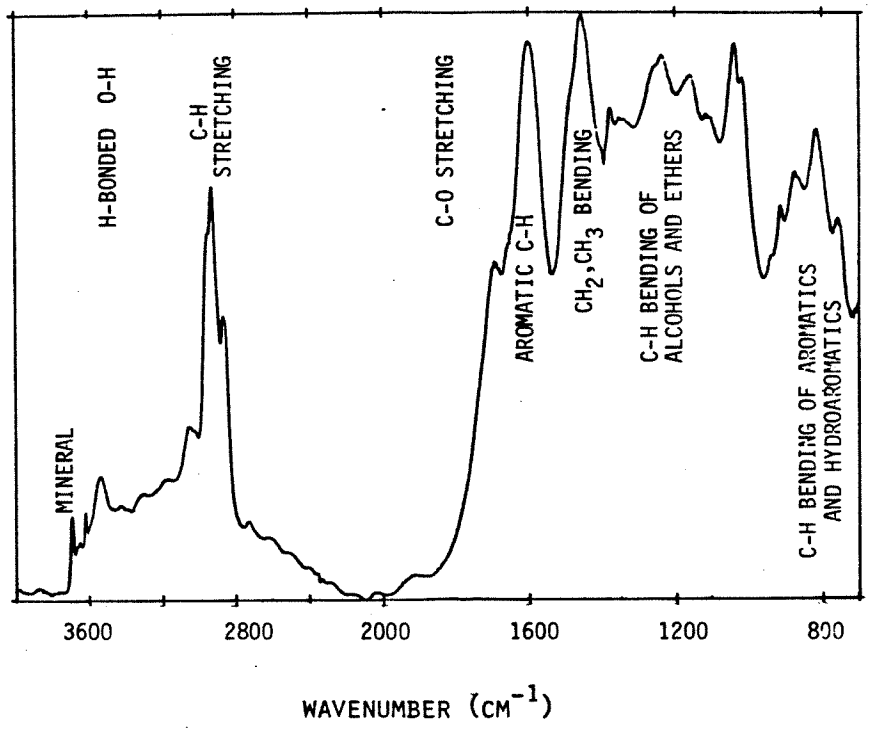

FIGURE 4.1: Regions of the Infrared Spectrum of a High-Volatile Bituminous Coal (PSOC 704)

FIGURE 4.2: Fourier Self Deconvolution of FTIR Spectra of PSOC 704 Coal

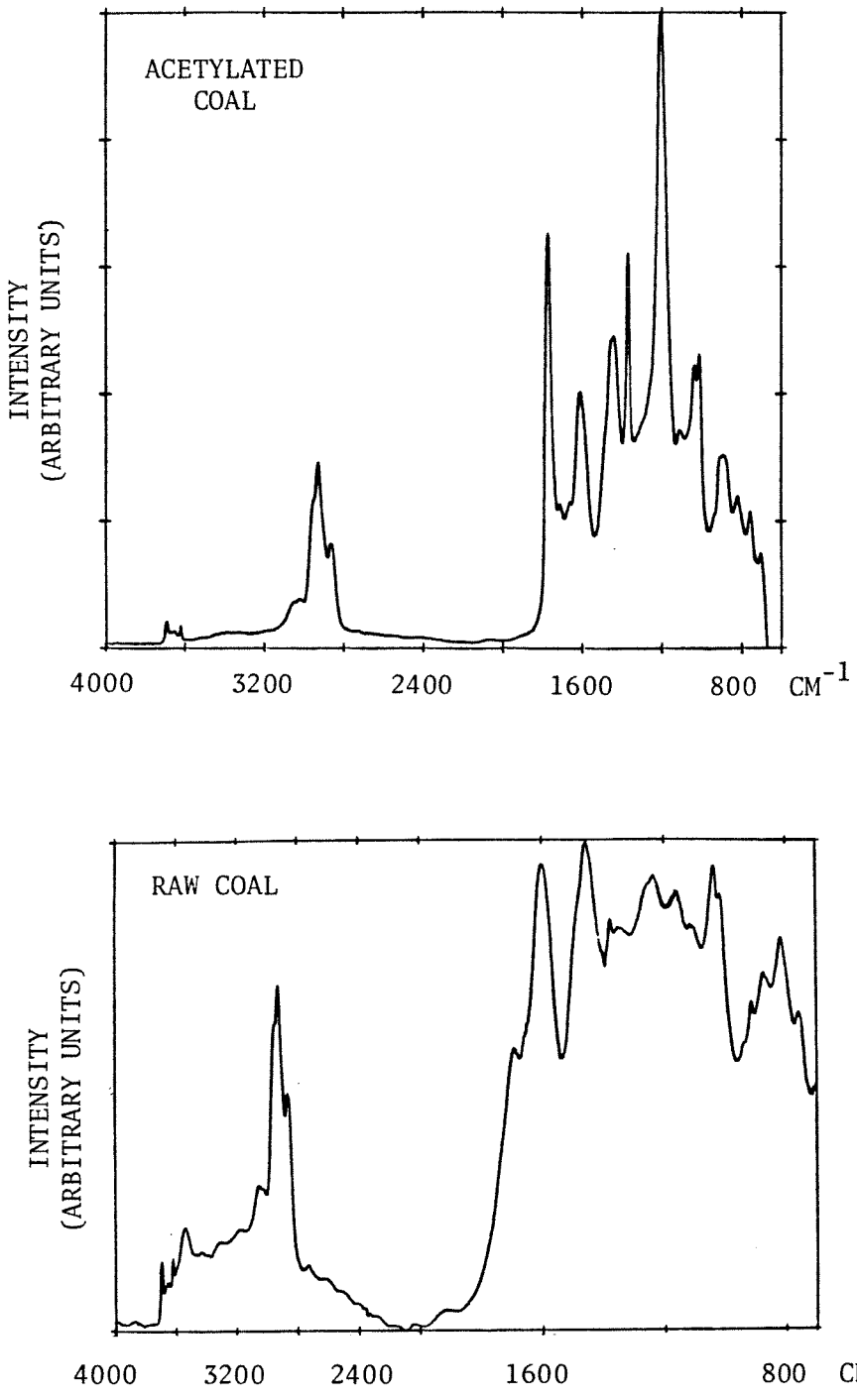

FIGURE 4.3: FTIR Spectra of Raw and Acetylated PSOC 704 Coal

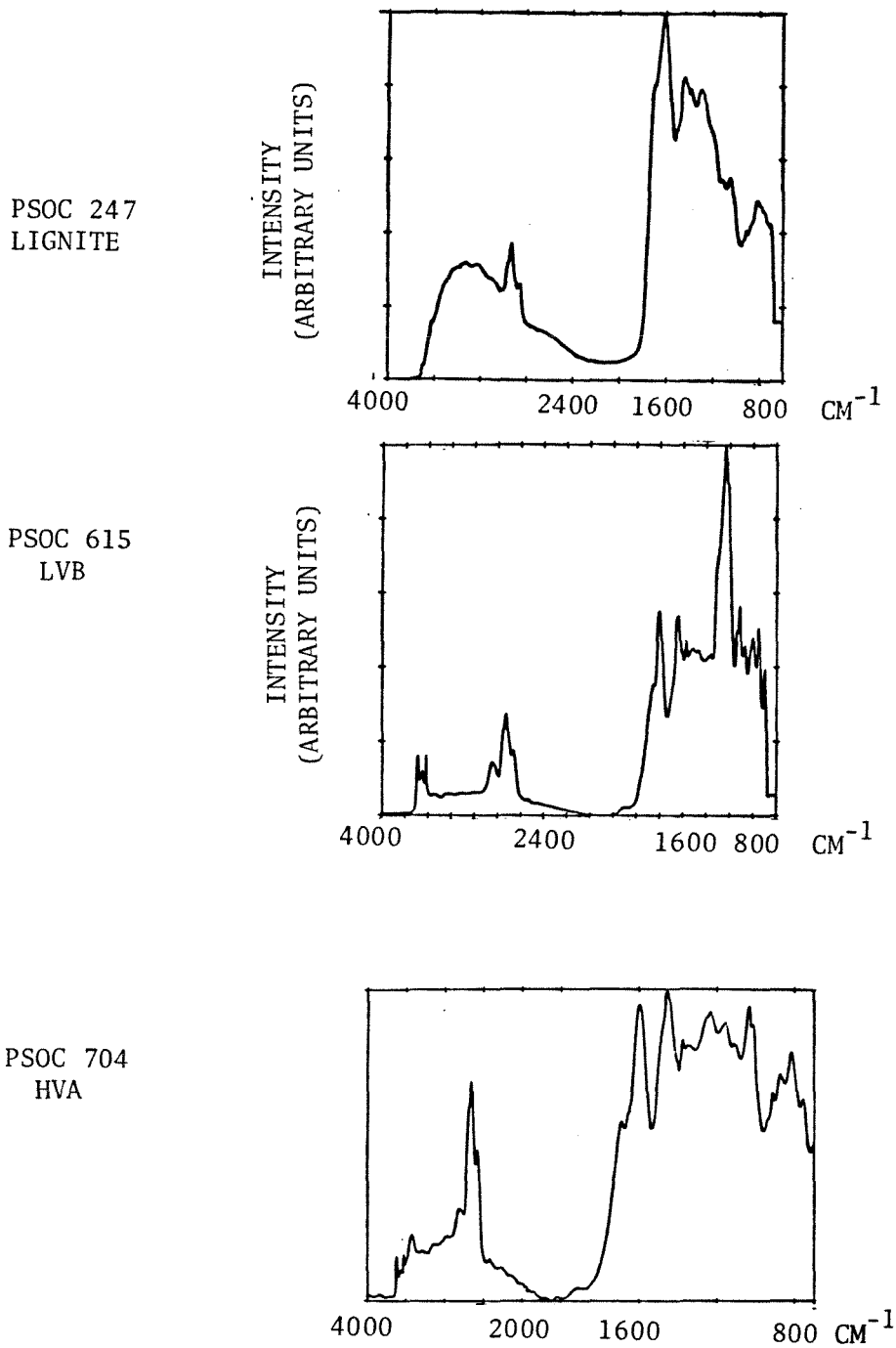

FIGURE 4.4: FTIR Spectra of Three Unoxidized Coals.

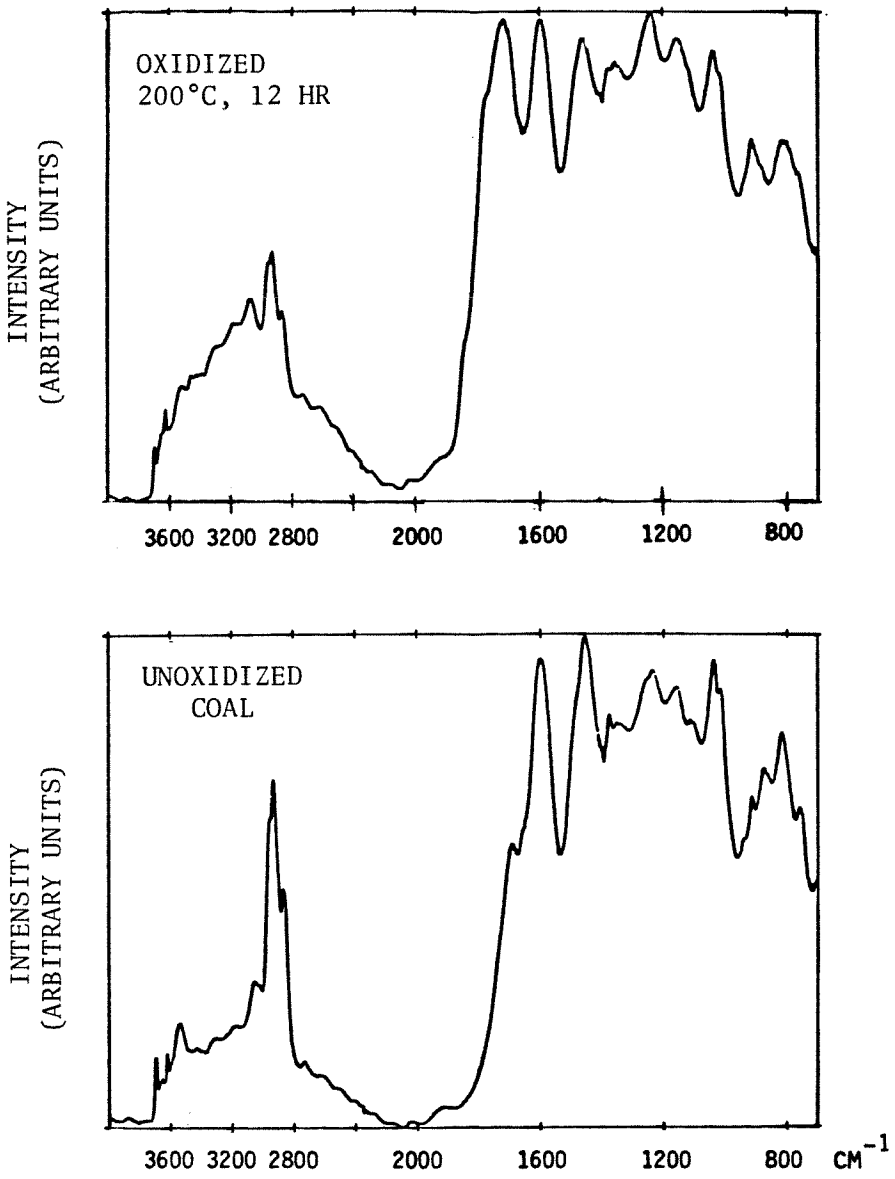

FIGURE 4.5: FTIR Spectra of PSOC 704 Coal Samples

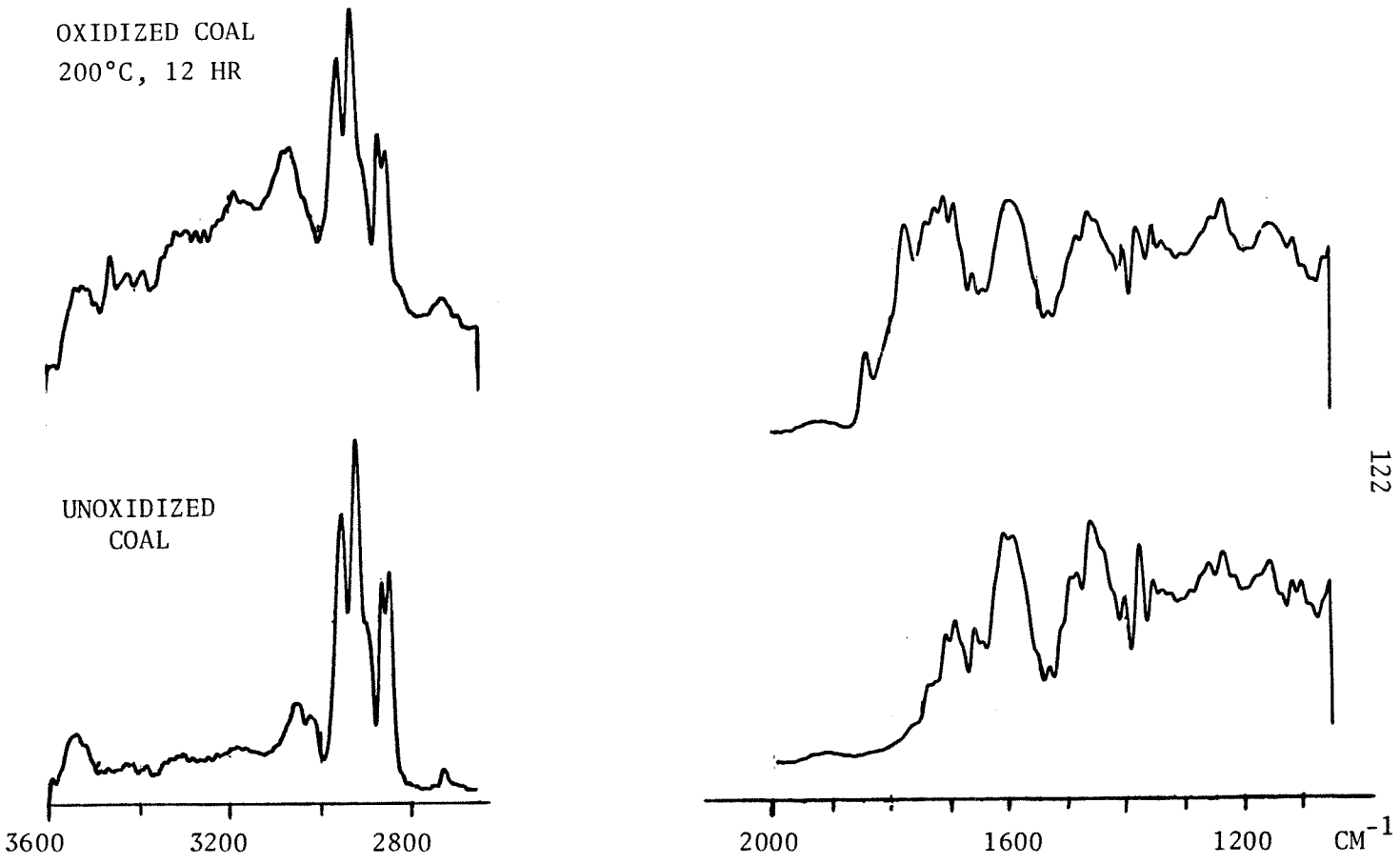

FIGURE 4.6: Fourier Self Deconvolved FTIR Spectra of PSOC 704 Coal Samples

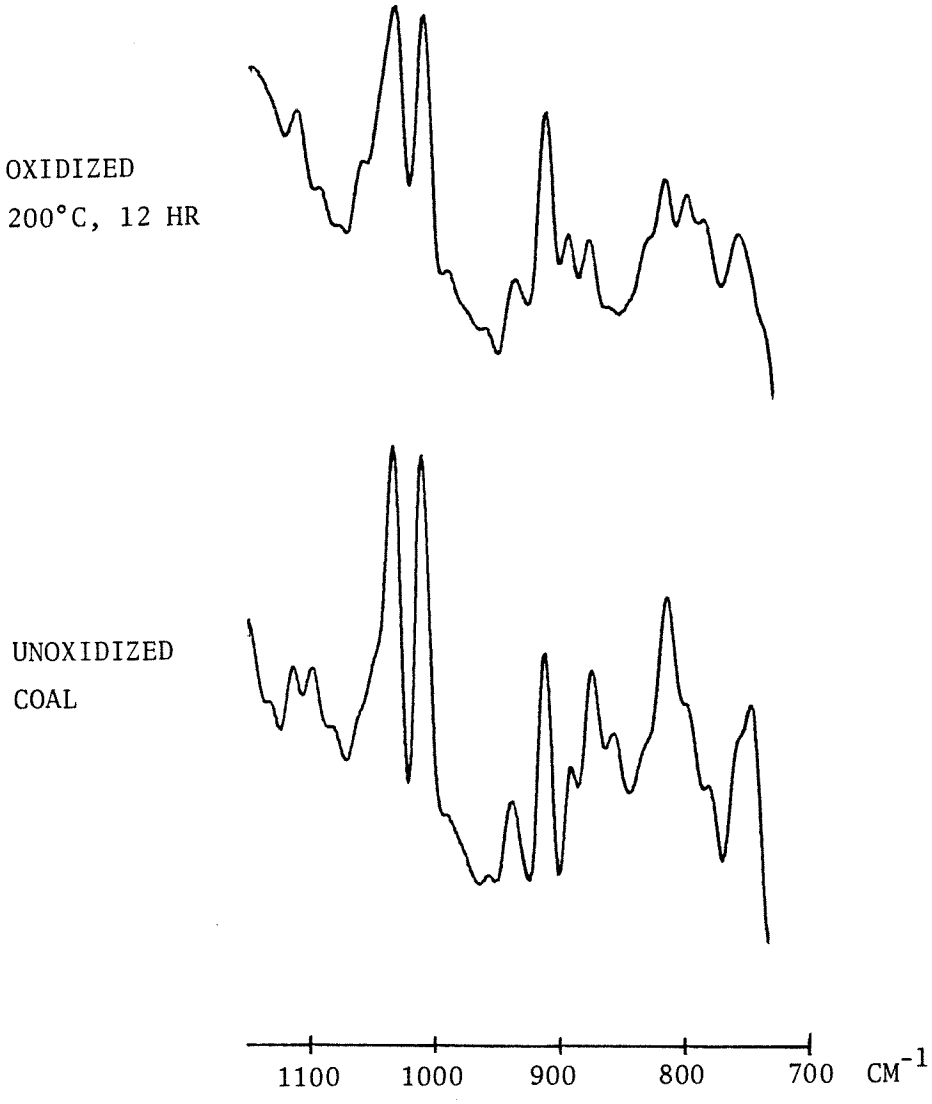

FIGURE 4.7: Fourier Self-Deconvolved FTIR Spectra of PSOC 704 Coal Samples

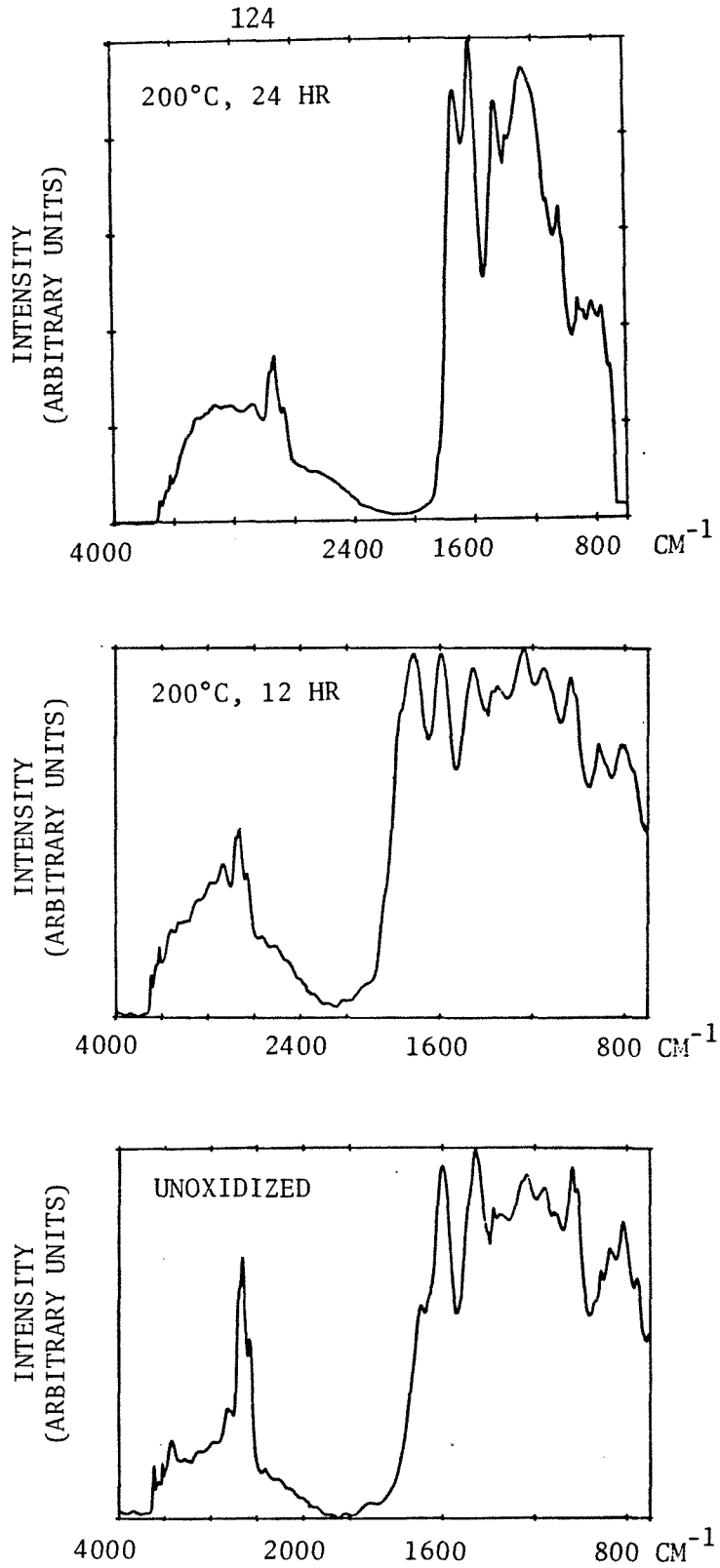

FIGURE 4.8: FTIR Spectra of PSOC 704 Coal Samples

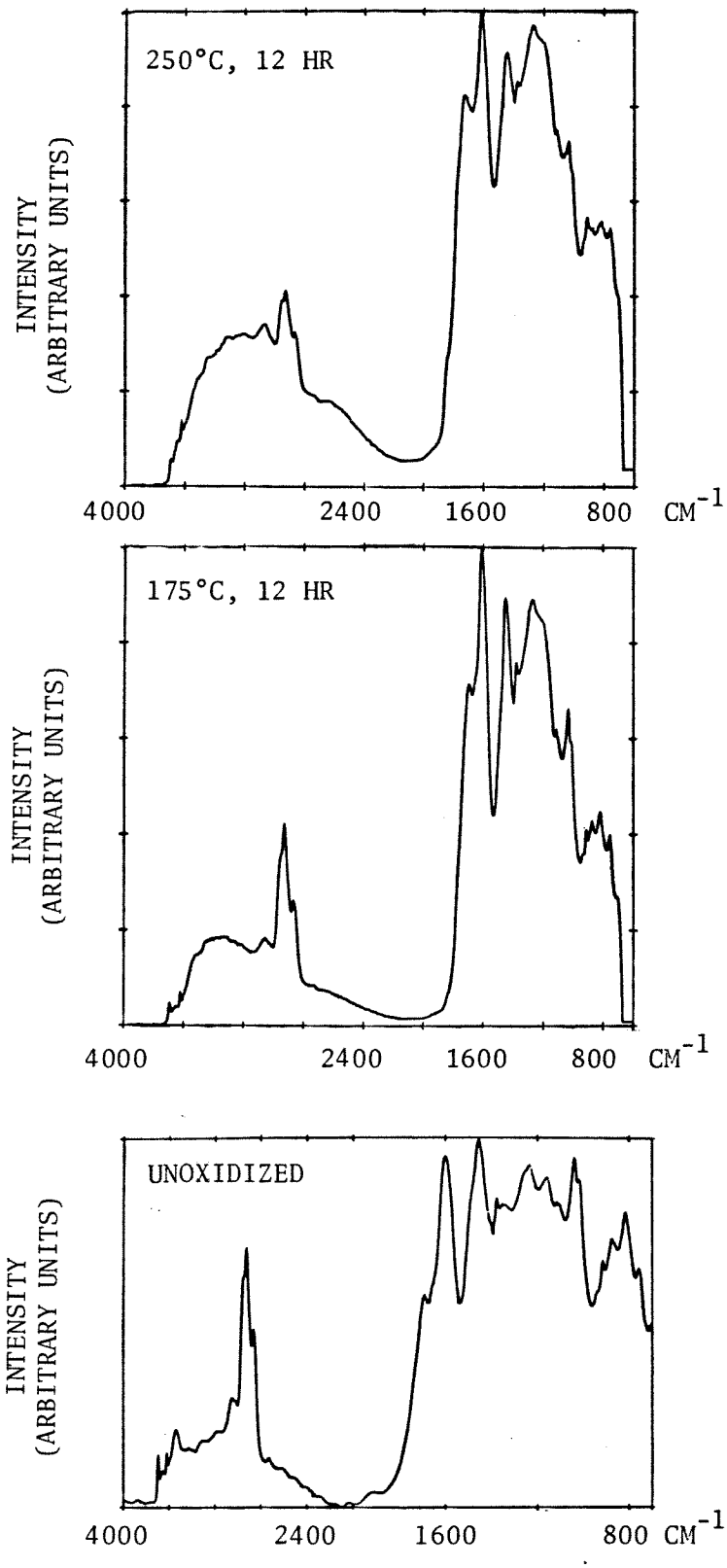

FIGURE 4.9: FTIR Spectra of PSOC 704 Coal Samples

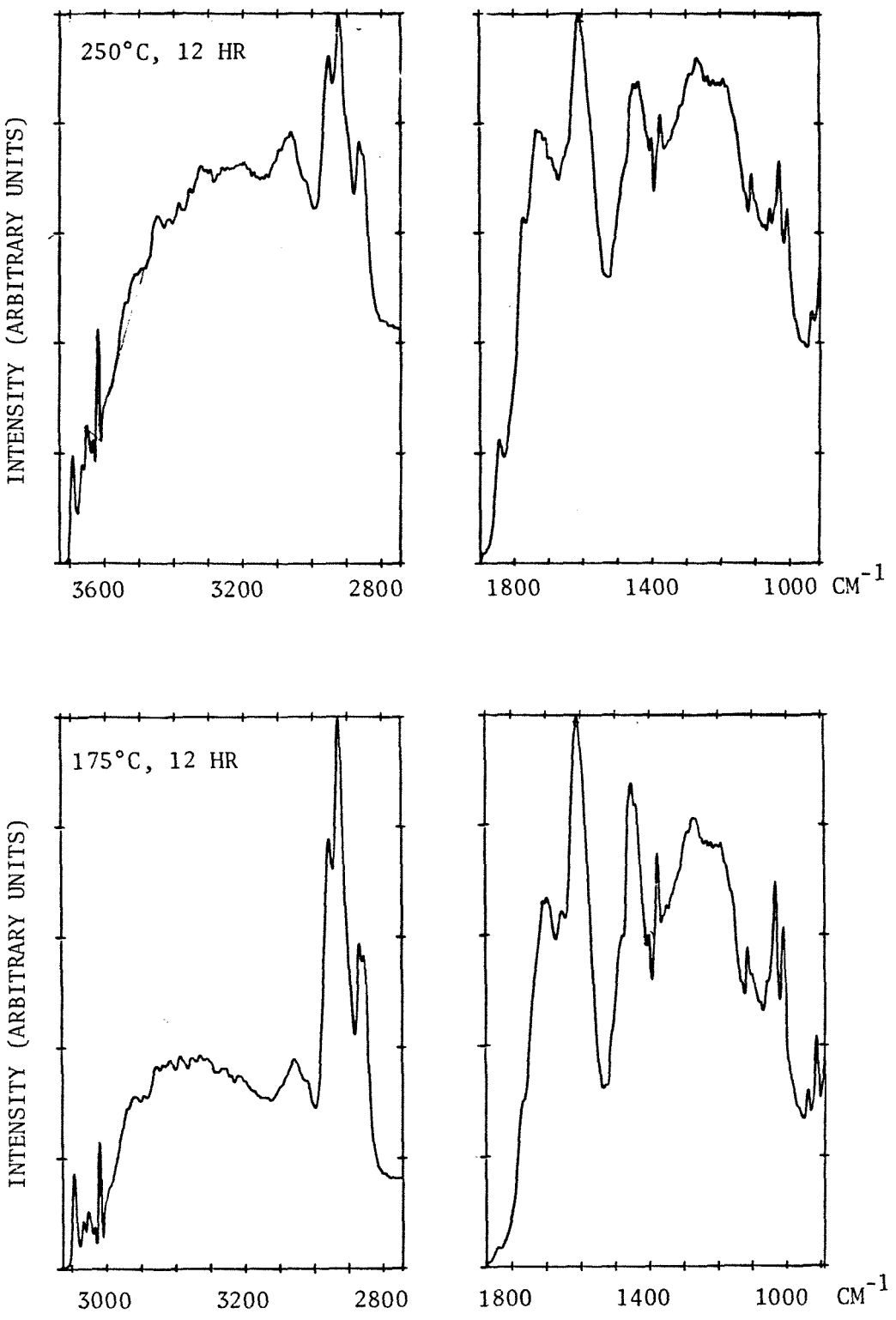

FIGURE 4.10: Fourier Self-Deconvolved FTIR Spectra of Oxidized PSOC 704 Coal Samples

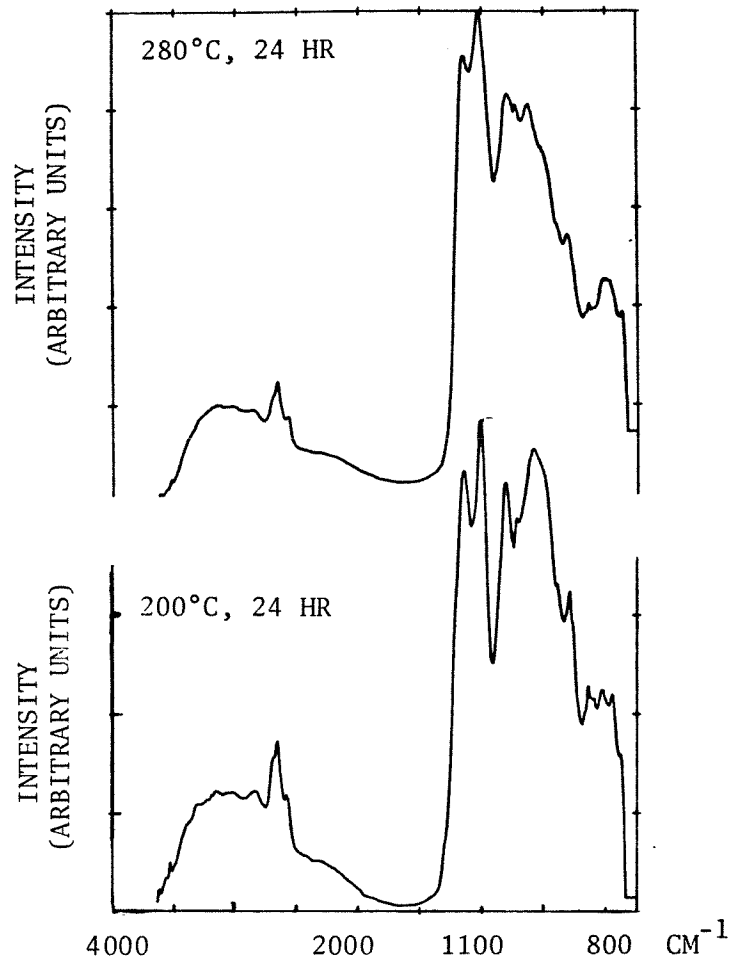

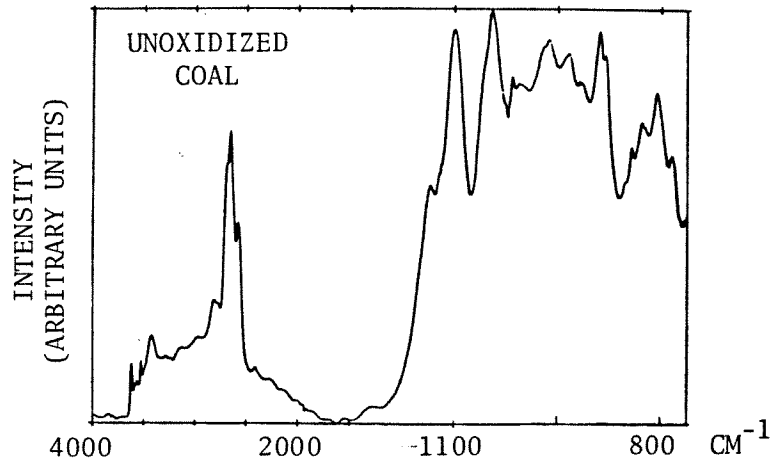

FIGURE 4.11: FTIR Spectra of PSOC 704 Coal Samples

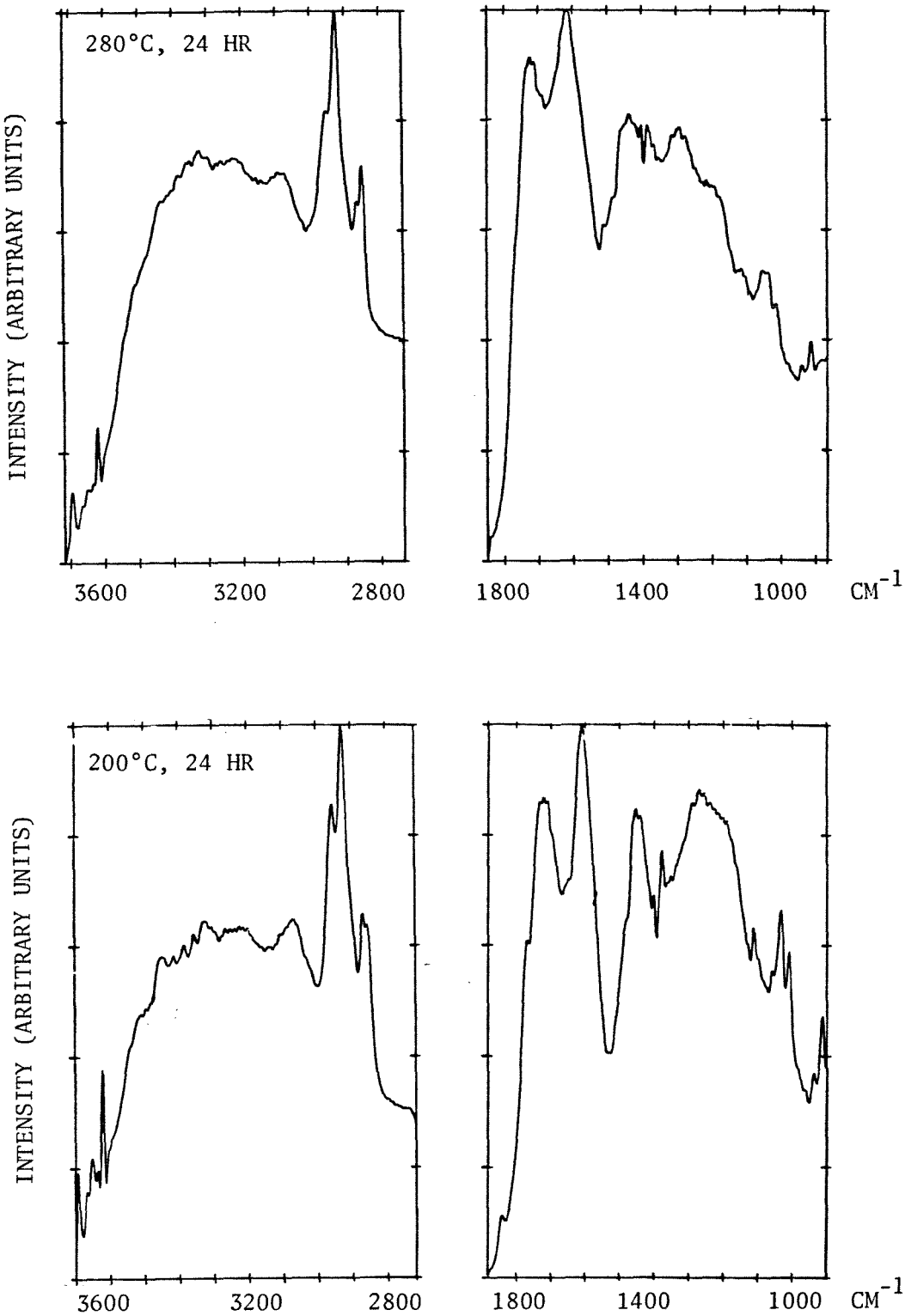

FIGURE 4.12: Fourier Self-Deconvolved FTIR Spectra of Oxidized PSOC 704 Coal Samples

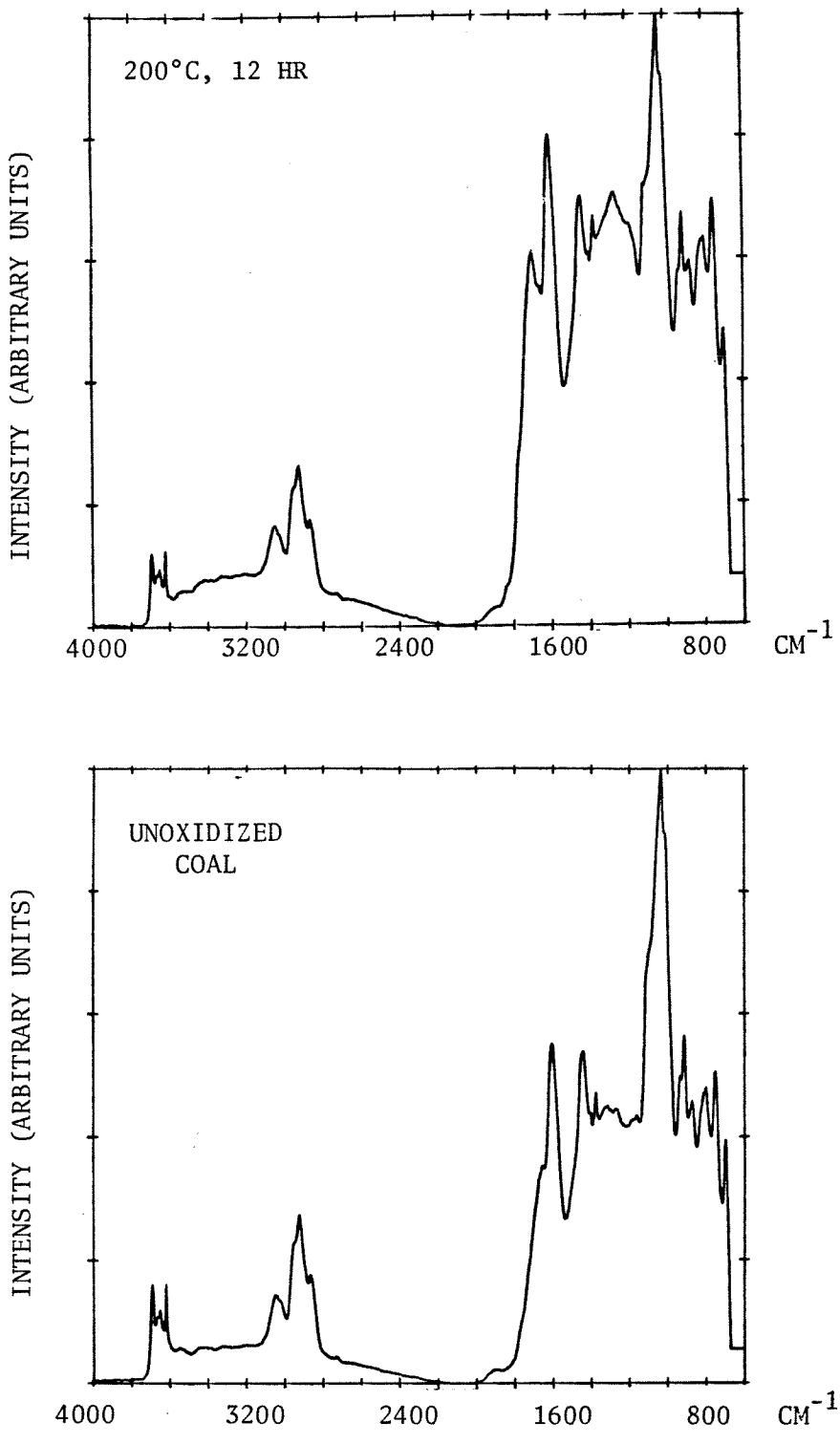

FIGURE 4.13: FTIR Spectra of PSOC 615 Coal Samples

References

[1] Griffiths P.R (Ed), Transform Techniques in Chemistry, Plenum Press, New York, 1978

[2] Painter P.C, Rimmer S.M, Snyder R.W, and Davis A, Appl. Spectrosc., **35**, 102, 1981

[3] Painter P.C, Coleman M.M, Snyder R.W, Mahajan O, Komatsu M, and Walker P.L, Appl. Spectrosc., **35**, 106, 1981

[4] Griffiths P.R, Dept. of Energy Report DOE/PC/30210-T3, 1982

[5] Fuller M.P and Griffiths P.R, Anal. Chem., **50**, 1906,1978

[6] Smyrl N.R and Fuller E.L, in Coal and Coal Products: Analytical Characterization Techniques, ACS Symp. Ser. 205,American Chemical Society, Washington D.C, 1982

[7] Osawa Y and Shih J.W, Fuel, **50**, 53, 1971

[8] Painter P.C, Snyder R.W, Starsinic M, Coleman M.M, Kuehn D.W, and Davis A, Appl. Spectrosc., **35**, 475, 1981

[9] Solomon P.R and Carangelo R.M, Fuel, **61**, 663, 1982

[10] Fuller M.P and Griffiths P.R, Appl. Spectrosc., **34**, 533, 1980

[11] Maddams W.F, Appl. Spectrosc., **34**, 245, 1980

[12] Painter P.C, Recent FTIR and Carbon-NMR Studies of Coal Structure, Penn State Univ., 1983

[13] Fraser R.D. B and Suzuki E, in Physical Principles and Techniques of Protein Chemisty, S.J Leach (Ed), Academic Press, New York, 1973

[14] Vandegniste B.G.M and De Galan L, Anal. Chem., **47**, 2124, 1975

[15] Butler W.L and Hopkins D.W, Photochem. and Photobiol., **12**, 439,1970

[16] Kauppinen J.K, Moffatt D.J, Mantsch H.H, and Cameron D.G, Appl. Spectrosc., fB35, , 1981

[17] Kuehn D.W, Snyder R.W, Davis A, and Painter P.C, Fuel, **61**, 682, 1982

[18] Wang S-H and Griffiths P.R, Fuel, Submitted 1984

[19] Fuller M.P and Griffiths P.R, Appl. Spectrosc., **34**, 533, 1980

5. NMR SPECTROSCOPIC ANALYSIS

5.1 Background and Review

5.1.1 The Carbon Aromaticity of Coal

The carbon aromaticity, f_a , of a sample of coal or of a coal-like material is defined as the ratio of aromatic carbon to total organic carbon in the sample.

Today, ^{13}C-NMR spectroscopy provides the most satisfactory basis for measuring carbon aromaticity. Another method, due to Brown and Ladner [1], has been used for many years to obtain good estimates of f_a. That method requires the results of elemental analysis on the sample, together with integrated intensities on the high-resolution proton magnetic resonance spectrum of an extract of the sample in a suitable solvent, such as methylene chloride, pyridine, or carbon disulfide.

Brown and Ladner defined f_a by the following equation:

$$f_a = \frac{\left(\left(\frac{C}{H}\right) - \frac{f_{ali}^{H}}{(H_{ali}/C_{ali})}\right)}{\left(\frac{C}{H}\right)} \qquad (1)$$

where f_{ali}^{H} is the ratio of aliphatic hydrogen to total hydrogen, which is obtained the integrated intensities of the proton NMR spectrum.

The ratio $\left(\frac{C}{H}\right)$ is determined from elemental analysis, and the ratio (C_{ali}/H_{ali}) is estimated as 2 , implying that the average aliphatic group is the methylene group. The normal range of total $\left(\frac{C}{H}\right)$ ratios for coals requires that, in practice, the aliphatic $\frac{H}{C}$ ratio is restricted to values within the range 1.5-

2.5. It turns out that f_a is not very sensitive to the aliphatic $\frac{H}{C}$ ratio.

There are two major objections to the Brown-Ladner method. First, the need to assume an average $\frac{H}{C}$ ratio for the aliphatic groups introduces some arbitrariness into the calculation. Second, the aliphatic ratio for hydrogen is obtained from high-resolution proton NMR analysis of a solvent *extract* , rather than the coal itself.

Nevertheless Retcofsky *et al.* [2] found surprisingly good agreement between f_a values obtained by the Brown-Ladner method and corresponding results based on ^{13}C-NMR analysis of solvent extracts. The extracts used for ^{1}H and ^{13}C NMR spectroscopy were obtained by Soxhlet extraction of the given sample with pyridine, followed by CS_2 extraction of the pyridine-soluble fraction. They examined five coals as well as a variety of coal-derived liquids such as H-coal, SRC liquid, and SYNTHOIL. Statistical analysis of their results using the " student's *t* " test indicated no difference between the two sets of data, at the 95 % confidence level. The assumed $(\frac{H}{C})$ ratio of 2.0 for the aliphatic component seems therefore to be valid for the solvent extracts of the coals and coal-like materials studied. There remains, however, some doubt as to whether those extracts were chemically representative of the whole coals or coal-like materials from which they were derived.

5.1.2 Nuclear Magnetic Resonance Spectroscopy

The principles of nuclear magnetic resonance are well established [3-5]. When nuclei with non-zero nuclear spin quantum numbers, such as ^{1}H, ^{19}F, and ^{13}C are placed in a magnetic field they can undergo transitions between energy levels, by absorbing electromagnetic radiation in the radiofrequency range, typically

10-100 Hz. The frequency, ν (Hz), is related to the strength of the magnetic field, H, and the gyromagnetic ratio, γ, by the equation

$$\nu = \frac{\gamma H}{2\pi}$$

The local magnetic field experienced by the nuclei depends on the shielding parameter, σ, and the applied magnetic field, H_0.

$$H = H_0 (1 - \sigma)$$

The chemical shift, δ (ppm), of a given peak with reference to a standard signal, such as the proton signal or carbon signal of tetramethyl silane (TMS), is defined by the relation

$$\delta = \frac{\nu_{peak} - \nu_{TMS}}{(Op.Freq.inMHz)}$$

The chemical shift of a particular peak is characteristic of the local environment of the nucleus giving rise to that peak. Under the proper conditions, the area under a peak is proportional to the number of nuclei responsible for the peak. One notable exception to this rule occurs when, in ^{13}C NMR, interactions between ^{13}C nuclei and protons lead to a phenomenon known as the Nuclear Overhauser Effect (NOE). As we shall see later, there are effective techniques for supressing the NOE. Thus NMR can yield quantitative as well as qualitative information about molecular structure.

In recent years pulsed, fourier-transform techniques have been used to produce spectra with significantly higher signal-to-noise ratios than those produced by conventional, continous-wave spectroscopy. As a result, high-resolution NMR spectroscopy of nuclei such as ^{13}C, which have low natural abundance, have become feasible. Further advances in solid-state NMR

techniques have allowed researchers to obtain high-resolution NMR spectra from solids. In our work, we used pulsed, fourier-transform ^{13}C NMR spectroscopy to measure the carbon aromaticity of coal. The fundamentals of this powerful technique are described below.

5.1.2.1 Pulsed, Fourier-Transform NMR Spectroscopy

The technique of pulsed fourier-transform NMR is based on the measurement of the response of magnetic nuclei to a pulsed oscillating secondary magnetic field. In a pulsed NMR experiment, a constant magnetic field $\mathbf{H_0}$ is applied along the z axis, and an oscillating field $\mathbf{H_1}$ is applied along the x axis. After the pulsed signal is turned off, the resulting magnetization of the sample is measured by a detector in the x-y plane. Several hundred decay signals are co-added to average out any transients and give a high signal-to-noise (S/N) ratio. A dedicated computer is used for the acquisition and storage of data, implementation of fast fourier transformations, and plotting of NMR spectra. The fourier transformation of the "free induction decay" gives us the frequency spectrum.

An isolated spinning magnetic moment μ, inclined at an angle ϑ to a static magnetic field $\mathbf{H_0}$, as in Figure 1, will be subject to a torque μ x $\mathbf{H_0}$ in a direction perpendicular to the plane containing μ and $\mathbf{H_0}$. That torque will cause μ to precess about $\mathbf{H_0}$ with angular velocity $\omega_0 = (\gamma H_0)$. If a small additional field, H_1 , rotating at a variable angular velocity ω , is applied in the x-y plane it will create a torque μ x H_1 which will tip μ away from H_0 and increase the angle ϑ. Resonance will occur when $\omega = \omega_0$.

The same observations hold true for an ensemble of magnetic nuclei with a net magnetic moment $\mathbf{M}$. Momentary application of $\mathbf{H_1}$ tips $\mathbf{M}$ and generates

transverse magnetic components M_x and M_y, which decay to zero exponentially, with characteristic time T_2, called the spin-spin relaxation time. This so-called Free Induction Decay (FID) generally has the form of an exponentially-decaying sine wave. At the same time the longitudinal component M_z is restored to its equilibrium value, with characteristic time T_1, the spin-lattice relaxation time. In general, the measured FID consists of the superposition of many exponentially-decaying sine waves, originating from different nuclear environments. The frequency spectrum is obtained by taking the Fourier Transform of the FID.

$$J(\omega) = \int_{-\infty}^{\infty} K(t) \exp(-i\omega t) dt$$

In a practical NMR experiment, spins in different nuclear environments will have slightly different Larmor frequencies. The ideal pulse, able to rotate the different spins by the same angle, should have

$$\gamma H_1 >> 2\pi \Delta$$

where Δ is the range of Larmor frequencies.

The angle through which **M** is tipped determines the size of M_y and hence the intensity of the signal detected by the receiver. This angle is called the flip angle, α, and is related to H_1, γ, and t_p (the length of time for which H_1 is applied) by the equation

$$\alpha = \gamma H_1 t_p$$

In a pulse experiment, t_p is chosen to be much shorter than T_1 . Suitable combinations of $\alpha = (\frac{\pi}{2})$ and $\alpha = (\pi)$ pulses are used to measure T_1 and T_2. For

example, Gerstein *et al.* used the sequence $180^0 - \tau - 90^0$ to measure T_1 and $90^0 - \tau - 180^0$ to measure T_2 for protons in a sample of coal-derived liquid. τ is some arbitrary interval between pulses.

Actually, the optimal value of α is not $\frac{\pi}{2}$. For a system with a long T_1, t_p should be shortened in order to limit the required delay time between successive pulses. The optimal value of α is given by the relation

$$\cos(\alpha) = \exp(-\frac{\tau}{T_1})$$

For ^{13}C NMR, for example, α must be small because the spin-lattice relaxation time is long. For nuclei with long spin-lattice relaxation times, loss of quantitative information may occur if the interval between successive pulses is too short relative to T_1 for nuclei in some given configuration. For example, unprotonated ^{13}C nuclei have longer relaxation times than ^{13}C nuclei attached to protons. These adverse effects of long spin-lattice relaxation may be controlled by adding a paramagnetic species to the sample, thus providing a fast alternative relaxation mechanism for the ^{13}C nuclei.

Short spin-spin T_2 relaxation also increases the spectral line width and thereby reduces the precision of the spectrum. This effect follows from the uncertainty principle:

$$\Delta t \, \Delta E \geq h$$

Setting $\Delta t \geq T_2$ and $\Delta E \geq h \Delta\nu$ gives

$$\Delta \nu \geq \frac{1}{T_2}$$

5.1.2.1.1 Decoupling Techniques Usually we are interested in magnetic resonance experiments involving several nuclei, whose nuclear magnetic resonances are coupled. In a double resonance experiment, two kinds of nuclei are excited simultaneously, using separate radiofrequency magnetic signals. The interaction between the nuclei causes a broadening of the spectral lines and makes high-resolution spectroscopy difficult with liquids and impossible with solids.

Heteronuclear decoupling of protons and carbon-13 nuclei eliminates dipolar broadening. In this method, a second radiofrequency field is applied at or near the Larmor frequency of the protons, thereby inducing rapid transitions between proton energy levels, so that the ^{13}C nuclei see an averaged proton field. The technique is now used routinely in obtaining decoupled, high-resolution spectra of coal-like liquids [6,7]. Because of the low natural abundance of the ^{13}C isotope, carbon-13 homonuclear interactions are relatively small, and so homonuclear decoupling is not neccesary.

Proton decoupling, while essential in order to reduce line broadening, creates, with liquid samples, the often undesirable Nuclear Overhauser Effect, by which the distribution of ^{13}C nuclei among magnetic spin quantum states is distorted and the natural intensities of the peaks altered. In the presence of NOE, integrated peak intensities are not directly proportional to the number of atoms responsible for the respective peaks, and useful quantitative information is thereby lost. The technique of *gated* proton decoupling [8] is used to supress the NOE. In that method, the proton-decoupling field is switched off during relaxation, between pulses.

5.1.3 High Resolution NMR of Solids

Magnetic interaction between nuclei affects the breadth and the shape of NMR spectra. In liquids those interactions are time-averaged to zero because of the rapid random motion of liquid molecules. In solids, however, pairs of neighboring magnetic nuclei interact like magnetic dipoles, such that each of the two nuclei experiences an induced magnetic field due to the presence of the other. As a result, the spectral lines are broadened. For a sample in a static external field H_0, the total static field experienced by each nuclear magnet in the dipole is given by

$$H = H_0 \pm \frac{3}{2}\mu r^{-3} (3\cos^2\vartheta - 1) \qquad (2)$$

where

r is the internuclear separation

ϑ is the angle between r and H_0

In an NMR experiment such a dipole would give rise to a doublet. In general we have an ensemble of nuclear dipoles, interacting together, and the result is that the spectrum is broadened.

If the sample is rotated at high frequency at the "magic angle" of 54.7^0 to the static field, for which angle the quantity $(3\cos^2\vartheta - 1)$ equals zero, the effects of dipolar *magnetic* interaction are removed. Typical spinning frequencies are 2-5 KHz. Magic Angle Spinning (MAS) also reduces peak width by minimizing chemical shift anisotropy. MAS is thus an indispensable requirement in the ^{13}C NMR spectroscopy of solid coal [9].

Unfortunately, MAS usually also produces undesirable spinning sidebands,

symmetrically displaced from the true position of the peak. Those bands lead to difficulties in assigning peak areas, especially when they overlap with genuine peaks in the spectrum. The intensity of the sidebands increases with operating frequency. The displacement of the sidebands is equal to the spinning frequency, expressed relative to the operating frequency, in parts per million. Therefore a low operating frequency and high spinning rate would minimize the overlap and intensity of the spinning sidebands.

In solids, as in liquids, rare spins (S) can be decoupled from neighboring abundant spins (I) by applying a strong rf field to the abundant spins, in a so-called Bloch delay experiment. Solids, however, require a much stronger decoupling field than liquids. High-power decoupling can only be applied for short periods of time because it tends to cause significant heating of the sample. To avoid overheating, very long accumulation times are neccesary. Also, gated decoupling must be used in order to avoid the effects of NOE.

The Cross Polarization technique [8] is especially suited to systems in which one type of nucleus is more abundant than the other, such as ^{1}H and ^{13}C. In the technique, polarization is transferred from the abundant species to the rare species when the I and S spins precess at the same frequency in their respective rotating frames.

$$\omega = \gamma_I H_{1,I} = \gamma_S H_{1,S} \qquad (3)$$

Under that condition, the Zeeman energy levels of the two nuclei are matched, and so energy can be transferred from I nuclei to S nuclei. Equation (3) is known as the Hartmann-Hahn condition. In addition to removing I-S dipolar coupling, the I-spin decoupling field can be used to enhance the sensitivity of the dilute spin, S, by use of the cross-polarization (CP) technique.

One protocol for implementing cross polarization is as follows :-

1. Allow the I spins to become magnetized in the static field H_0.

2. Rotate the resulting magnetization so that it coincides with the $H_{1,I}$ field, in the rotating frame of reference. The I spins are then said to be " spin-locked ".

3. Apply a $H_{1,S}$ rf field such that the Hartmann-Hahn condition (Equation (3)) is met, allowing transfer of polarization from I to S. The contact time for cross polarization, t_c, must be established by experiment.

4. Switch off $H_{1,S}$ and record the FID of the S spins. The FID acquisition time, t_a, should be long enough to allow all the nuclei to undergo relaxation. While the S spins decay to zero, the $H_{1,I}$ field is left on, and used to decouple the I spins.

5. After a delay of a few seconds, turn off $H_{1,I}$ and repeat the whole sequence over and over again, co-adding the FID signals. If a multiple-contact experiment is to be run, steps 3 and 4 are repeated several times before $H_{1,I}$ is turned off. The number of multiple pulses is limited by the decay of the spin-locked I magnetization, which is characterized by a relaxation time $T_{1\rho}$, called the rotational-frame spin-lattice relaxation time.

Following from the Hartmann-Hahn condition, the intensity of the S signal is enhanced by a factor equal to the ratio of the gyromagnetic ratios of I and S spins. In a ^{1}H- ^{13}C cross-polarization experiment, for example, the carbon-13 signal is enhanced by a factor of 4. The time required to effect cross polarization depends on the particular nuclear invironment. Thus non-protonated ^{13}C nuclei undergo much slower cross-polarization than do protonated ^{13}C nuclei.

The combination of CP with magic-angle allows us to obtain spectra having sharp peaks and narrow lines. Any structural information that could be obtained from observing the effects of heteronuclear interactions is thereby destroyed, however.

5.1.4 Review of NMR Studies of Coal and Coal Products

NMR analysis of coal-derived liquids provides much more spectroscopic information than is obtainable from NMR analysis of solid coal. Of course, results obtained with liquids are not always directly applicable to the parent solid coal. Nonetheless useful qualitative, and even semi-quantitative, conclusions about coal structure can be inferred from the analysis of coal-derived liquids. Proton NMR spectroscopy has been successfully applied to the qualitative and quantitative analysis of coal-derived liquids. Solid coal samples, however, are not accessible to proton NMR analysis. With solid coal samples, the amount of qualitative information is generally limited to the division of the spectrum into two regions corresponding to resonances of aromatic and aliphatic carbon, respectively. The carbon aromaticity can then be calculated using the integrated peak areas of the two regions.

5.1.4.1 Coal-Derived Liquids

Several groups of researchers obtained high-resolution ^{1}H NMR spectra together with proton-decoupled ^{13}C-FT-NMR spectra of coal-derived liquids [2,6,9,11] and were thus able to characterize the distribution of hydrogen in those liquids and to assign the chemical shifts of different peaks in the ^{13}C spectrum .

Bartle *et al* [6] started with a supercritical-toluene extract of a low-rank coal and extracted it with petroleum ether and with benzene. About 85 % of the

original extract was soluble in either solvent. The soluble liquids were separated into different fractions using gel-permeation chromatography, and the fractions were then analyzed using high-resolutuon ^{1}H NMR, proton-decoupled ^{13}C FT-NMR, infra-red spectroscopy, and mass spectrometry. From the spectrum, different proton environments were distinguished - aromatic and phenolic, olefinic, methylenic, hydrogens on carbon atoms α to aromatic rings (H_α), hydrogens on carbon atoms β to aromatic rings (H_β), and hydrogens on methyl carbons and on carbons γ or further from aromatic rings. Quantitative information was obtained from the proton NMR spectrum, based on the proportionality between peak areas and numbers of relevant protons. Several peaks in the ^{13}C NMR spectrum were also assigned: alkyl carbon, olefinic carbon, C-OH, C-O of heterocyclic and aromatic ethers, aromatic C-H, and aromatic C-C. Owing to the nuclear overhauser effect, the atomic distribution of carbon among different nuclear environments could not be determined.

Yokoyama *et al.* [10], working with the heavy-oil product of coal hydrogenation, also used solvent fractionation and gel-permeation chromatography to produce a large number of liquid fractions which were then analyzed by ^{1}H and ^{13}C NMR. They sought to measure carbon aromaticities (f_a) using peak areas of the ^{13}C spectrum and to compare them with f_a values obtained using the Ladner-Brown method. The two sets of figures were in fair agreement but, as the authors themselves acknowledged, the ^{13}C spectra could not be justifiably used for quantitative calculations as long as the NOE was not somehow suppressed. Therefore the reported agreement between the two sets of f_a values was probably fortuitous. In subsequent work, using liquids produced by coal hydrogenation, Yokoyama and his colleagues [11] successfully used gated proton decoupling to suppress the NOE in ^{13}C NMR, and were thus able to calculate the distribution of carbon atoms among different aliphatic and

aromatic environments. The quantitative results were also used to estimate relative amounts of oxygen and nitrogen attached to carbon atoms.

Yoshida *et al.* [12] performed ^{13}C NMR spectrometry of the liquid produced by the hydrogenation of an oxygen-rich brown coal. Chemical shifts were measured relative to TMS and the spectrum was divided into several regions, and assigned on the basis of known ^{13}C peaks for a series of oxygen containing aromatic model compounds. Chemical shifts of 93 ppm and below were assigned to aliphatic carbon. The range 171-240 ppm was associated with resonances due to carbonyl, aldehyde, and carboxylic groups. Aromatic resonances were assigned to chemical shifts in the range 93-171 ppm. Within the aromatic region, the 93-148 ppm range was assigned to carbon atoms attached to hydrogen or connected to substituted aliphatic , alkyl, and benzylic carbons while the region from 148 to 171 ppm was assigned to aromatic carbon atoms bound to hydroxyl, methoxyl, and aryl-ether oxygen atoms. Using peak areas, carbon aromaticities were calculated. Those calculations, however, suffered from the same error which marred the work of some earlier workers. They were invalid because no steps had been taken to suppress the nuclear overhauser effect and hence restore the proportionality between peak areas and corresponding numbers of atoms.

5.1.4.2 Solid Coals

When ^{13} C spectra of solid coal were first reported, a number of researchers examined them in terms of their similarity to the spectra of the corresponding coal-liquefaction product. Zilm *et al.* [13] found that the artificially-broadened ^{13}C NMR spectrum of the liquid had the same general shape as the spectrum of the solid, but that the fine structure of the original spectrum of the liquid was

quite different from that of the solid. Not much additional information was available from solid state ^{13}C NMR spectra until high-resolution techniques were developed.

Vanderhart and Retcofsky [14] reported the first high-resolution ^{13}C-NMR spectrum of a coal in 1976. Since then the technique has been developed and widely applied [14-19]. By the use of cross polarization (CP) and magic-angle spinning (MAS) quantitative estimates of coal aromaticity, reproducible to within less than ± 2 %, are now obtainable. In addition, we can distinguish between resonances due to carbons attached to hydrogen atoms and those due to unprotonated carbon atoms by introducing a delay before the proton decoupling signal [15,18,19]. The technique, known as " dipolar de-phasing ", or " delayed decoupling " depends on the fact that carbons attached to hydrogen atoms have shorter spin-spin relaxation times (T_2) than do unprotonated carbons.

In recent years, several groups have investigated the factors that determine the quantitative reliability of solid state ^{13} C NMR spectra. Sullivan and Maciel [16] conducted detailed investigations into the effects of contact time and rotational-frame relaxation time on the reliability of f_a values for a U.S bituminous coal. In the CP experiment, the contact time (t_C) must be long enough to allow polarization to be transferred from the protons to the carbon atoms. Because of the heterogeneous nature of coal, carbon atoms in different environments have different characteristic CP times, t_{CH}. On the other hand, the magnetization of the spin-locked protons decays exponentially in a characteristic time $T_{1\rho H}$, the rotational-frame spin-lattice relaxation time, which must be longer than t_C in order that all the carbon atoms should be counted. The magnetization of the carbon atoms also decays with $T_{1\rho C}$ which, however, is

about an order of magnitude longer than $T_{1\rho H}$ [16]. Thus the desired condition for analytical reliability is

$$t_{CH} < t_C < T_{1\rho H} \quad (4)$$

Sullivan and Maciel showed that the minimum required contact time for quantitative measurement of f_a was 0.5 ms, and that the plot of f_a vs. contact time reached a plateau at about 1 ms. They also measured the intensity of the ^{13} C signal as as they varied the contact time from 20 μs to 7 ms. The signal intensity and the shape of the ^{13} C spectrum remained constant from t_C = 1 ms to t_C = 3 ms, indicating that significant proton rotational-frame relaxation had not set in during the first 3 ms. Using the sequence developed by Schaefer and Stejskal [17], they also measured proton $T_{1\rho H}$ values as 3.8 ± 0.5 ms for the aromatic fraction and 4.4 ± 0.5 ms for the aliphatic fraction, values which were consistent with the results of the variable-contact-time experiments. Thus they showed that the requirements of equation (4) had been met. Further, the f_a values they obtained with CP/MAS agreed well with values measured using MAS and high-power decoupling, in Bloch decay experiments. Given that the two kinds of experiment involved different relaxation mechanisms, they provided mutual confirmation. Thus the authors concluded that, for the bituminous coal studied, reliable values of coal aromaticity could be derived from CP/MAS measurements.

Packer *et al.* [15] also considered the validity of f_a data calculated from the relative areas of aromatic and aliphatic spectral peaks of ^{13}C-NMR spectra of coals and coal-like materials, using a British bituminous coal and its liquid extract. They noted that the presence of free radicals in a solid coal sample could significantly shorten $T_{1\rho H}$ values. When they measured f_a values for solid coal samples they found that the measured f_a value increased with contact time,

reaching an asymptotic value at 1 millisecond (ms), which implied that, to obtain reliable f_a values for that coal, the contact time had to be at least 1 ms. For the coal studied they also found that, for some protons, the measured rotational-frame relaxation time $T_{1\rho H}$ was shorter than the cross polarization contact time. Considering that the aromatic carbons would polarize more slowly than the aliphatic, and thus tend to be undercounted, they concluded that, for such a coal, measured values of f_a could be lower than the correct values by as much as 0.05-0.15.

Dipolar de-phasing allows us to observe ^{13}C-NMR spectra of unprotonated carbon atoms. Havens *et al.* [19] used dipolar de-phasing in their studies of a series of vitrinites, and found that the quarternary aromatic carbon content of the vitrinites decreased with total carbon content. That finding was confirmed by the observed agreement between values of aromatic hydrogen content as estimated by Fourier-Transform Infra-Red (FTIR) spectroscopy and those calculated from the amount of protonated carbon, obtained by NMR. The authors also took CP/MAS ^{13}C spectra of a high-volatile " A " bituminous coal which had been oxidized in an oven at 140 deg C for periods of up to 16 days. Carbon aromaticity values (f_a) were calculated from integrated peak areas. For the first few days there was no appreciable change in f_a but after 16 days f_a had increased from 0.68 to 0.75. This result confirmed the FTIR results of Painter *et al.* [21], who had noted that the aliphatic fraction of the coal was preferentially consumed during oxidation, but contradicted the reported findings of MacPhee and Nandi [20] who had oxidized a coal at 105 deg C and reported decrease in carbon aromaticity, based on ^{13}C-NMR data. Quite possibly, the NMR experimental technique used in ref [20] was incorrect.

Dipolar de-phasing was also used by Hagaman and Woody [18] to resolve the

aliphatic and aromatic peaks in the spectra of solid bituminous coal into separate contributions attributed to carbons attached to oxygen atoms, carbons connected to protons, and quaternary carbons. Based on peak areas, they concluded that the relative amounts of carbonyl and quinonic carbon in the raw coal were not significant.

5.2 ^{13}C - NMR Analysis of Coal Samples

Past work on air oxidation of coal has indicated that the aliphatic fraction of coal is preferentially attacked by oxygen, producing CO and CO_2. Havens *et al.* [19] found evidence for the preferential oxidation of aliphatic carbon atoms by oxygen at 140^0 C. They were not able to establish whether any aromatic carbon atoms were lost during air oxidation at that temperature because they did not perform carbon-balance calculations based on chemical analysis of raw and oxidized coal. Lahiri *et al.* [22] believed that a basic change in mechanism occurred at 225^0 C and attributed that change to the incipient oxidative destruction of aromatic rings.

In our investigations we used ^{13}C-NMR to measure f_a for a bituminous coal oxidized in a fluidized-bed reactor at temperatures ranging from 175 to 280^0 C. The carbon content (C), ash content (Ash), and iron content (Fe) of the samples were determined using methods described in chapter 2. We intended to use ash and iron as independent tracers, to calculate weight losses due to oxidation and thus perform carbon-balance calculations.

We obtained relevant data on the following samples of PSOC 704 coal, which we had obtained from the Penn State Coal Bank.

1. Raw, unoxidized coal

2. Coal oxidized at 175^0 C for 12 hours

3. Coal oxidized at 200^0 C for 12 hours

4. Coal oxidized at 200^0 C for 24 hours

5. Coal oxidized at 250^0 C for 12 hours

6. Coal oxidized at 280^0 C for 24 hours

5.2.1 NMR Experimental Procedure

^{13}C spectra of the solid coal samples were recorded by Mr Mark Davis at the Colorado State University Regional NMR Center at Fort Collins, Colorado. The center is funded by National Science Foundation Grant Number CHE-8208821. Cross Polarization (CP) and Magic Angle Spinning (MAS) were used. Chemical Shifts were measured relative to tetramethylsilane (TMS).

The ^{13}C frequency was 15.1 MHz and the proton frequency was 60 MHz. The MAS spinning rate was 2.5 kHz. As can be seen in Figure 5.3 , the values of those parameters were sufficient to minimize the intensity of the spinning side bands and the extent of their overlap with the main peaks.

The experimental protocol used was essentially the single-contact CP procedure described earlier in this chapter, with an added provision for delaying the decoupling signal and thus obtaining a spectrum due only to the unprotonated carbon atoms, the technique known as " delayed decoupling " or " dipolar de-phasing ". The repeated sequence of steps included spin locking of the protons, cross-polarization, delaying the proton decoupling signal if desired, proton decoupling and measurement of the ^{13}C FID signal, and relaxation delay. The sequence is shown schematically in Figure 5.2.

Most of the experiments were performed using a contact time of 1 millisecond (ms) and a repetition time of 1 second. The suitability of these values was tested by running additional experiments with 2 ms contact time and 2 seconds repetition time, respectively. The acquisition time, t_A , was 32 ms and the duration of the proton pulse, t_P , was 5.5 μs. Spectra were obtained by co-adding data from 10,000 scans.

5.2.2 Determination of Aliphatic and Aromatic Carbon Consumption

5.2.2.1 Calculation

We estimated the percentage consumption of aromatic and aliphatic carbon using equations (5) and (6) below. C is carbon content and T the content of some tracer, such as ash. The subscripts *i* and *f* refer to the initial and final states, respectively.

$$\text{Fraction aromatic C consumed} = \left[\left(\frac{C\,f_a}{T}\right)_i - \left(\frac{C\,f_a}{T}\right)_f\right] \Big/ \left(\frac{C\,f_a}{T}\right)_i \qquad (5)$$

$$\text{Fraction aliphatic C consumed} = \frac{\left[\left(\frac{C\,(1-f_a)}{T}\right)_i - \left(\frac{C\,(1-f_a)}{T}\right)_f\right]}{\left(\frac{C\,(1-f_a)}{T}\right)_i} \qquad (6)$$

Thus the extent of oxidation of aromatic and aliphatic carbon was estimated, as a function of time and of temperature.

5.3 Results and Discussion

5.3.1 Results

5.3.1.1 Chemical Analysis of Coal

Results of chemical analysis of the coal samples for iron and ash are shown in Table 5.1. The iron analyses were performed by Galbraith Laboratories Inc., of Knoxville Tennessee, using Atomic Absorption, according to ASTM Method D 3682-78. Officially, this method determines the iron content of the ash to within 2 % . Our coal samples contained 8.2-11.0 % ash; therefore the iron analyses should have been reproducible to within ± 0.2 %. Actually,the results were not so reproducible. Ash contents were determined in our laboratory. The analytical procedure used is described in Chapter 3. Iron and ash analyses were intended to be used to estimate the relative masses of organic matter in the coal samples, and thereby calculate the mass of coal consumed in oxidation.

Results of the iron analyses were generally rather inconsistent. The figures in Table 5.1 are best estimates based on triplicate analytical data. Figures for two of the samples showed only a ± 2 % (relative) variation, but the rest varied by 10-50 %. The reliability of the iron data is indicated in Table 5.1. The wide variability of the iron analyses was probably due to non-uniformity in the iron contents of particles in a given sample of coal, which could occur if different-sized grains of pyrite were attached to the coal particles during grinding.

Ash content data were more consistent than the iron analyses, The measurement error (relative basis) was about ± 3 %. We therefore based our calculations on those results.

5.3.1.2 Carbon Aromaticity

Under the conditions used to obtain our solid state ^{13} C NMR spectra, the area under a given peak was proportional to the number of carbon atoms giving rise to that peak. Normalization routines developed at the Colorado State University

NMR Center were used to correct for any baseline drift in the spectra.

The ^{13} C NMR spectrum of coal, such as that shown in Figure 5.3, broadly consists of an aromatic region ranging from 0 to 80 ppm and an aromatic region between 80 and 220 ppm. Olefins, dienes, quinones, carbonyl groups and carboxylic acids also show up in the aromatic region. Those functional groups, however, occur in fairly small concentrations and the carbonyl and carboxylic groups have relatively low ^{13} C NMR intensities in raw coals.

Spinning sidebands arising from the aromatic envelope appeared at 300 ppm and at -40 ppm, well resolved from the main aromatic and aliphatic peaks. In estimating the carbon aromaticity we added the areas under those lobes back into the aromatic peak area. A trace of integrated peak area as a function of chemical shift is also shown in Figure 5.3.

As a rule, in order to obtain reliable, quantitative ^{13} C NMR spectra of coal, the contact time for cross polarization must be long enough to allow complete transfer of magnetization from the protons to all the carbon atoms in the sample, and the repetition time must be sufficient for spin-lattice relaxation to be completed before the proton pulse is applied again. In our experiments the contact time (t_C) was 1 ms and the repetition time (t_R) was 1 second. We also ran two additional spectra of the raw PSOC 704 coal with a contact time of 2 ms and a repetition time of 2 seconds, respectively. Those spectra are shown in Figure 5.4 and are virtually indistinguishable from the spectrum taken with t_C = 1 ms and t_R = 1 second Aromaticity values based on integrated areas for the three peaks in Figure 5.4 are shown in Table 5.2 ; the differences between them amount to less than 1 %, well within the measurement error of ± 2 %.

5.3.1.3 Effect of Oxidation on ^{13} C NMR Spectra

Results of chemical analysis and FTIR spectroscopy had shown that oxidation consumed mainly aliphatic carbon and produced phenolic, carboxylic, and other C-O functional groups. The solid state ^{13} C NMR spectra of oxidized coal samples shown in Figures 5.5, 5.6, and 5.7 clearly indicate that the aliphatic-peak area decreases with increasing oxidation, while the peaks associated with phenolic and carbonyl groups increase in intensity.

Figure 5.5 shows the gradual reduction in relative aliphatic carbon content with oxidation time at 200 ^{0} C. Simultaneously, the intensity of the small carbonyl peak at 192 ppm slowly increases. The size of the aliphatic peak also decreases with increasing oxidation temperature, as is shown in Figure 5.6. The increase in carbon aromaticy accompanying oxidation is clearly shown by the f_a values in Table 5.3. For coal oxidized at 280 ^{0} C for 24 hours, the aliphatic peak almost disappears, as we see in Figure 5.7, while the intensities of the phenolic peak at 154 ppm and carbonyl peak at 192 ppm increase.

The increase in aromaticity with oxidation confirms the findings of Havens *et al.* [19] and again contradicts the published work of McPhee and Nandi [20]. While the NMR data of Havens *et al.* and the FTIR data of several authors, including Painter *et al.* [21], have shown that aliphatic carbon is preferentially consumed, there remains some ambiguity as to whether any aromatic carbon is also consumed. Havens *et al.* believed that no aromatic carbon was consumed when a bituminous coal was oxidized at 140 ^{0} C for 16 days. Lahiri *et al.* [22] believed that aromatic material in coal was consumed only above a transition temperature, which they believed to be 225 ^{0} C.

We used equations (5) and (6) to calculate percentage aromatic and aliphatic consumption for each of our oxidized coal samples, based on f_a values obtained

from ^{13} C NMR peak areas and on data of carbon content and ash content. The results, shown in Table 5.3, indicated that some aromatic carbon is consumed even at 175 ^{0} C, with the relative consumption of aliphatic and aromatic carbon increasing with temperature.

The absolute error in the calculated values of percent aliphatic carbon consumption and percent aromatic carbon consumption was estimated as ± 3 % . That estimate was obtained using a procedure which utilized standard results from the theory of variances. The procedure is described in Appendix B. In that calculation, we used best estimates of measurement errors, on a relative basis, for ash content (± 3 %), carbon aromaticity (± 2 %), and carbon content (± 0.4 %).

Contrary to the results of Lahiri *et. al.*, there was no evidence of a transition temperature at which the oxidation of aromatic carbon supposedly would begin.

5.3.1.4 Effect of Delayed Decoupling

By introducing a 50 μs delay in the proton decoupling signal, we were able to obtain a spectrum representing carbonyl and quaternary carbon atoms only. The appropriate delay in the decoupling signal was chosen on the basis of past experience with bituminous coals at the Regional NMR Center.

Figure 5.8 and 5.9 show standard and delayed-decoupling spectra of raw and oxidized PSOC 704 coal, respectively. In Figure 5.8 we see that the aromatic portion of the raw coal has the higher proportion of unprotonated carbon atoms, consistent with the conventional view that a part of the aromatic carbon in coal is composed of fused polycyclic rings.

The proportion of unprotonated carbon atoms cannot simply be calculated

from ratios of corresponding areas in the delayed-decoupling and standard spectra because NMR signals from unprotonated carbons in different environments may have different intensities. A semi-quantitative analysis of corresponding peak areas , however, is still valid and the comparison of spectra from different samples can provide useful information. In Figure 5.10 we note significant differences between delayed-decoupling spectra of the raw coal and the oxidized coal. Coal oxidation intensifies the carbonyl peak at 180-220 ppm and the phenolic peak centered around 154 ppm, while nearly all the quaternary aliphatic carbon is consumed.

5.3.2 Discussion

The main findings from this ^{13}C NMR study of the oxidation of an Eastern high-volatile bituminous coal also apply to other types of coal. Our results clearly show that coal aromaticity is increased by oxidation. Estimates of percentage consumption of aliphatic and aromatic carbon, though subject to some error, indicate that both types of carbon are oxidized at all temperatures down to 175 ^{0} C. Our data disprove Lahiri's [22] theory that aromatic rings are oxidized only above 225 ^{0} C. The data do show that aliphatic carbon is consumed about three times faster than aromatic carbon. The spectra taken with delayed proton decoupling show that, in the raw coal, the aromatic fraction has the greater proportion of unprotonated carbons. With oxidation, the quarternary aliphatic carbon is consumed much faster than the aromatic.

Based on the identity of the aromaticity values obtained from spectra taken using different contact times, we believe our reported values of carbon aromaticity to be reliable. The extensive work of Sullivan and Maciel [16], using a similar Eastern high-volatile bituminous coal, showed that proton rotational-frame relaxation times ($T_{1\rho H}$) for that coal were long enough to ensure

quantitative reliability of the ^{13} C NMR spectrum, and showed that the f_a vs. t_C curve reached a plateau at $t_C = 1$ ms and then remained flat for $t_C < T_{1\rho H}$. Strictly speaking, the detailed investigations of ref [16] should be repeated for each particular coal studied, to establish unequivocally the quantitative reliability of the spectral data. In our case, however, such investigations were not practical.

Possible small errors in the measured f_a values would not significantly alter our overall conclusion that both aromatic and aliphatic carbon are consumed at 175-280 ^{0} C, with the consumption of the aliphatic carbon being faster than that of the aromatic.

Table 5.1

Analytical Data of PSOC 704 Coal Samples

Sample		Analytical Data		
Oxidation Temp (^{0} C)	Hours Oxidized	Iron Content (Percent)	Reliability	Ash (Percent)
-	-	4.13	Good	8.24
175	12	-	-	8.54
200	12	4.06	Poor	8.80
200	24	4.41	Poor	9.24
250	12	4.28	Poor	10.05
280	24	5.49	Good	10.95

Table 5.2

Effect of Repetition Time and Contact Time on Apparent Aromaticity of PSOC 704 Coal Sample

Repetition Time (seconds)	Contact Time (milliseconds)	Carbon Aromaticity
1.0	1.0	0.702
1.0	2.0	0.708
2.0	1.0	0.706

Table 5.3

Analytical Data, Carbon Aromaticity, and Percent

Carbon Consumption for Oxidized PSOC 704 Coal

Oxidation Conditions		Carbon Content	Ash Content	Carbon Aromaticity	Carbon Consumed (%) (± 3 %)	
Temp (^{0} C)	Time (hr)	(%)	(%)	f_a	Aromatic	Aliphatic
-	-	75.82	8.24	0.70	-	-
175	12	72.64	8.54	0.71	6.2	10.6
200	12	69.28	8.80	0.78	4.7	37.3
	24	66.64	9.24	0.80	10.4	47.8
250	12	63.96	10.05	0.82	19.0	58.5
280	24	61.96	10.95	0.86	24.4	71.3

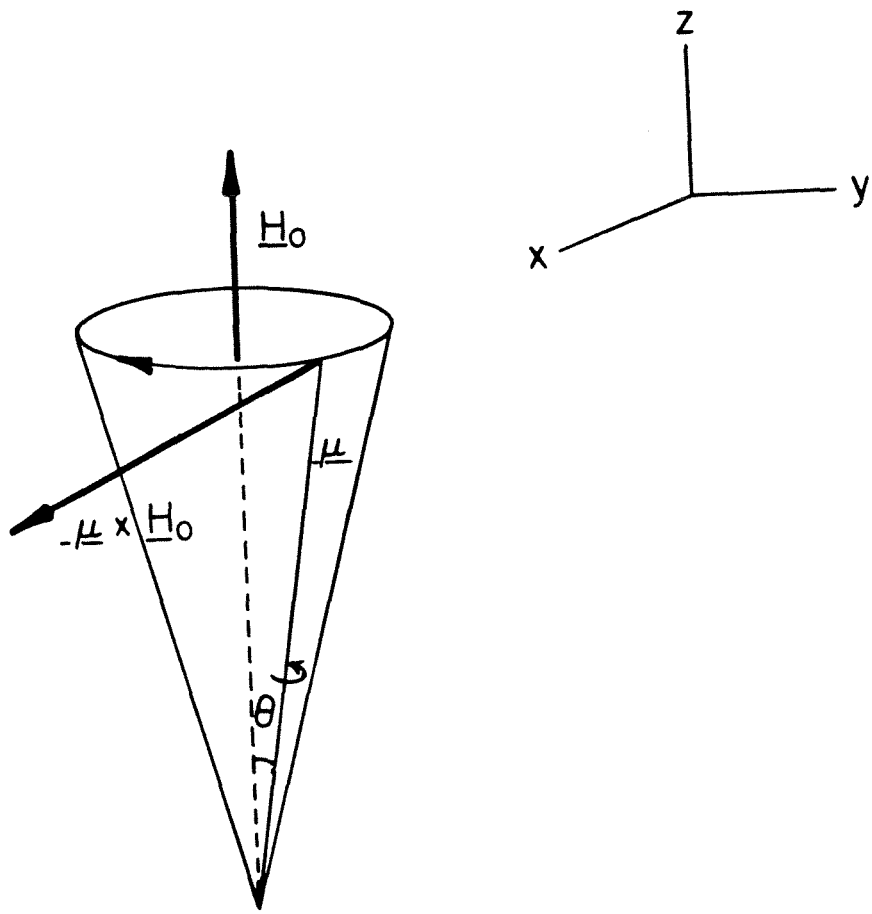

FIGURE 5.1: Forces on an Isolated Spinning Magnet $\underline{\mu}$ in a Magnetic Field of Strength $\underline{H}_o$

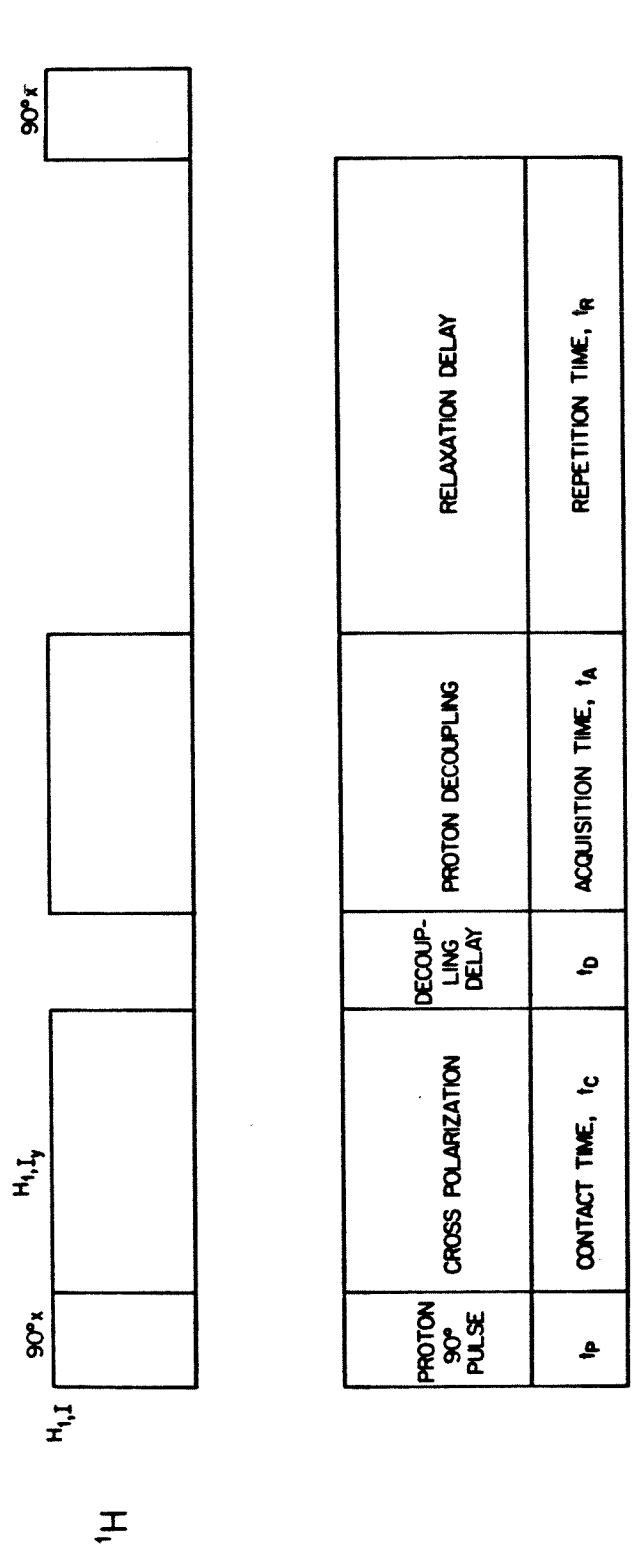

FIGURE 5.2: PULSE SEQUENCE USED IN ^{13}C-^1H CROSS POLARIZATION EXPERIMENTS

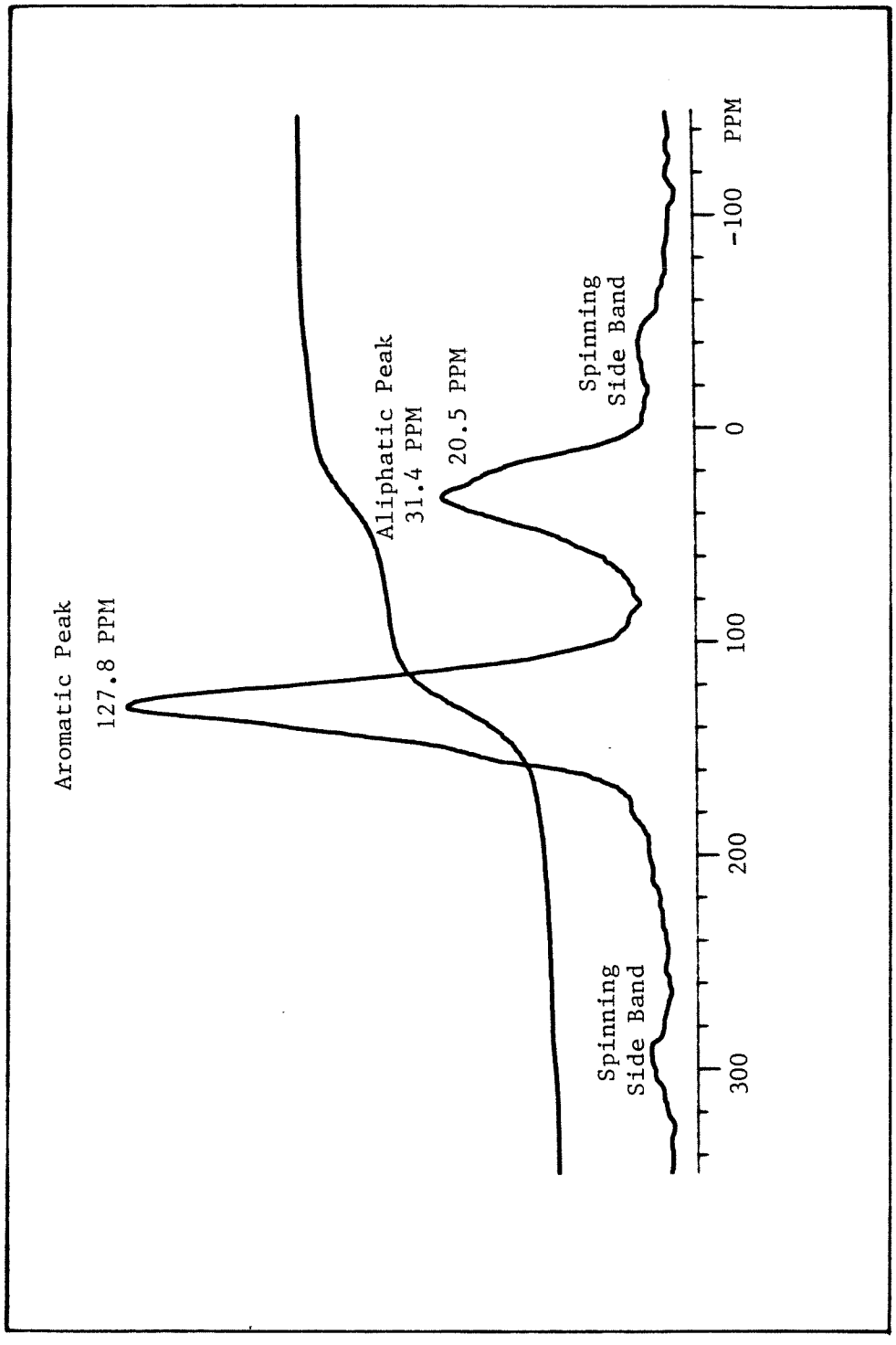

FIGURE 5.3: ^{13}C NMR Spectrum of Unoxidized PSOC 804 Coal

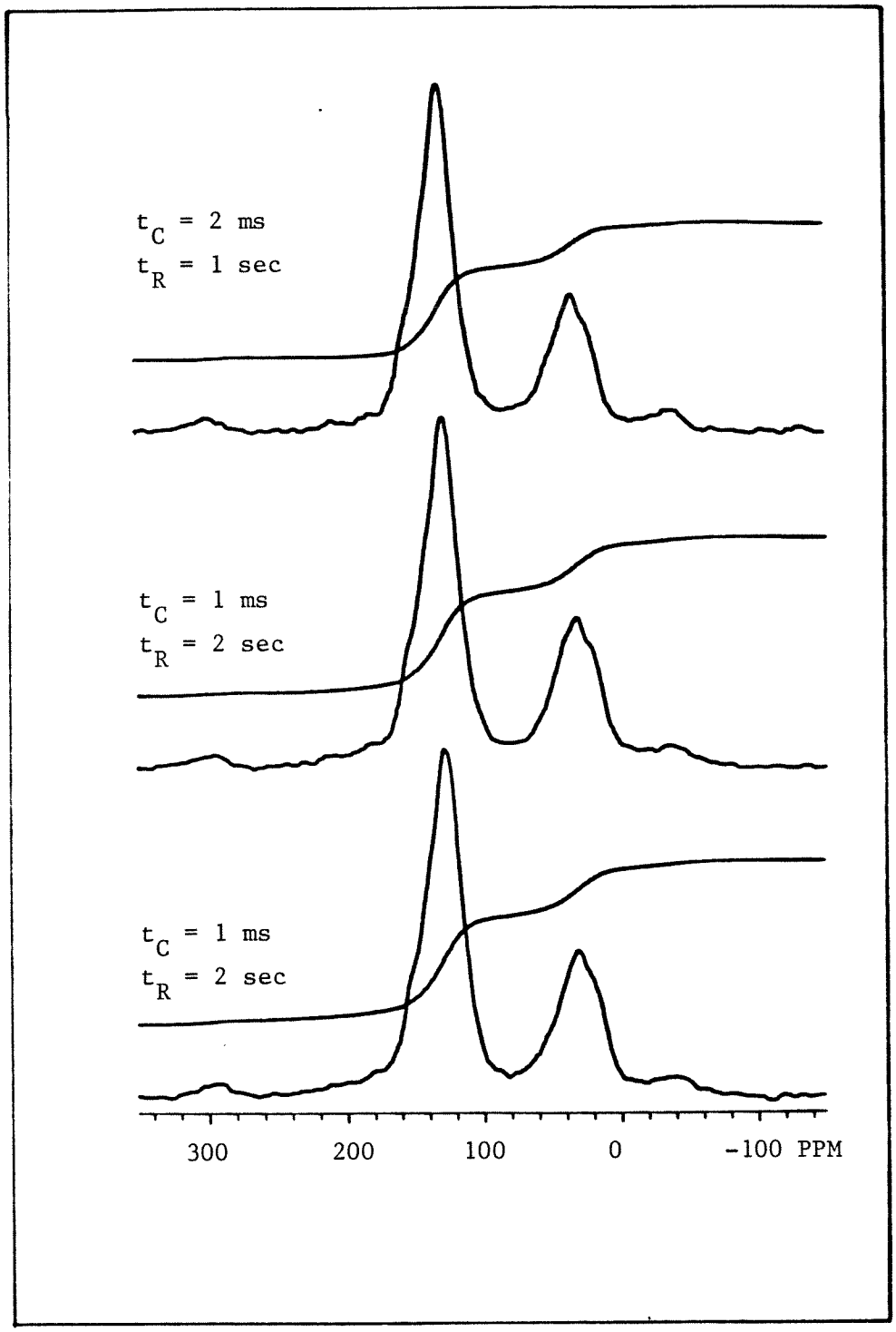

FIGURE 5.4: ^{13}C NMR Spectra of PSOC 704 Coal, Obtained Using Different Contact Times (t_C) and Repetition Times (t_R)

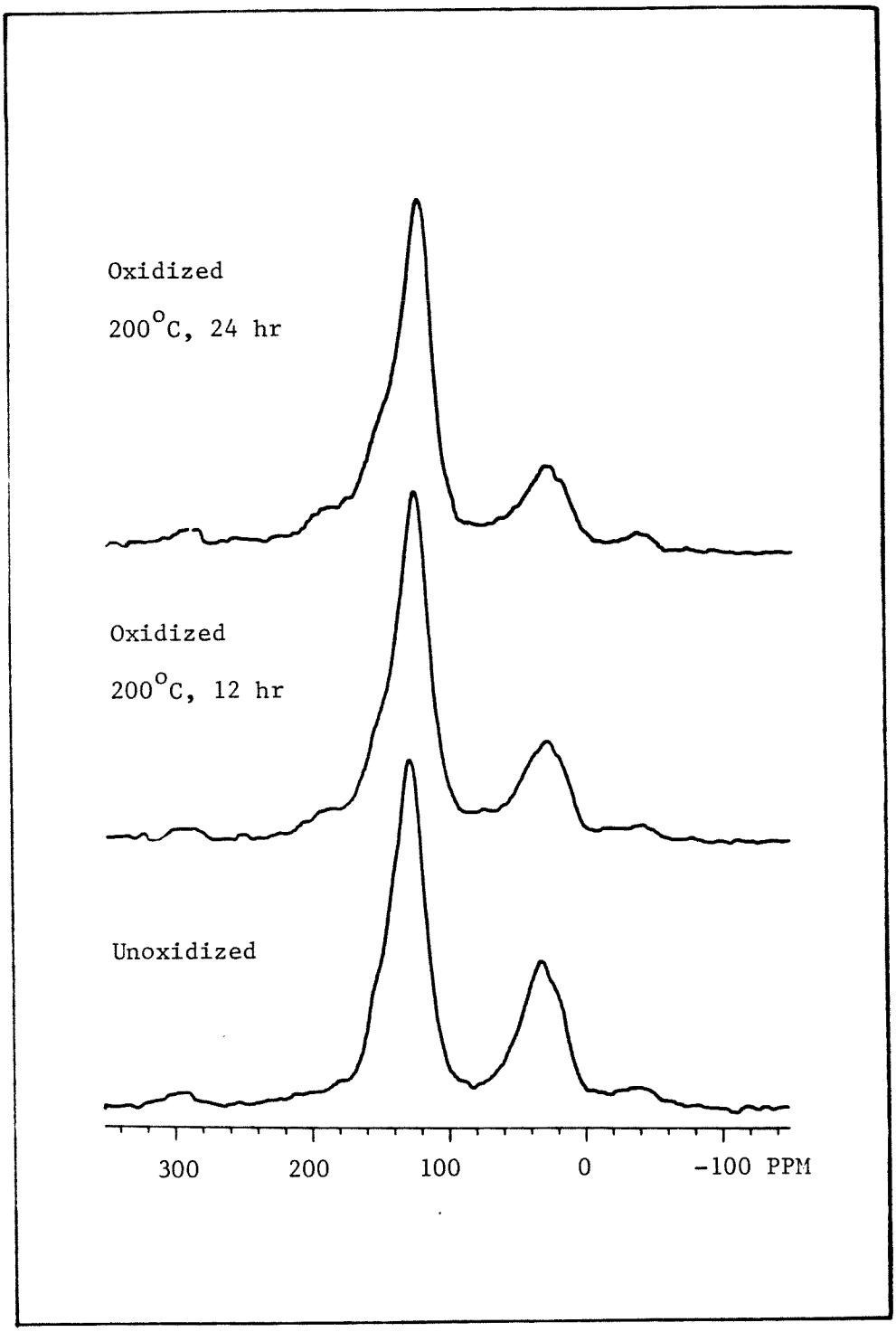

FIGURE 5.5: ^{13}C NMR Spectra of PSOC 704 Coal Samples, Showing Effect of Oxidation Time at 200°C

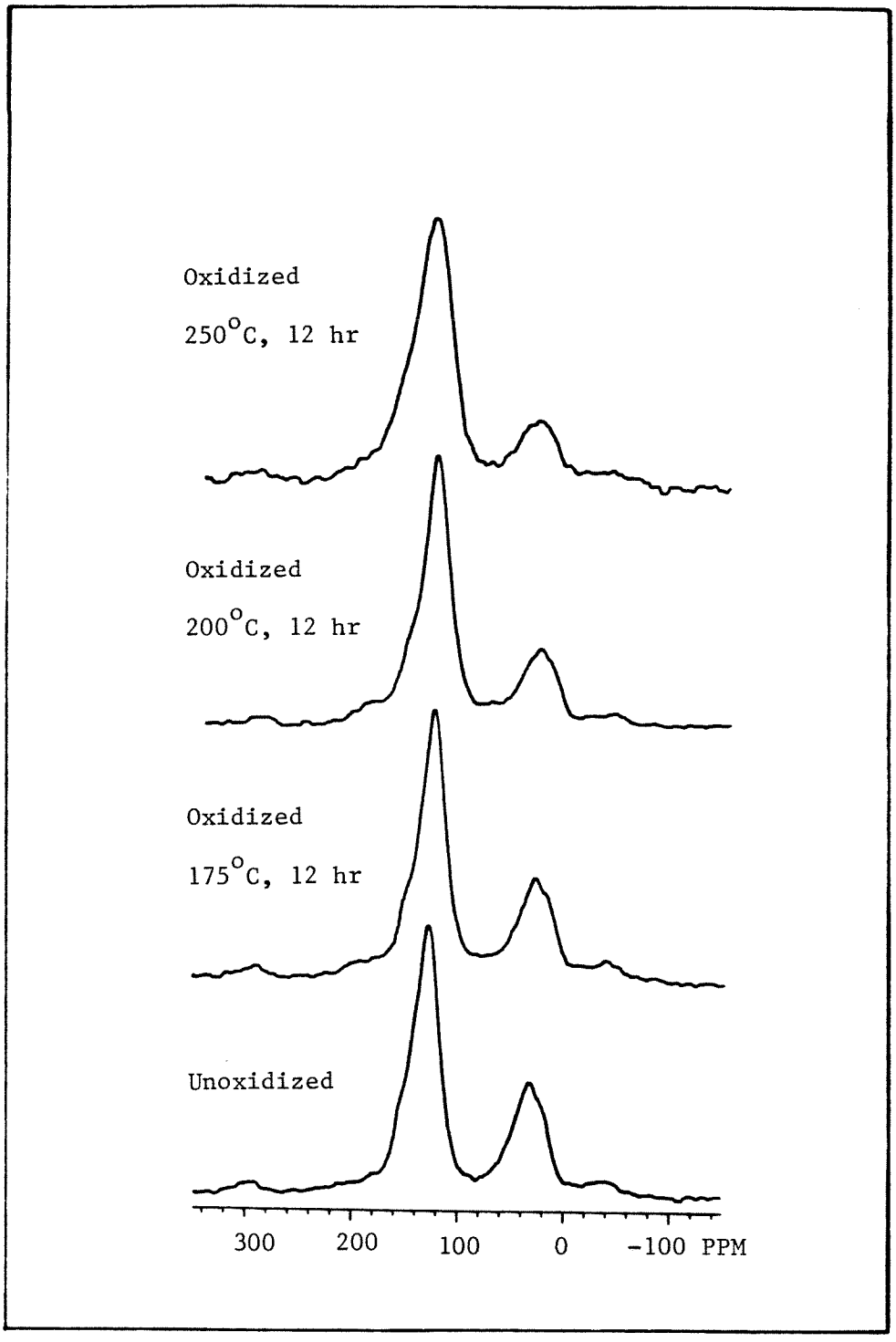

FIGURE 5.6: ^{13}C NMR Spectra of PSOC 704 Coal Samples, Showing Effect of 12-hr Oxidation at Different Temperatures

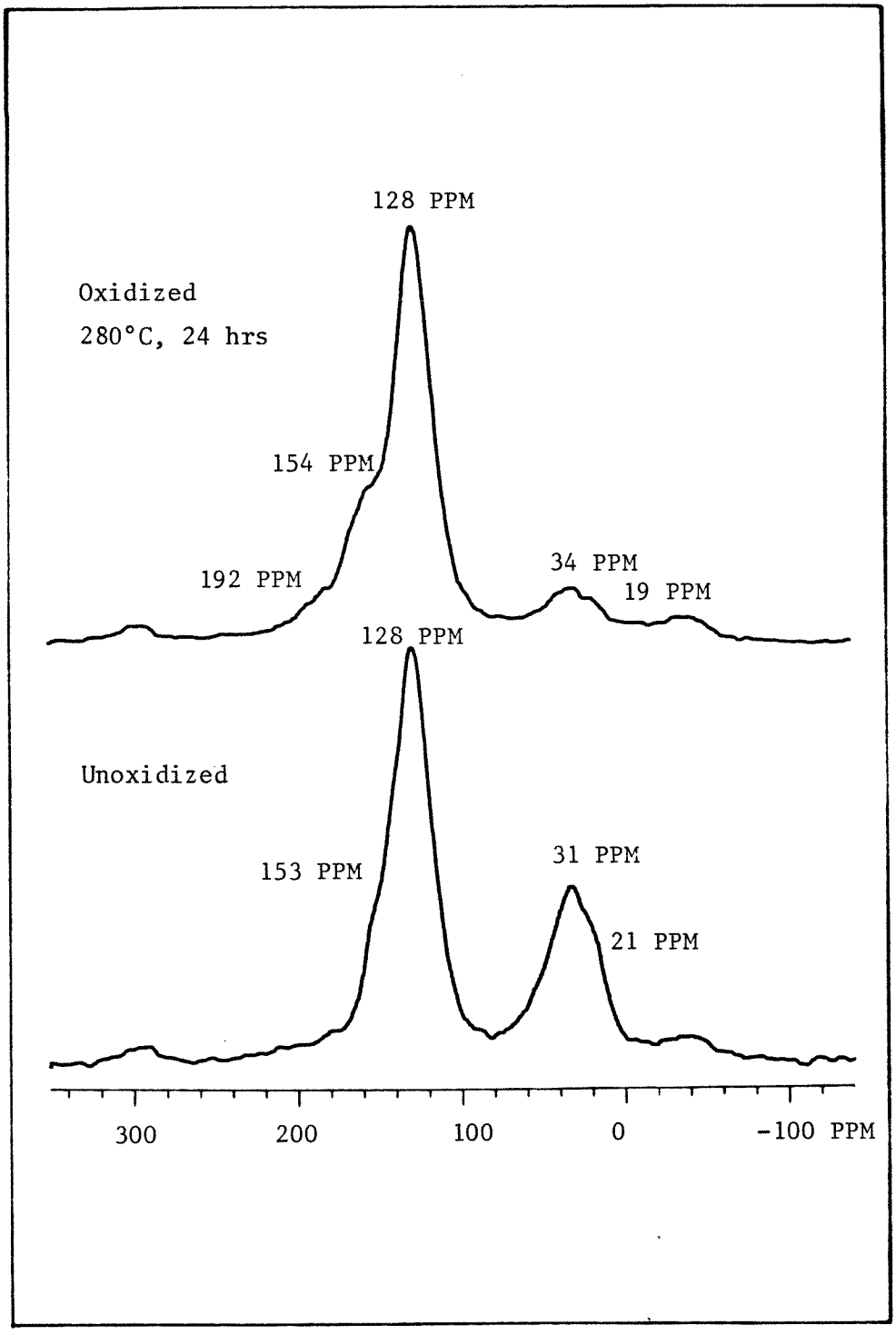

FIGURE 5.7: ^{13}C NMR Spectra of PSOC 704 Coal Before and After Oxidation at 280°C for 24 hours

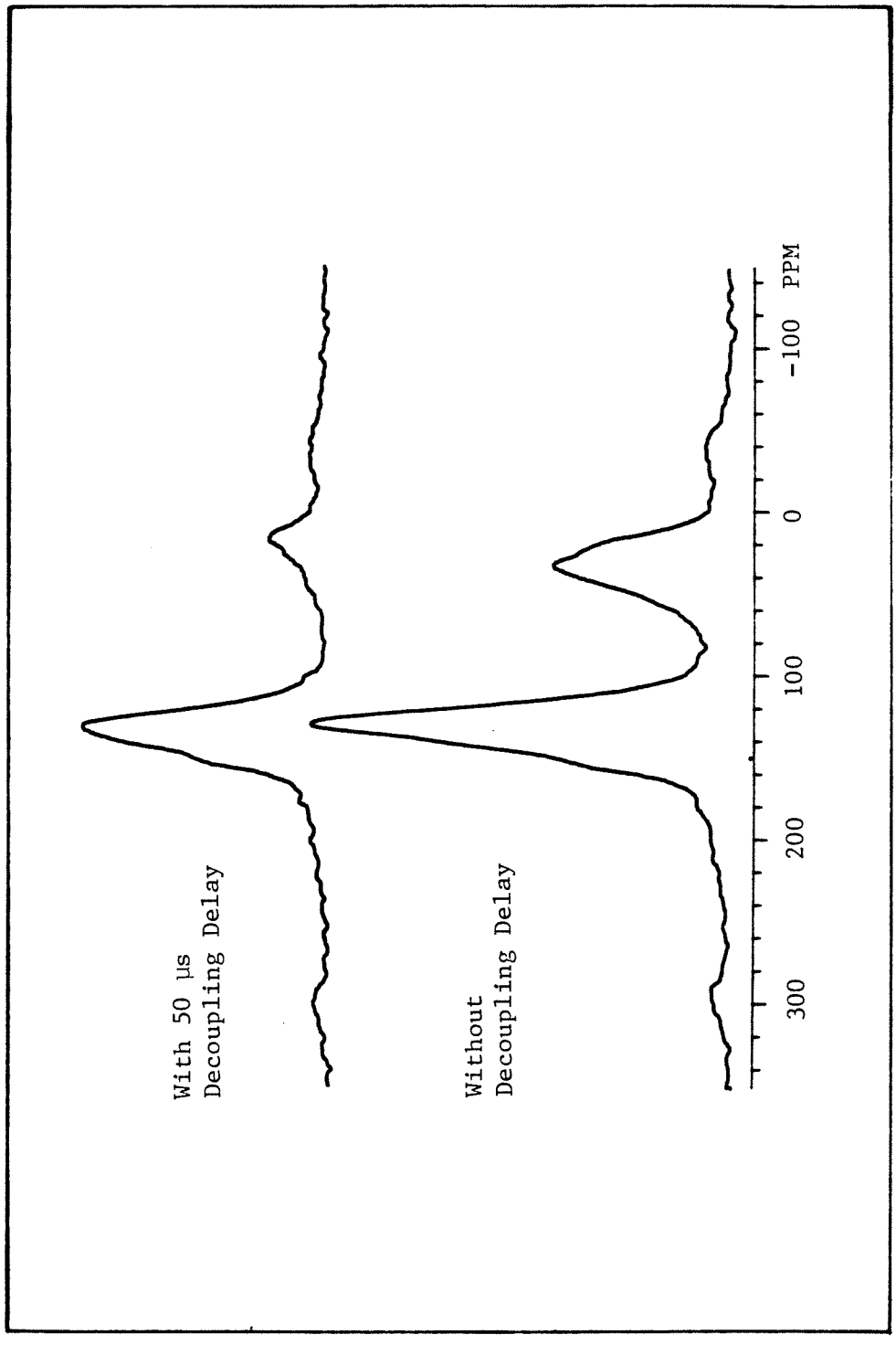

FIGURE 5.8: Effect of Decoupling Delay on ^{13}C NMR Spectrum of Unoxidized PSOC 704 Coal

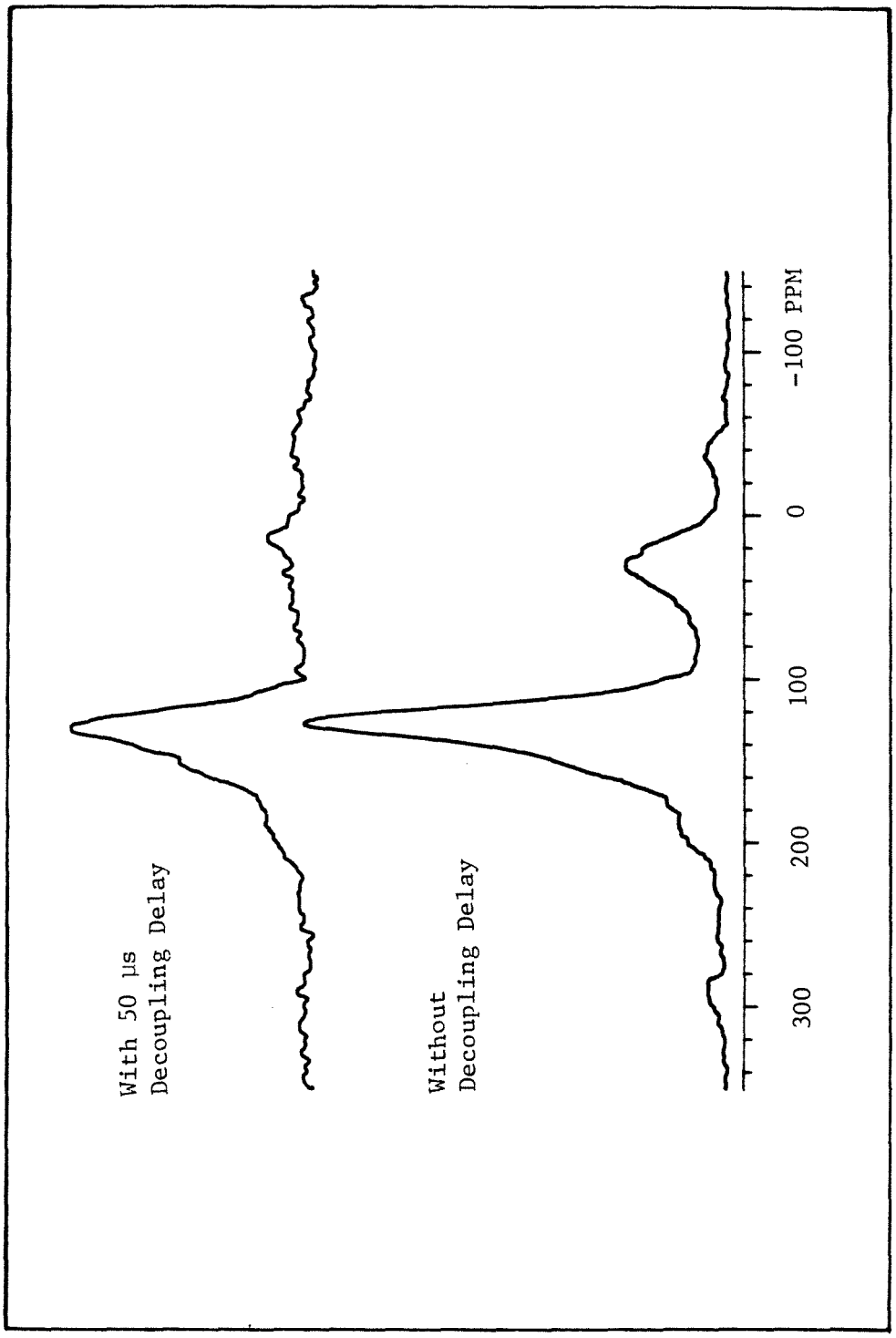

FIGURE 5.9: Effect of Decoupling Delay on ^{13}C NMR Spectrum of PSOC 704 Coal Oxidized at 200°C for 24 hours

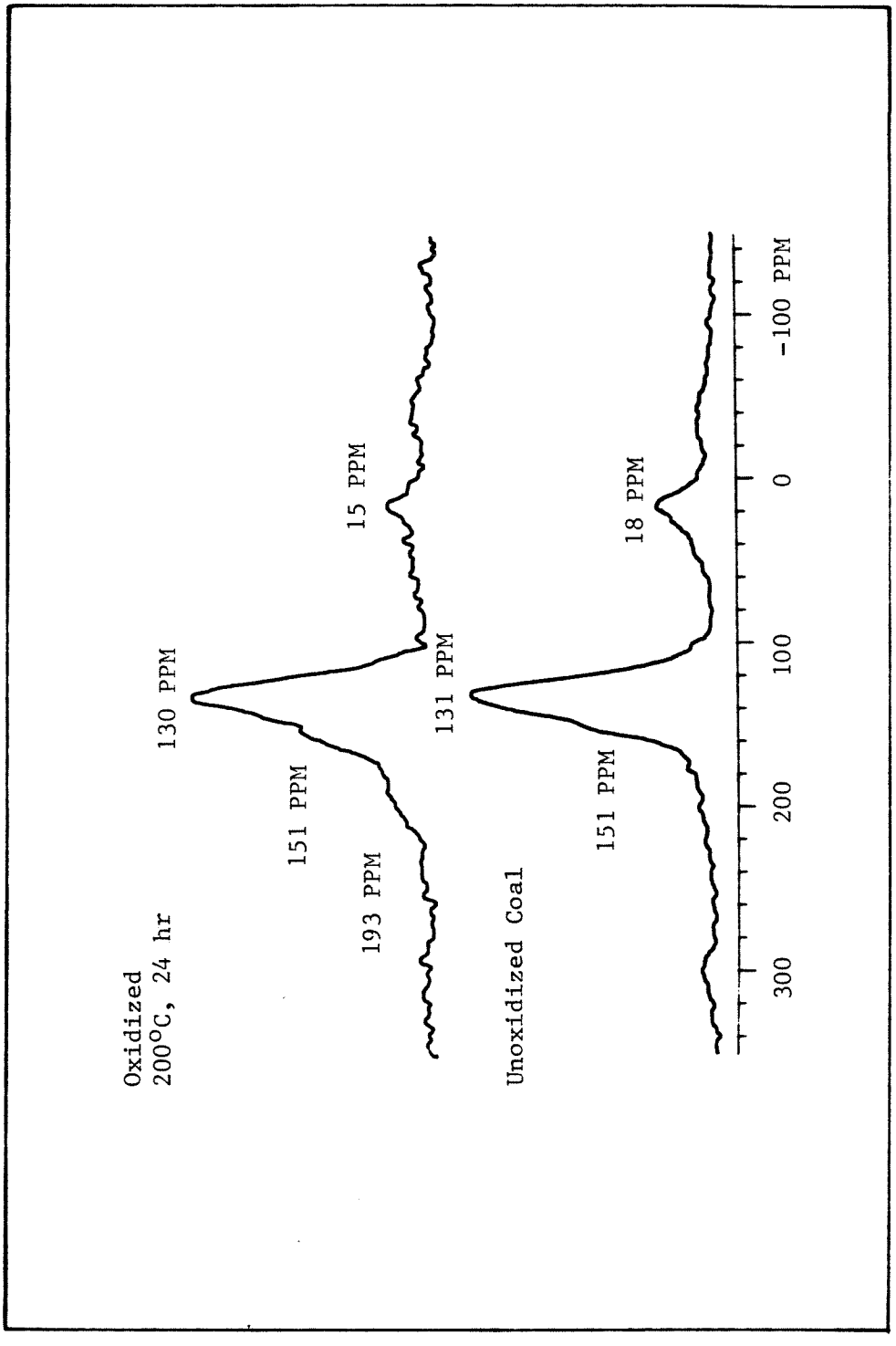

FIGURE 5.10: ^{13}C Spectra of Raw and Oxidized PSOC 704 Coal, Obtained with Decoupling Delay of 50 microseconds

References

[1] Brown J.K and Ladner W.R, Fuel, **39**, 87, 1960

[2] Retcofsky H.L, Schweighardt F.K, and Hough M, Anal. Chem, **49**, 585, 1977

[3] Karr C (Ed), Analytical Methods for Coal and Coal Products, Vol.II, Academic Press, New York, 1978

[4] Mullen K and Pregosin P.S, Fourier Transform NMR Techniques: A Practical Approach, Academic Press, New York, 1976

[5] Fukushima E and Roeder S.B.W, " Experimental Pulse NMR - A Nuts and Bolts Approach ", Addison-Wesley, Reading, Massachusetts, 1981

[6] Bartle K.D, Martin T.G, and Williams D.F, Chem. and Ind., April 1975, 313

[7] Gerstein B.C, Chow C, Pembleton R.G, and Wilson R.C, J.Phys. Chem., **81**, 565, 1977

[8] Pines A, Gibby M.G, and Waugh J.S, J.Chem.Phys., **59**, 569, 1973

[9] Andrew E.R, Progr. Nucl. Mag. Reson. Spectrosc., **8**, 1, 1971

[10] Yokoyama S, Uchino H, Katoh T, Sanada Y, Yoshida T, Fuel, **60**, 254, 1981

[11] Yokoyama S, Bodily D.M, Wiser W.H, Fuel, **58**, 162, 1979

[12] Yoshida T, Nakata Y, Yoshida R, Ueda S, Kanda N, and Maekawa Y, Fuel, **61**, 824, 1982

[13] Zilm K.W, Pugmire R.J, Grant D.M, Wood R.E, and Wiser W.H, Fuel, **58**, 11, 1979

[14] Vanderhart D.L and Retcofsky H.L, Fuel, **55**, 207, 1976

[15] Packer K.J, Harris R.K, Kenwright A.M, and Snape C.E, Fuel, **62**, 999, 1983

[16] Sullivan M.J and Maciel G.E, Anal. Chem., **54**, 1615, 1982

[17] Schaefer J, Stejskal E.O, Buchdahl R, Macromolecules, **20**, 384, 1977

[18] Hagaman E.W and Woody M.C, Fuel, **61**, 53, 1982

[19] Havens J.R, Koenig J.L, Kuehn D, Rhoads C, Davis A, and Painter P.C, Fuel, **62**, 936, 1983

[20] MacPhee J.A and Nandi B.N, Fuel, **60**, 169, 1981

[21] Painter P.C, Snyder R.W, Starsinic M, Coleman M.M, Kuehn D.W, and Davis A, Appl. Spectrosc., **35**, 475, 1981

[22] Lahiri A, Mukherjee P.N, Bhowmik J.N, Fuel, **38**, 469, 1959

6. REVIEW AND DISCUSSION OF OXIDATION CHEMISTRY

6.1 Background and Review

6.1.1 Intraparticle Heat and Mass Transfer

The brief discussion in this section will show that the measured rates of reaction were free of intra-particle transport limitations. In Appendix A we show that *extra*-particle heat and mass transfer resistances were negligible. Thus the measured rates of reaction must be regarded as intrinsic rates of chemical reaction, unaffected by heat or mass transport.

6.1.1.1 Mass Transfer

Standard theory states that if the overall rate of reaction was limited by mass transfer the observed activation energy of reaction would be equal to one half of the true activation energy and the apparent order of reaction with respect to gaseous reactant would be $((n + 1)/2)$, where n is the true order of reaction. Our results obtained with PSOC 704 coal gave an activation energy of 15.0 kcal/g. mole and the observed order of reaction was 2.0 at the beginning of the reaction, falling to 1.4 after 12 hours of reaction. The variable order of reaction implies complicated chemical kinetics or, perhaps, possible intra-particle diffusional control. That possibility is considered below.

By the Weisz criterion, intra-particle mass transport will not be controlling if

$$f = \frac{r_p^2 \rho_p R}{C_s D_e} \leq 1 \qquad (1)$$

where ρ_p and r_p are particle density and radius, C_s is reactant concentration at the particle, and D_e is the effective diffusivity of reactant.

We calculated f using data for the oxidation of 60-80 mesh PSOC 704 coal particles at 200 ^{0} C, with C_s = 5.38 gmol O_2/m^3, particle radius of 213.5 microns, and ρ_p = 785 kg/ m^3, and estimating the rate of oxygen consumption as 2.5 times the rate of production of CO_2, viz. 1.25 x 10^{-4} gmol O_2/kg coal-sec. We obtained

$$f = \frac{4.72 \times 10^{-10}}{D_e}$$

with D_e expressed in m^2/s . Thus mass transfer would be limiting if $D_e \leq 4.72 \times 10^{-10}\ m^2/s$.

The diffusivity of gases in coal varies with pore diameter. In a typical subbituminous coal, for example, pores may be roughly distributed among five characteristic diameters - micropores (0.0004-0.0012 μm , 0.008 μm , 0.1 μm , 1.0 μm , and 3.0 μm , with the smallest pores accounting for most of the available pore volume [1]. The Knudsen diffusion coefficient for a pore of 0.0012 μm , the largest micropore, is about 6 x 10^{-7} m^2/s , which is three orders of magnitude larger than the minimum value necessary for intra-particle diffusional control. We therefore conclude that the overall rate is not controlled by Knudsen diffusion.

Within micropores, however, transport is believed to occur primarily by activated, or surface, diffusion [2] with the term $(D_e^{1/2}/r_0)$ equal to about 10^{-2} at room temperature, where r_0 is an appropriate diffusional distance. A typical activation energy for surface diffusion is about 5 kcal/ gmol. Activated diffusion, if present, is inextricably linked with intrinsic chemical kinetics. We cannot measure one without interference from the other. For all practical purposes, therefore, no intra-particle diffusional effects were apparent in our fluidized-bed oxidation experiments.

Could the observed decay in reaction rate be due to blockage of micropores ? In fact, some published work suggests otherwise. In the work of Oda *et al.* [3], micropore volume increased by about 70 % after oxidation in air for 10 hours at 150 ^{0} C. Leon *et al.* [4] increased the nitrogen-absorption surface area of a bituminous coal by a factor of 50 following oxidation for 4 hours in a 6:1 mixture of oxygen and nitrogen at 400 ^{0} C , and also found that heating in pure nitrogen under the same conditions had no effect on the nitrogen-adsorption surface area of the coal. Therefore the decay in reaction rate observed in our experiments cannot be explained by a reduction in micropore volume.

6.1.1.2 Heat Transfer

A good measure of intra-particle temperature gradients is given by the Prater temperature, ΔT_{max} , which is the maximum temperature difference between the core of the particle and the surface of the particle. In calculating ΔT_{max} , using equation (2), it is assumed that the particle temperature is at steady state and that heat and mass transport are not coupled. Coupled heat and mass transfer was considered by Lee and Luss [5], while unsteady transfer of heat and mass was analyzed by Wei [6].

$$\Delta T_{max} = - \frac{\Delta H \, D_e \, c_s}{k_e} \qquad (2)$$

where

k_e is effective thermal conductivity, ΔH is enthalpy of reaction, and the other quantities are as defined earlier.

We calculated ΔT_{max} as 5.3 ^{0} C, using data of Run 1, with $D_e \approx 10^{-7}$ m^2/s and $k_e \approx 2.0 \times 10^{-4}$ kW /m^{0}K [7] . The enthalpy of reaction was estimated by dividing the slope of the heating value vs. time curve at 2 hr by the rate of reaction at 2 hr. The rate of oxygen consumption was estimated as 2.5 times

the rate of production of CO_2.

The Prater temperature in fact describes the limiting case when the concentration of gaseous reactant at the center of the particle is zero, implying that the reaction is limited by intra-particle diffusion. As seen earlier, intra-particle diffusion was not the limiting process in our experiments, and so the actual intra-particle temperature difference was probably much lower than the calculated Prater temperature. Thus we conclude that intra-particle temperature gradients were negligible.

6.1.2 Chemistry of Autoxidation

Autoxidation is the term generally used in the literature of organic chemistry to describe slow, direct oxidation of C-H bonds by air at temperatures between ambient temperature and about 200 ^{0} C. The accepted view is that autoxidation is a free-radical reaction initially giving peroxides which then further react to give complex mixtures of more stable products [8,9] The general mechanism, regarded as applicable to a wide range of organic substrates [8], is as follows:

Initiation

$$RH \longrightarrow R^{\bullet} + H \qquad (3)$$

$$RH + O_2 \longrightarrow R^{\bullet} + HO_2^{\bullet} \qquad (4)$$

Propagation

$$R^{\bullet} + O_2 \longrightarrow RO_2^{\bullet} \qquad (5)$$

$$RO_2^{\bullet} + RH' \longrightarrow RO_2H + R'^{\bullet} \qquad (6)$$

Chain Branching

$$RO_2H \longrightarrow RO^{\bullet} + HO^{\bullet} \qquad (7)$$

$$RO^{\bullet} + R'H \longrightarrow ROH + R'^{\bullet} \quad (8)$$

$$HO^{\bullet} + R'H \longrightarrow H_2 + R'^{\bullet} \quad (9)$$

Termination

$$2\,RO_2^{\bullet} \longrightarrow \text{Inert Products} \quad (10)$$

$$RO_2^{\bullet} + R^{\bullet} \longrightarrow \text{Inert products} \quad (11)$$

$$2\,R^{\bullet} \longrightarrow RR \quad (12)$$

Initiation may occur by thermolysis, photolysis, or proton abstraction by some radical initiator. Walters [9] notes that experimental evidence indicates that, at room temperature, $k_4 >> k_5$. If so, reaction (6) is the rate-controlling step . For that reason $[RO_2] >> [R]$, and hence equation (10) is the dominant termination reaction. The estimated activation energy of reaction (6) is about 5 kcal/ g mol for methylenic C-H bonds and about 15 kcal/ g mol for methyl C-H bonds [9]. The rough order of reactivity is ethers > aldehydes > phenols > olefins > ketones > aromatic side chains at α positions > tertiary aliphatic C-H > secondary aliphatic C-H > primary aliphatic C-H. Ethers, phenols, and olefins are more reactive because the resulting radicals are stabilized by resonance.

Hoare and Walsh [10] studied the gas-phase photochemical oxidation of acetone at 200 ^{0} C and established that methyl radicals react with O_2 according to the reaction

$$CH_3^{\bullet} + O_2 + M \longrightarrow CH_3O_2^{\bullet} + M' \quad (13)$$

where M is some third body. Christie [11] also came to the same conclusion from her study of the oxidation of ethyl iodide at 18-22 ^{0} C. She found that the rate was proportional to total pressure but that the rate extrapolated to zero total pressure was still finite. Therefore she suggested that the addition of oxygen to the methyl radical could also occur without the participation of a

third body, as in equation (14), and an overall rate constant k_{15} could be written as shown in equation (15) below.

$$CH_3^{\bullet} + O_2 \longrightarrow CH_3O_2 \qquad (14)$$

$$k_{15} = k_{14} + k_{13,M}\,M \qquad (15)$$

In equation (13), the rate of reaction is proportional to the oxygen partial pressure and to the total pressure. Thus, if the oxygen partial pressure is systematically altered by varying the total pressure of the oxidizing gas mixture, the rate of reaction will exhibit an apparent second-order dependence on oxygen concentration.

In the oxidative degradation of high-molecular-weight polymers, the concentration of hydroperoxides , RO_2H , is reported to increase rapidly to a high value which then gradually falls as, presumably, reactive sites are depleted [8]. Hydroperoxides have been observed by infra-red spectroscopy [12] and by iodometry [13]. Rugg *et al.* [12] oxidized polyethylene films in air at 140 ^{0} C and observed an infra-red absorption at around 3560 cm^{-1}, which they attributed to hydroperoxides. When the oxidized film was cooled to room temperature, the absorption at 3560 cm^{-1} virtually disappeared.

Walters [9] points out that autoxidations are generally greatly accelarated by the addition of small amounts of salts of manganese, copper, cobalt, iron, and lead. The transition metal cations promote the decomposition of hydroperoxides by oxidation or by reduction , thus :

$$RO\text{-}OH + Fe^{2+} \quad RO + (FeOH)^{2+} \quad \text{Oxidation}$$

$$RO\text{-}OH + Co^{3+} \quad RO\text{-}O + Co^{2+} + H^{+} \quad \text{Reduction}$$

The products of decomposition include assorted oxygenated species, water, and carbon oxides. The ultimate products of autoxidation are alcohols, aldehydes,

ketones, acids, acid anhydrides, and esters [8].

6.1.3 Review of Past Work

Several authors have proposed a so-called " dual-path " mechanism for the oxidation of coal in air [7,14,15]. Jensen *et al.* [15] and Berkowitz [7] proposed the reaction scheme shown in Figure 1.1 to describe the reaction of coal and air above 250 ^{0} C:

In that scheme, water and carbon oxide gases were believed to originate from two separate sources: direct " burn-off " and humic-acid decomposition. The production of phenolic acid groups was believed to be typified by the oxidation of naphthalene to give phthalic anhydride, according to the mechanism of Tronov shown in Figure 1.2 . Actually, we would expect the carbon oxide gases and water to arise from some oxidized intermediate species, not necessarily humic acids . In fact, given their chemical stability, we would not expect humic acids to be the primary source of the carbon oxide gases and water produced during oxidation. Indeed, our data of Chapter 2 showed that acid decomposition was not a significant source of carbon oxide gases. The gases and water must arise from some other oxidized intermediate species.

The presence of oxygenated intermediate species during coal oxidation seems logical. Jones and Townsend [16] thought such species to be " peroxygen-like bodies "which they believed to be unstable above 90 ^{0} C. Jensen *et al.* [14] saw humic acids as the intermediate species while Kam *et al.* [15] did not specify the chemical nature of the " activated complex " species. Jones and Townsend [16] studied the weathering of coal below 90 ^{0} C and concluded that " peroxygen complex " species or " peroxidic bodies " played a key role in the oxidation of coal. The so-called peroxygen complex was said to be unstable above 70 ^{0} C and

the overall rate was apparently controlled by the rate of breakdown of the complex. The authors devised a technique for measuring " peroxygen " in coal, by shaking the coal sample with a solution containing ferrous and thiocyanate (CNS^-) ions and estimating the amount of ferric thiocyanate produced by titration against titanous chloride. The concentration of " peroxygen " initially increased with exposure to oxygen, rising to a peak and then declining with time. The method which Jones and Townsend used to estimate " peroxygen " concentrations might not have been accurate; nonetheless their findings were significant in that they showed the importance of some oxygenated intermediate in coal oxidation. Later other authors, such as Chakrabarty *et al.* [17], were to echo the idea that a " coal oxygen complex " was formed in the early stages of oxidation. Based on the known oxidation chemistry of organic compounds, there is good reason to believe that hydroperoxides, hydroperoxy radicals, and peracids are the principal intermediate species in the reaction between oxygen and the organic matter in coal.

The idea of a " burn-off " reaction path, distinct from slow oxidation via intermediate, appears arbitrary and unsubstantiated. There is no apparent reason why oxidation should occur by two competing reaction paths. The precise meaning of the term " burn off " is not really clear. Assuming that it is akin to the combustion of graphite, we find that the rate of such a reaction is negligibly slow at around 250 ^{0} C. Hawtin and Murdoch [18] reported the oxidation rate of graphite as about 1.59×10^{-4} hr^{-1} at 769 ^{0} C, based on loss of weight. The activation energy was reported as 45.4 kcal/g mole. If the ratio of CO to CO_2 produced is assumed to be 1.0 the rate of consumption of oxygen is about 2.75×10^{-9} kg mol/kg coal-sec at 500 ^{0} C and 1.45×10^{-15} at 250 ^{0} C. By comparison, oxygen consumption rates for bituminous coal at 250 ^{0} C, reported in Chapter 2 of this thesis, were about 10^{-7} kg mol/kg coal-sec. Thus it appears

that " burn-off ", if present, would be negligible compared with the overall rate of oxidation.

From the above discussion of autoxidation it seems clear that the air oxidation of coal occurs by a free-radical mechanism. Rather surprisingly, although the role of free radicals in combustion has long been an accepted fact, free-radical mechanisms have only recently been proposed for coal oxidation [19,20]. Dack *et al.* [21] established the presence of free radicals in a Victorian brown coal using electron spin resonance (e.s.r) and noted that the concentration of free radicals increased significantly when the coal was exposed to air at 21 ^{0} C.

6.2 Mechanism of Oxidation

We propose that the mechanism of coal oxidation is a free-radical mechanism, based on the established mechanism of autoxidation which is represented by equations (3) through (12).

Coal contains a large diversity of organic functional groups, and the free radicals they form can participate in various different chemical reactions. Therefore a detailed chemical mechanism would not be practical. We can only discuss coal oxidation chemistry in terms of broad classes of functional groups, such as aliphatic and aromatic C-H groups, aldehydes, and acids. The scheme represented by equations (3) through (12), however, covers most of the important autoxidation reactions of the different reactive functional groups in coal.

The initial species RH in equation (3) could be an aliphatic or aromatic functional group in coal or an aldehyde. Bradley [26] states that, at lower temperatures, initiation by reaction (4) is favored over initiation by the direct

decomposition reaction (3), and regards the reaction between RH and oxygen as the primary step in the oxidation of hydrocarbons at lower temperatures. Direct thermal cracking requires a high energy input, about 70-100 kcal/mole, and is therefore significant only at higher temperarures as in, for example, oxidation of pre-mixed gases. A reaction like equation (26), on the other hand, would require about 30-45 kcal/mole for an alkane [27]. The relative ease of homolytic fission for alkyl C-H bonds is: R_3C-H > R_2CH-H > RCH_2-H > CH_3-H . The activation energy for reaction (3) will be lower for the formation of radical species which can be stabilized by delocalization of the unpaired electron, as shown in Figure 6.1. Thus, for example, methyl and methylene groups directly attached to aromatic rings, and C-H bonds at tertiary carbons, will be oxidized relatively fast.

Reaction between R and oxygen produces the a peroxyalkyl or a peroxyacyl radical, RO_2 , which readily forms the hydroperoxide. The hydroperoxide is not stable at the temperatures used in our experiments, and decomposes fast according to equation (10), producing an alkoxy or a phenoxy radical and the hydroxyl radical, OH . This radical is highly reactive, abstracting H atoms and also attacking aromatic rings. Tronov's scheme is an example of OH radical-induced oxidation of an aromatic ring. Also, RO_2 radicals can isomerize or decompose, depending on the nature of the R group, producing a variety of possible products including aldehydes, ketones, olefins, cyclic ethers, and the radicals RO and OH.

The literature of atmospheric photochemistry contains accounts of the chemistry of alkoxyl radicals, alkylperoxy radicals, and aldehydes [22,23]. Alkoxyl radicals RO can react with O_2 to give the reactive hydroperoxy radical HO_2 and an aldehyde [22], and can also abstract a hydrogen from some group

RH' to form an alcohol and the radical R' . In the presence of oxygen, aldehydes can be oxidized to peracids and carboxylic acids [24]. They can also react with the OH radical, or decompose, to give CO and further radicals, and can abtract a hydrogen atom from some RH group to form alcohols. The formation of CO from aldehydes proceeds as follows:

$$RCHO \longrightarrow R\dot{C}O + H^{\bullet}$$

$$RCHO + O_2 \longrightarrow R\dot{C}O + HO_2^{\bullet}$$

$$R\dot{C}O \longrightarrow R^{\bullet} + CO$$

CO is itself converted to CO_2 by the OH radical, thus:

$$CO + {}^{\bullet}OH \longrightarrow H^{\bullet} + CO_2 \qquad (16)$$

followed immediately by

$$H^{\bullet} + O_2 \longrightarrow HO_2^{\bullet}$$

Equation (16) is widely regarded as the ultimate CO_2-producing reaction in fuel combustion [25], which occurs at temperatures of 500 ^{0} C and above. At the lower temperatures used in our experiments, a more important source of CO_2 is the thermal decomposition of peracids. CO_2 could also possibly be produced by the decomposition of carboxylic acids. Our data reported in Chapter 2, however, showed that the decomposition of carboxylic acids does not apparently contribute to the formation of CO_2 during coal oxidation at the temperatures used in this work. We believe that the CO_2 produced during coal oxidation originates mainly from peracid decomposition, with some contribution from equation (16). Peracids are formed by the sequence

$$RCHO \longrightarrow R\dot{C}O + H$$

$$R\dot{C}O + O_2 \longrightarrow RCO_3^{\bullet}$$

$$RCO_3^{\bullet} + RH \longrightarrow RCO_3H + R^{\bullet}$$

The reactions of peracids can lead to the formation of CO_2 as well as carboxylic acids, as follows:

$$RCO_3H \longrightarrow RCO_3^{\bullet} + H^{\bullet}$$

$$RCO_3^{\bullet} \longrightarrow RO^{\bullet} + CO_2$$

$$RCO_3H \longrightarrow RCO_2^{\bullet} + {}^{\bullet}OH$$

$$RCO_2^{\bullet} + RH \longrightarrow RCO_2H + R^{\bullet}$$

Thus aldehydes, which arise from methyl and methylene groups, are precursors of both carboxylic acids and carbon oxides. Accordingly, the formation of acids cannot be explained separately from the production of oxide gases.

Phenolic groups are most probably produced by the addition of hydroxyl radicals to aromatic groups. The hydroxyl radicals, which are highly reactive, are produced mainly by the decomposition of hydroperoxides. When an OH radical adds to an aromatic ring it produces a free radical, which may lose a hydrogen atom to form a phenol or gain a hydrogen atom from some group RH and form a cyclic diene, which then undergoes further oxidative degradation. The two possibilities are shown in Figure 6.2

As we observed in Chapter 2, the ratio of CO_2 to CO in the exit gas from the coal-oxidation coal-oxidation reactor increased linearly with temperature. For

PSOC 704 coal the ratio was about 1.0 at 200 ^{0} C and about 1.45 at 300 ^{0} C. The 45 % increase in the relative amount of CO_2 could be due to a higher rate of formation and decomposition of peracids and a rise in the rate of the reaction (16), caused by an increase in the concentration of OH radicals and a higher rate constant for equation (16) at the higher temperature. That rate constant has been the subject of theoretical and experimental study. It turns out to have a temperature-dependent activation energy [25]. At temperatures below about 600 ^{0} K the rate is relatively insensitive to temperature. Data from ref [25] show that the rate constant goes up by 16 % from 200 ^{0} C to 300 ^{0} C. Therefore we attribute the higher rate of CO_2 production at higher temperatures mainly to an increased rate of peracid decomposition.

In Chapter 3 we noted that, while significant amounts of carbon and hydrogen were lost from the coal during oxidation, especially in the first few hours, very little material was lost if the coal was merely heated in a fluidizing stream of nitrogen. Thus the process of devolatilization apparently was enhanced by the oxidation reactions taking place in the pores of the coal, either by localized exothermic effects or, more likely, by the scission of methylenic and other bonds, thus releasing molecular fragments as gaseous species which may or may not be oxidized. Coal contains material which can devolatize within the pores and possibly undergo gas-phase oxidation.

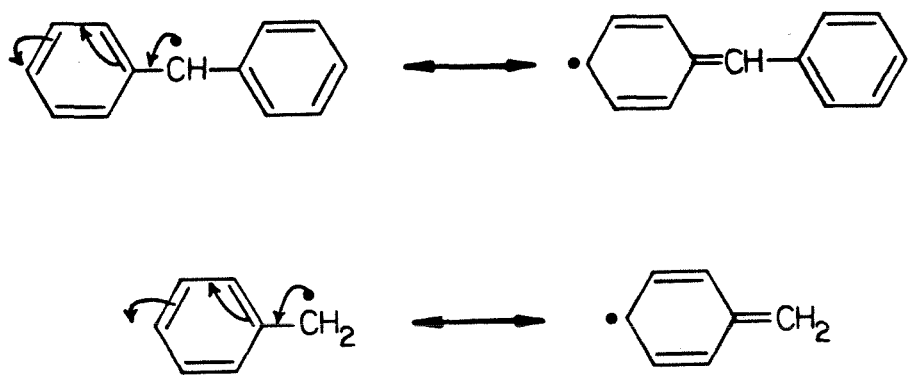

FIGURE 6.1: Stabilization of Free Radicals by Delocalization

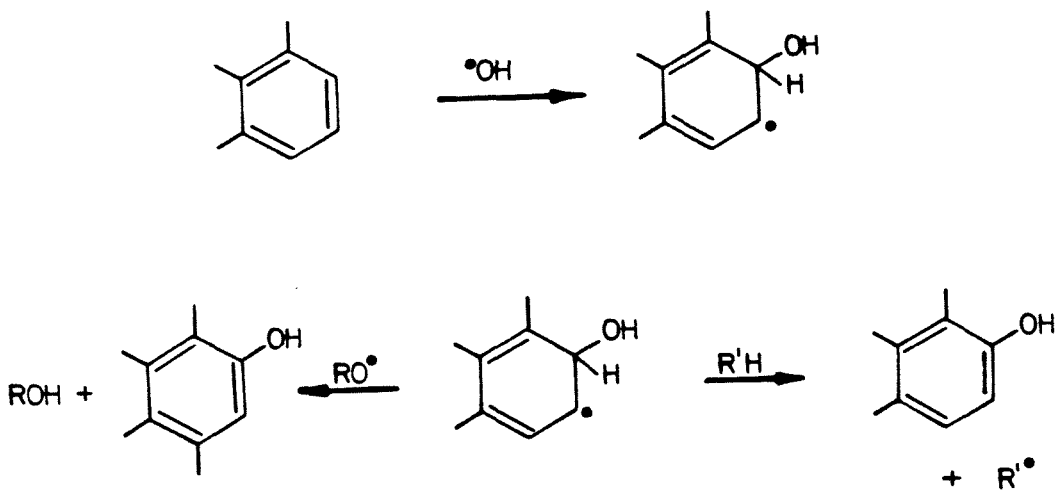

FIGURE 6.2: Attack of the Hydroxyl Radical on an Aromatic Ring

References

[1] Gavalas G.R and Wilks K.A, AIChEJ, **26**, 201, 1980

[2] Nandi S.P and Walker P.L, Fuel, **43**, 385, 1965

[3] Oda H, Takeuchi M and Yokokawa C, Fuel, **60**, 390, 1981

[4] Leon S, Klotzkin M, Gard G, and Emett P.H, Fuel, **60**, 673, 1981

[5] Lee J C M and Luss D, Ind. Eng. Chem. Fundam., **8**, 596, 1969

[6] Wei J, Chem. Eng. Sci., **21**, 1171, 1966

[7] Berkowitz N, An Introduction to Coal Technology, Academic Press, New York,1979

[8] Hawkins W.L, Oxidation and Combustion Reviews, **1**, 170, 1965

[9] Walters W.A, Mechanisms of Oxidation of Organic Compounds, John Wiley & Sons, New York, 1964

[10] Hoare D.E and Walsh A.D, Trans. Faraday Soc., **53**, 1102, 1957

[11] Christie M.I, Proc. Roy. Soc. (London), Series A, **244**, 411, 1958

[12] Rugg F.M, Smith J.J, and Bacon C.R, J. Polymer Sci., **13**, 535, 1964

[13] Bell and Thodstop U.S Patent 2,921,048

[14] Jensen E.J, Melnyk N, Wood J.C, and Berkowitz N, in Coal Science, Given P.H (Ed), Advances in Chemistry Series No. 55, American Chemical Society, Washington D.C, 1966

[15] Kam A.Y, Hixson A.N, and Perlmutter D.D, Chem. Eng. Sci., **31**, 815, 1976

[16] Jones R.E and Townsend D.T.A, J. Soc. Chem. Ind., **68**, 197, 1949

[17] Chakrabarty S.K, Mazumdar B.K, and Lahiri A, Nature, **187**, 502, 1960

[18] Hawtin and Murdoch, Chem. Eng. Sci., **19**, 819, 1964

[19] Rhoads C.A, Senftle J.T, Coleman M.M, Davi} A, and Painter P.C, Fuel, **62** , 1387, 1983

[20] Liotta R, Brons G, and Isaacs J, Fuel, **62**, 781, 1983

[21] Dack S.W, Hobday M.D, Smith T.D, and Pilbow J.R, Fuel, **63**, 39, 1984

[22] Carter W.P.L, Darnall K.R, Graham R.A, Winer A.M, and Pitts J.N, J.Phys. Chem., **83**, 2305, 1979

[23] Falls A.H and Seinfeld J.H, Environ. Sci. and Technol., **12**, 1398, 1978

[24] Hendrickson J.B, Cram D.J, and Hammond G.S, Organic Chemistry, Third Edition, McGraw-Hill, 1970

[25] Smith I.W.M, Kinetics and Dynamics of Elementary Gas Reactions, Butterworths, Boston, Massachusetts, 1980

7. CONCLUSIONS AND RECOMMENDATIONS

7.1 Conclusions

Our experimental investigations of coal oxidation in air in a fluidized bed at 175 - 280 ^{0} C and 126 - 274 kPa total pressure, and subsequent characterization of the oxidized coal by chemical analysis and by FTIR and ^{13} C NMR spectroscopic analysis of the solid, led to the following findings and conclusions:

[1] The rate of production of CO and CO_2 decayed with time, with a slope which increased as temperature and partial pressure were increased. The decline in CO and CO_2 rates as afunction of time was believed to be due to the gradual loss of oxidizable material initially available in the coal. The CO and CO_2 rate , and the CO / CO_2 ratio, were different for different coals. Of the coals studied the order of reactivity was

Lignite > High Volatile A > Low Volatile

The CO / CO_2 ratio increased linearly with oxidation temperature . Based on initial rates of reaction for PSOC 704 coal, activation energies were 68.2 MJ / kg mole (16.3 kcal / g mole) for the CO_2 rate and 49.0 MJ / kg mole (11.7 kcal / g mole) for the CO rate. There was no minimum in CO / CO_2 ratio, as had been reported by Kam *et al* [1], at around 225 ^{0} C.

[2] Using PSOC 704 Coal, we found no significant differences among CO and CO_2 rates for particles of different sizes within the range 125 - 354 μm . This finding was consistent with the results of calculations (Appendix A) which indicated that gas-to-particle mass-transfer resistance was negligible.

[3] Based on experiments in which we varied the total pressure of the

fluidizing air and measured CO and CO_2 rates the apparent order of reaction with respect to oxygen concentration, based on initial CO_2 rates, was 2.1 ± 0.2 . The order of reaction based on rates after 6 hours of oxidation was 1.5 ± 0.1 . The variability in reaction order indicated that many different reactions could be occurring, with time-dependent rates, such that the overall CO_2 rate was not simple.

[4] Based on the observation that when oxidized coal was heated in a stream of nitrogen the rates of production of carbon oxide gases were much lower, and decayed much faster, than rates observed during oxidation, and that chemical analysis of heated coal showed virtually no change in the concentration of carboxylic acid groups, we concluded that carboxylic acids are not the proximate source of carbon oxide gases during oxidation. The gases must originate from some other oxygenated intermediates whose concentration falls off rapidly when not replenished by the reactions of coal and oxygen. The concentration of phenolic groups fell significantly with heating, as those groups condensed to give ethers and water.

[5] A sharp loss of heating value during the first few hours of oxidation was consistent with the observed loss of carbon and hydrogen. Yet heating in pure nitrogen caused no significant loss of carbon or hydrogen. Therefore sharp the loss of material must have occured by a process of devolatilization, possibly accelarated by the heat generated by the oxidation reaction or by release of small molecular fragments by oxidative fission of methylenic bonds in the coal.

[6] Oxidation enhanced significantly the cation exchange capacity of coal. Total and carboxylic acidity rose about equally, and increased with time and with temperature. For PSOC 704 coal, rates of production of carbon

oxide gases and rates of creation of acidic groups were comparable in magnitude.

[7] In the FTIR spectrum, the intensity of the broad band at 2800 - 3100 cm^{-1} , due to hydrogen bonded phenolic and carboxylic groups, increased with oxidation while the peaks due to aromatic and aliphatic C-H stretching fell steadily in intensity as oxidation progressed. The aliphatic peaks were reduced more than the aromatic peaks.

[8] The carbonyl region of the FTIR spectrum showed clear evidence of the formation of aliphatic and aromatic acids and acid anhydrides, esters, aldehydes and ketones.

[9] Oxidation increased the aromaticity of coal. This finding contradicted the published work of McPhee and Nandi [2], and confirmed the results of Havens *et al* [3].

[10] ^{13} C NMR spectroscopy, combined with chemical analysis, showed that air oxidation consumed more aliphatic than aromatic carbon but that both were consumed, at temperatures as low as 175 ^{0} C. This finding disproved the idea, proposed by Lahiri *et al* [4] and accepted by a number of other workers, that the aromatic material in coal was oxidized only above a threshold temperature, believed to be around 225 ^{0} C.

[11] The aromatic fraction of the coal had a higher proportion of quarternary, or unprotonated, carbon than did the aliphatic, thus supporting the conventional view that a part of the aromatic carbon in coal occurs in fused aromatic rings. Upon oxidation, proportionately more of the quarternary aliphatic carbons were lost.

[12] From a review of the published literature of autoxidation, together with

our results, we conclude that the air oxidation of coal proceeds by a free-radical mechanism, in which the initiation reaction is probably the rate determining step, producing oxygenated products such as hydroperoxides, aldehydes, peracids, which further react or decompose to give other products. CO is produced by the thermal decomposition of aldehydes and CO_2 by decomposition of peracids. Carboxylic groups arise from the oxidation of aldehydes, which in turn are derived from methyl and methylene groups in the coal. The attack of the reactive OH radicals upon aromatic rings produces phenolic groups and can also lead to rupture of the rings and consumption of aromatic material.

7.2 Recommendations

The work described in this thesis could be extended in the following ways:

[1] Subject to the availability of a sufficiently-accurate instrument to measure oxygen concentration in air, the rate of consumption of oxygen by coal should be measured as a function of time and temperature. Thus a more complete understanding of the kinetics of coal oxidation could be developed.

[2] The rates of oxygen consumption and CO and CO_2 production should be measured at different total pressures, while keeping the oxygen partial pressure constant, so that any possible effects of total pressure may be observed.

[3] Our data indicated that oxidation appears to enhance the devolatilization of organic material from coal. This phenomenon should be further investigated so as to understand better how devolatilization occurs under oxidative conditions.

[4] The total and organic content of the coal should be measured as a function of oxidation; however, given the high degree of uncertainty associated with the difference method suggested by the ASTM, the more accurate method based on neutron activation should be used for measurement of oxygen content.

[5] With a view to the possible commercial application of oxidation as a means of pre-treating coal to enhance its cation-exchange capacity, and subsequently to achieve sulfur capture during combustion, desired values of cation-exchange capacity should be established from combustion tests and then achieved by oxidizing coal at lower lower temperatures, so as to minimize loss of heating value.

References

[1] Kam, A. Y., Hixson, A. N. and Perlmutter, D. D., Chem. Eng. Sci. **31**, 821, 1976.

[2] MacPhee J.A and Nandi B.N, Fuel, **60**, 169, 1981

[3] Havens J.R, Koenig J.L, Kuehn D, Rhoads C, Davis A, and Painter P.C, Fuel, **62**, 936, 1983

[4] Lahiri A, Mukherjee P.N, Bhowmik J.N, Fuel, **38**, 469, 1959

APPENDIX A : Estimation of Mass-Transfer Resistances

Gas-to-Particle Mass-Transfer Calculations for Packed-Bed Reactor of Kam *et al* (Chem. Eng. Sci., **31**, 821, 1976), Run No.20, and for Fluidized-Bed Reactor Used in the Present Work

Summary

Mass transfer coefficient, k_c (m/s):

Packed Bed : 3.73×10^{-2} Fluidized Bed: 5.12×10^{-1}

External surface area of particle, amt (m^2/kg.coal)

Packed Bed: 6.34 Fluidized Bed: 35.8

Oxygen concn. in bulk gas, at reactor inlet, c_b (gmol/m^3)

Packed Bed: 5.17 Fluidized Bed: 5.38

Change in O_2 concn. across external mass-transfer film, ($c_b - c_s$), (gmol/m^3):

Packed Bed: 1.34×10^{-3} Fluidized Bed: 6.82×10^{-3}

$(c_b - c_s) / c_b$, where c_s is O_2 concn. at particle surface

Packed Bed: 2.60×10^{-4} Fluidized Bed: 1.27×10^{-5}

Conversion of O_2 at beginning of experiment, percent

Packed Bed: 72.9 Fluidized Bed: 1.46

Notes

1. The above figures indicate that gas-to-particle mass-transfer resistance was negligible in both reactors.

2. The high conversion of oxygen for the packed-bed experiments implies the existence of a

large concentration gradient of oxygen in the reactor, which causes the rate of reaction to vary with axial position and bed temperatures to be non-uniform.

1. Calculation

1.1 Data

1.1.1 Physical Properties of air at 1 Atmosphere and 200 ^{0} C

Density, ρ : 0.742 kg/m^3

Viscosity, μ : 2.58x10^{-5} kg/m–s

Diffusivity, D_{O_2-Air} : 4.06x10^{-5} m^2/s

Schmidt Number Sc $= \frac{\mu}{\rho D}$: 0.903

1.1.2 Experimental Conditions

Reactor, internal diam. (inches)

Packed Bed: 0.411 Fluidized Bed: 0.625

Reactor Temperature (^{0} C)

Packed Bed: 200 Fluidized Bed: 200

Reactor Pressure (atm)

Packed Bed: 1.0 Fluidized Bed: 1.24

Mass of coal used (gms)

Packed Bed: 45 Fluidized Bed: 10

Mean coal particle size , d_p (mm)

Packed Bed: 1.205 Fluidized Bed: 0.2135

Specific external area of particle, $a_{ext} = 3/\rho_{coal}R$ (m^2/kgcoal), based on approx. bulk density of coal of 785 kg/m^3

Packed Bed: 6.34 Fluidized Bed: 35.8

Air Flowrate (cm^3/ min at 1 atm., 25 ^{0} C)

Packed Bed: 142.2 Fluidized Bed: 600

Air flow per unit reactor area, G (kg/m^2s)

Packed Bed: 3.259×10^{-2} Fluidized Bed: 5.946×10^{-2}

Reynolds number, $Re = d_p G/\mu$

Packed Bed: 1.522 Fluidized Bed: 0.492

Percent O_2 in incoming air

Packed Bed: 20.23 Fluidized Bed: 20.95

Rate of inflow of O_2 (gmol/ min)

Packed Bed: 1.176×10^{-3} Fluidized Bed: 5.121×10^{-3}

Initial O_2 consumption rate, r_{O_2} (gmol/ kg coal-min)

Packed Bed: 1.91×10^{-2} Fluidized Bed: 7.5×10^{-2}

Initial conversion of oxygen (%)

Packed Bed: 72.9 Fluidized Bed: 1.46

1.2 Mass Transfer Correlations

1.2.1 Packed Bed

$$\varepsilon_B j_D = \varepsilon_B \left(\frac{k_c \rho\, Sc^{2/3}}{G}\right) = \frac{0.357}{Re^{0.359}}$$

from Petrovic and Thodos, Ind. Eng. Chem. Fundam., **7**, 247, 1978

ε_B estimated as 0.4

Calculated $k_c = 3.73 \times 10^{-2}$ m/s

1.2.2 Fluidized Bed

$$j_D = \left(\frac{k_c \rho Sc^{2/3}}{G}\right) = 5.7\, Re'^{-0.78}$$

$$Re' = \frac{Re}{(1 - \varepsilon_B)}$$

from Chu *et al*, Chem. Eng. Prog., **49**, 141, 1953

ε_B estimated as 0.4

Calculated $k_c = 5.12 \times 10^{-1}$ m/s

1.3 Calculation of External Film Resistance

Using reported initial rates of reaction, r_{0_2}, we calculated $\Delta c = c_b - c_s$ from the equation

$$r_{0_2} = k_c\, a_{mt}\, \Delta c$$

Results:

$\Delta c = 1.34 \times 10^{-3}$ gmol/m^3 for packed bed

$\Delta c = 6.82 \times 10^{-5}$ gmol/m^3 for fluidized bed

APPENDIX B : Error Analysis for Chapter 5

Estimation of Errors in Calculation of Aliphatic Carbon Consumption and Aromatic Carbon Consumption in Chapter 5.

According to Equations (5) and (6) of Chapter 5,

$$\text{Fraction aromatic C consumed} = [(\frac{C f_a}{T})_i - (\frac{C f_a}{T})_f] / (\frac{C f_a}{T})_i \qquad (1)$$

and

$$\text{Fraction aliphatic C consumed} = \frac{[(\frac{C(1-f_a)}{T})_i - (\frac{C(1-f_a)}{T})_f]}{(\frac{C(1-f_a)}{T})_i} \qquad (2)$$

Errors in the measurements of the relevant quantities in Equations (1) and (2) were estimated as follows:

Table 1B

Measurement Errors

Quantity	Relative Error (2σ)
Carbon Content	0.4 %
Carbon Aromaticity	2 %
Ash Content	3 %

Standard theory (see, for example, G.U Yule and M.G Kendall, An Introduction to the Theory of Statistics, Hafner Publishing Company, New York, 1950) gives the following relationships:

$$\text{Var}(X_1 + X_2) = \text{Var}(X_1) + \text{Var}(X_2) \pm \text{Cov}(X_1, X_2) \qquad (3)$$

$$\text{Var}\left(\frac{X_1}{X_2}\right) = \frac{\text{Var}(X_1)}{M_2^2} + \frac{\text{Var}(X_2)}{M_1^2} - \frac{2\,\text{Cov}(X_1, X_2)}{M_1 M_2} \qquad (4)$$

where M_1 and M_2 are the means of of X_1 and X_2, respectively.

If X_1 and X_2 are uncorrelated, Cov (X_1, X_2) is zero.

The errors in the calculation of aliphatic and aromatic carbon consumption were calculated using the relationships of Equations (1) through (4) above, together with the figures in Table 5.3 and Table 1B. For convenience, let:

AX = Fraction of aromatic carbon consumed

AY = Fraction of aliphatic carbon consumed

$$P = (Cf_a/T)_i \quad , \quad P' = (C(1-f_a)/T)_i$$

$$Q = (Cf_a/T)_f \quad , \quad Q' = (C(1-f_a)/T)_f$$

Then

$$\text{Var}(AX) = \text{Var}\left(1 - \frac{Q}{P}\right) = \text{Var}\left(\frac{Q}{P}\right)$$

We made the conservative assumption that the terms $(Cf_a/T)_i$, T_i, $(Cf_a/T)_f$, and T_f were uncorrelated. That assumption was conservative in that it gave a higher estimate of the variance than that which would be given by including the covariance terms in Equations (3) and (4). Hence we obtained the following equations:

$$\text{Var}(AX) = \text{Var}\,\frac{(Q)}{P^2} + \text{Var}\,\frac{(P)}{Q^2}$$

$$\text{Var}(P) = \frac{\text{Var}\left(\left(Cf_a / T \right)_i \right)}{T_i^2} + \frac{\text{Var}(T_i)}{\left(\left(Cf_a / T \right)_i \right)^2}$$

$$\text{Var}(Q) = \frac{\text{Var}\left(\left(Cf_a \right)_f \right)}{T_f^2} + \frac{\text{Var}(T_f)}{\left(\left(Cf_a \right)_f \right)^2}$$

In the corresponding equations for Var (AY) , C f_a is replaced by (1 − C f_a). From Equation (3) we can see that

$$\text{Var}\left(1 - C f_a \right) = \text{Var}\left(C f_a \right)$$

and therefore,

$$\text{Var}(P) = \text{Var}(P') \quad , \text{Var}(Q) = \text{Var}(Q') \quad \text{and} \quad \text{Var}(AX) = \text{Var}(AY)$$

Thus the error in AY was the same as the error in AX.

We noted that the error in the carbon content, C, was much smaller than the error in the carbon aromaticity, f_a , So we simplified the calculation by disregarding the error in C.

Values of Var (AX) were calculated using data for the 175 ^{0} C, 12 hr oxidized sample and data for the 280 ^{0} C, 24 hr oxidized coal sample. The results were very similar; 2.019×10^{-4} and 2.326×10^{-4}, respectively. Therefore the error in the value of AX , which we defined as 2σ , was estimated as 0.03. The numerical calculation is outlined below.

1. Calculation of Var (P)

$$C_i = 75.82. \quad , \sigma_{C_i} / C_i = 0.002$$

$$T_i = 8.24 \quad , \ \sigma_{T_i} / T_i = 0.015$$

$$\text{Var}\,((\,Cf_a)_i) = (\,0.01 \times 75.82 \times 0.70\,)^2 = 0.2816$$

$$\text{Var}\,(T_i\,) = (\,0.015 \times 8.24\,)^2 = 0.01528$$

and hence

$$\text{Var}\,(P) = 0.004153$$

2. Calculation of Var (Q)

2.1 Using Data for 175 ^{0} C, 12 hr Oxidized Coal Sample

$$\text{Var}\,(\,Cf_{af}) = (\,0.01 \times 72.64 \times 0.71\,)^2 = 0.2660$$

$$\text{Var}\,(\,T_f\,) = (\,0.015 \times 8.54\,)^2 = 0.01641$$

$$\text{Hence} \quad \text{Var}\,(Q) = 0.003652$$

2.2 Using Data for 280 ^{0} C, 24 hr Oxidized Coal Sample

$$\text{Var}\,(\,Cf_{af}) = (\,0.01 \times 61.96 \times 0.86\,)^2 = 0.2839$$

$$\text{Var}\,(\,T_f\,) = (\,0.015 \times 10.95\,)^2 = 0.02698$$

$$\text{Hence} \quad \text{Var}\,(Q) = 0.002378$$

3. Calculation of Var (AX)

The values of Var (AX) calculated using two values of Var (Q) above were

2.02×10^{-4} and 2.33×10^{-4}, and the average value was 2.18×10^{-4}. Thus, σ_{AX}, the standard deviation in AX, which is the square root of the variance, was calculated as 1.47×10^{-2}. The standard error at the 95 % confidence level, which is given by $2\ \sigma_{AX}$, was therefore about 2.9×10^{-2}. As shown earlier, that was also the standard error in the calculated fractional consumption of aliphatic carbon.